NOVEMBER 26, 2018

PRE- AND POST-NOURISHMENT MORPHOLOGIC BEHAVIOUR ALONG THE DUTCH AND DANISH NORTH SEA COAST

MASTER THESIS

DAVID BARMENTLOO
UNIVERSITY OF TWENTE, RIJKSWATERSTAAT

UNIVERSITY OF TWENTE.

Rijkswaterstaat
Ministry of Infrastructure and Water Management

Interreg North Sea Region Building with Nature
European Regional Development Fund

EUROPEAN UNION

Pre- and post-nourishment morphologic behaviour along the Dutch and Danish North Sea coast

By

D.S.G. Barmentloo
November 2018

To be publicly defended on 26 November 2018

Committee members:

Prof. dr. K.M. Wijnberg	*University of Twente*
Dr. ir. J. van der Zanden	*University of Twente*
Ir. R.J.A. Wilmink	*Rijkswaterstaat*
Drs. Q.J. Lodder	*Rijkswaterstaat*

In order to obtain the Master of Science degree in Civil Engineering and Management

Department of Civil Engineering and Management (CEM)
Faculty of Engineering Technology
University of Twente

I. Preface

In front of you lies my master thesis *'Pre- and post-nourishment behaviour along the Dutch and Danish North Sea coast'*, which is my final project of the Master Water Engineering & Management at the University of Twente. The master thesis is carried out at Rijkswaterstaat, where I took an internship during the last eight months.

During my master thesis I applied knowledge learned in most of the courses in the master programme. This master thesis showed me the practical use of these courses and gave me a good impression on how these learned capacities can be used in the field.

I would like to thank my graduation committee for their support and feedback. Rinse Wilmink, the weekly discussions kept me on track and helped me to not get stuck, thanks for your help. Joep van der Zanden, your feedback, especially on the method and structure of the report helped me a lot. I really appreciated that you continued to support me in your free time, after starting working somewhere else. Quirijn Lodder, your input based on field knowledge and more fundamental questions you asked were very helpful, thank you for your support. Kathelijne Wijnberg, thank you for your feedback and help, especially with details on the eigenfunction analysis. Finally, to the whole graduation committee, I appreciated it very much that the assignment was not yet completely defined on forehand, which gave me the possibility to define my own scope. This increased my motivation a lot.

I enjoyed my time at Rijkswaterstaat. I would like to thank my colleges and fellow students for the talks during lunch and coffee breaks. It made my stay at Rijkswaterstaat more pleasant and I got to know the tasks and projects of Rijkswaterstaat better.

I hope you find the report informative and that you enjoy reading it.

Utrecht, November 16, 2018.

David Barmentloo

II. Summary

In the shoreface of the Dutch and Danish coast nearshore sandbars are present. These sandbars play a vital role in the nearshore morphology; due to the decreased depth at the bar crest, waves break and dissipate a part of their energy before reaching the coast. The sandy North Sea coast of The Netherlands and Denmark are both prone to erosion, especially in case of storm events. Sandbars are important to reduce this coastal erosion.

Amongst other protection measures, shoreface nourishments are applied along both coasts aimed at counteracting erosion so that the coastline is maintained and the probability of flooding is decreased. In case of a shoreface nourishment, sand is supplied to the coastal zone, commonly around -6m MSL (mean sea level). A shoreface nourishment influences also the migration and position of nearshore sandbars.

In this research, eigenfunction analysis of cross-shore transect data measurements has been performed to investigate the influence of shoreface nourishments on nearshore morphologic behaviour, including sandbar migration. By using eigenfunctions analysis, dominant modes of variation (eigenfunctions) have been determined. The temporal component corresponding to the eigenfunctions (weightings) enables to examine the development of the nearshore morphology over time in terms of the shape of the eigenfunctions. The first eigenfunction, the most dominant pattern of variation, strongly resembles the time-averaged profile while the second and third eigenfunction generally account for migrating nearshore sandbars.

Pre-nourishment morphologic behaviour

This research concludes that the cyclic offshore bar migration along the Holland coast, as previously observed by Wijnberg (1995), remained present after 1990 until the application of the first shoreface nourishments. North and South of the IJmuiden harbour moles, offshore bar migration is observed, though on a completely different timescale. Bar cycle return periods of 15 (range: 12-18) and 4 (range: 3-4) years are observed respectively.

Along the Danish Midtjylland coast (km. 80-156), generally offshore migrating shore-oblique sandbars are observed. The sandbars have lengths of approximately 6-10 km and are generally attached to the shore in the north and extend seawards in the south. Due to the oblique orientation and relatively coarse resolution of the data used in this study, it seems like the sandbars are migrating northward. However, the apparent northward movement is likely the effect of offshore migration of the shore-oblique bars, combined with bar decay at the most offshore (southern) point and development of a new bar close to the shore in the north. The bar cycle return period is estimated between 8-12 years. Compared to the consistent bar migration along the Holland coast, the observed bar migration pattern along the Danish coast is more variable and less consistent.

Along major parts of the Danish west coast, the shoreface steepened up to 50% over the last century, combined with over 200m coastal retreat. The eigenfunction analysis used showed no off- or onshore bar migration pattern along the Danish coast from Hanstholm to Fjaltring (km. 0-79).

Post-nourishment morphologic behaviour

After the application of shoreface nourishments, reduced offshore migration, stagnation and temporal onshore migration of the offshore moving sandbars is observed. This effect is present for almost all shoreface nourishments along the analysed Holland coast with offshore migrating bars (km. 30-90).

The duration of affected bar behaviour due to a single nourishment in this area ranges from (at least) 13 years to only 1 year. This period of 13 years is significantly longer compared to many previous studies of individual nourishments along the Holland coast. Investigating the effect of single nourishments on the bar migration is often complicated due to the application of a subsequent nourishment shortly after the first nourishment. The application of multiple nourishments north of the IJmuiden harbour moles (transect km. 30-40) led to 9 years (2007-2016) of bar stagnation. Hence, the current nourishment practice seems to cause stagnation of the sandbars. The interval between the nourishments is not large enough to make offshore migration of the sandbars possible.

Results of this research show that along the Holland coast (repeated) nourishments influence the offshore bar migration up to 2km alongshore from the borders of the nourished section. Generally, the alongshore influence is very limited and bar switches occur directly at the borders of the nourished section.

In the area where no migrating sandbars are observed (between Den Helder and the former Pettemer Zeewering), the nourishments cause significant and long term (> 8 years) flattening of the shoreface.

In Denmark the observed pre-nourishment bar migration forms a less clear pattern, complicating the analysis of post-nourishment bar behaviour. Only at one location a clear bar signal has been observed over an 8-year period in which nourishments were applied frequently. In this particular case, the bars were relatively stable during the nourishment period. After this period, bar started migrating offshore.

No consistent relation between nourishment implementation characteristics and bar migration has been observed. Generally, large nourishments do affect the offshore migration for a longer period. However, also after one relatively small nourishment a long period of bar stagnation has been observed. Causal relationships are difficult to determine due to the many variables and non-linear relations between them (e.g. sediment diameter size and distribution, nourished volume per running metre, total nourished volume, wave-variability (storm-events), placement depth and the pre-nourishment morphologic behaviour).

Table of Contents

1. Introduction

1.1 Background

This master thesis is part of an EU Interreg Building with Nature (BwN) project. This project aims at making coast more adaptable and resilient to the effects of climate change, such as sea level rise (Wilmink et al., 2017). Improving the resilience of coasts goes hand-in-hand with Building with Nature, which is based on the philosophy that it is better to make use of natural processes for coastal protection instead of counteracting nature blocking its processes. A nourishment is seen as a nature-based solution to provide safety against flooding. Sand is supplied to the coast, so that the coast is strengthened, and erosion is counteracted. This is an alternative solution to hard coastal protection measures such as seawalls.

As a part of this transnational Building with Nature project, knowledge of (differences in) coastal protection of various countries along the North Sea Region (NSR) coast (Belgium, Netherlands, Germany, Denmark and Sweden) is exchanged. One of the recently completed products of the Building with Nature project is a combined dataset of yearly/biannual nearshore bathymetry transect measurements. The trans-national dataset allows for large-scale investigation of nearshore morphologic behaviour and differences herein within the NSR.

1.2 Motivation

Countries along the North Sea Region (NSR), including Belgium, The Netherlands, Germany and Denmark, all apply flood protection measures to strengthen or stabilize their (mostly sandy) coasts. Due to climate change (e.g. sea level rise and increased storminess), the need for flood protection measures is expected to increase over the coming decades. One of these flood protection measures are shoreface nourishments. This type of nourishments is increasingly applied over the last decades, mainly because they are cheaper than more traditional beach nourishments (Deltares, 2017b; Verwaest et al., 2000). In case of a shoreface nourishment, sand is supplied to the coastal zone, commonly around -6m MSL.

Research has shown that nearshore sandbar migration is influenced by a shoreface nourishment (Grunnet & Ruessink, 2005; Ojeda et al., 2008; Van Der Spek et al., 2007; Walstra, 2016) and that implementation and observed bar behaviour is different along the NSR coast (Lodder & Sørensen, 2015). Commonly, the shoreface nourishment causes onshore migration or stagnation of the previously offshore migrating sandbars. After a period of multiple years, in the order of 2 to more than 6 years, this bar starts migrating offshore again. It is unclear whether this offshore migration again forms the previously natural migration pattern or that changes are still present. Moreover, it is not clear whether the time it takes to return to pre-nourishment behaviour can be related to region characteristics (e.g. bar cycle return period) or by nourishment implementation characteristics (e.g. volume, grain size, placement location in cross-shore profile).

1.3 Problem definition

In the NSR, there is a need for improved understanding of nearshore morphodynamics and differences herein. Understanding the nearshore morphology is important since it influences the nearshore hydrodynamics, especially the energy dissipation of incoming waves. The

energy dissipation affects the wave energy that reaches the coast. In this way, the nearshore morphology and resulting wave energy dissipation is an important factor regarding coastal erosion and coastal safety.

During high wave events, waves generally break on the crests of sandbars and thereby lose their energy. Wijnberg (1995) has shown that these sandbars do migrate offshore and show cyclic behaviour along the Dutch coast in the period of 1965-1990. Nowadays, data until 2016 is available, enabling further analysis of recent coastal morphology. Moreover, data from countries outside the Netherlands with similar coasts can be studied, such as Denmark. By studying both coasts in a consistent way, more knowledge of recent nearshore morphodynamics and difference herein can be obtained.

Over the last decades, shoreface nourishments are increasingly applied in both countries. Shoreface nourishments are known to affect the bar migration and thereby the nearshore morphology.

The bar behaviour (after nourishments) is studied often for individual areas (or nourishments) (Ahrendt, 2001; Deltares, 2017b; Kaergaard et al., 2012), by comparing different areas (nourishments) (Ojeda et al., 2008; Van Duin et al., 2004) or by analysing on a country-level scale (Di Leonardo & Ruggiero, 2015; Wijnberg & Terwindt, 1995). However, a large-scale study with a consistent method to analyse bar behaviour (after nourishments) within the NSR has not been performed yet. A large-scale study could provide more insight in the bar behaviour and differences herein within the NSR. Possibly, correlating relations in the nearshore characteristics and observed bar behaviour can be found. Di Leonardo and Ruggiero (2015) for example conclude from a large-scale study of 260 km. US north-west Pacific coast that the width of the effective bar zone (the cross-shore locations where bars can be located) decreases with steeper shoreface slopes. Moreover, steepening of the shoreface was associated with a transition from multiple sandbars to a single sandbar.

Secondly, the effect of shoreface nourishments on the bar behaviour (e.g. bar migration) can be studied along these large coastal stretches. Possibly relations between the pre- and post-nourishment morphologic behaviour exist that can be found by examining a large quantity of nourishments on a large spatial and temporal scale. If these relations are known, the post-nourishment morphology can be predicted based on the pre-nourishment morphology and nourishment implementation. Also, it can be investigated if these effects are local effects (i.e., influence of nourishments is only observed along the coastal stretch where nourishments are applied) or that shoreface nourishments influence the coastal morphology along larger coastal stretches.
In this way, a more thorough understanding of the nourishments and its effectiveness in coastal protection can be obtained.

1.4 Objective

The research objective is stated as follows:

To characterise nearshore morphologic behaviour along the NSR and investigate the influence of shoreface nourishments on this morphologic behaviour.

The research objective is twofold. The first part is the characterisation of regions with similar morphologic behaviour along the NSR coast. Secondly, this research is aiming to relate post-nourishment behaviour to pre-nourishment behaviour. Therefore, this characterisation of the pre-nourishment morphologic behaviour is an evident pre-requisite in order to relate it to post-nourishment morphology.

1.5 Research questions

To meet the objective described above, the following research questions are formulated:

1. ***What regions with similar nearshore morphologic behaviour can be characterized along the Dutch and Danish North Sea coast?***

The analysed Dutch and Danish North Sea coast will be divided into regions with similar nearshore morphologic behaviour. This nearshore morphologic behaviour will be based on the movement of the shoreline (progradation/coastal retreat), (trends in) steepness, the presence of nearshore bars and their migration.

There will be focussed on various mostly inlet free sections. Here coasts are relatively uniform, which is expected to result in alongshore uniform bar behaviour. Also, since bar cycles can be up to 15 years, a large temporal dataset is needed to adequately study the bar behaviour. Areas that will be analysed are the Rijnland and North-Holland coast (Netherlands) and the Midtjylland, Agger and Nationalpark Thy coast (Denmark). All these areas do have a long history of at least biannual measurements.

Eigenfunction analysis will be used to characterize regions with similar bar behaviour, see 3.3 *Eigenfunction analysis of cross-shore profile data* for a comprehensive description of this data-analysis technique. Dominant patterns / cross-shore shapes that can explain most of the variance from the reference datum will be extracted and analysed. The most dominant pattern explaining most of the variance in the dataset, the first eigenfunction, strongly resembles the average profile. The second and third eigenfunction commonly originate from the variable position of the nearshore sandbars.

2. ***How do shoreface nourishments influence the nearshore morphologic behaviour?***

To clearly define what is incorporated in the term ‘influence’, this question is divided into three sub-questions.

a) ***How do shoreface nourishments influence the steepness of the shoreface?***
b) ***How do shoreface nourishments influence the migration of nearshore sandbars?***
c) ***Is the post-nourishment nearshore morphologic behaviour region-specific or do nourishment implementation characteristics govern this morphologic behaviour?***

Sub-questions a and b will be answered with the same technique as used in research question 1, namely the eigenfunction analysis. The expectation is that, in case of offshore migrating

sandbars, the influence of a nourishment on the bar migration is observable from the disturbance of the pattern of the second and third eigenfunctions weightings.

To answer sub-question c, the observed post-nourishment nearshore morphology (bar migration, steepness) will be evaluated against the pre-nourishment bar behaviour, total volume [m^3], volume per meter coastline [m^3/m] and the placement depth of the nourishment. These evaluation criteria contain as well important implementation characteristics of nourishments as a criterium assessing the original nearshore morphodynamics.

1.6 Reading guide

In Chapter 2 literature of nearshore morphologic processes and the influence of shoreface nourishments on these processes is summarized. Also, the shoreface nourishment practices in along the analysed coastlines are evaluated here.
In Chapter 3 *Methodology*, the study area, the dataset and the data-analysis technique used in this study are described.
In Chapter 4 the results of the eigenfunction analysis are given, based on pre-nourishment data. In this chapter Research Question 1 is answered. Results regarding the influence of nourishments on the nearshore morphologic behaviour are given in Chapter 5. With this post-nourishment morphologic behaviour Research Question 2 is answered. Discussion and conclusions can be found in Chapter 6 and 7 respectively.

2. Research background and nourishment practice

In this chapter literature on bar behaviour, shoreface nourishments and the effect of shoreface nourishments on the bar behaviour is summarized. Regarding the bar behaviour there is in particular elaborated on the migration processes and the alongshore uniformity or variability in the bar position. Regarding nourishments, there is elaborated on nourishment practice in both countries and the migration of shoreface nourishments. Finally, various studies about the effects of shoreface nourishments on the nearshore sandbars are summarized.

2.1 Bar behaviour

The coasts in the North Sea Region are generally wave-dominated, i.e. waves are the dominant factor that determines the coastal morphology. Wave-dominated beaches can be energy dissipative because of wave breaking on sandbars. Sandbars in the nearshore-zone are formed by cross-shore sediment accumulation due to a highly non-linear morphological relation between the bed profile and nearshore hydrodynamics (Walstra, 2016). Nearshore bars are present in the shoreface, where the sediment is to some extent mobilized by orbital motion of fair weather waves (Dashtgard et al., 2012). A wave-dominated beach can contain up to five bars (Walstra, 2016) and nearshore sandbars can be present up to a water depth of 10 m. In Figure 1 the position of nearshore sandbars in the shoreface is shown.

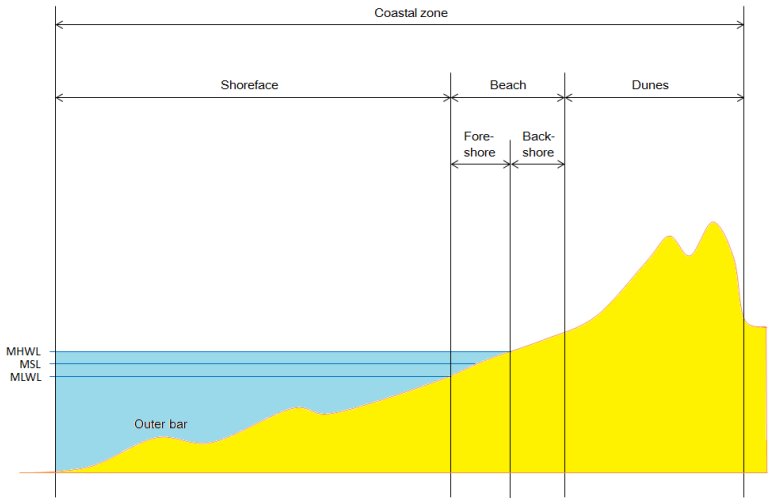

Figure 1: Schematization of nearshore sandbars in coastal zone (Bruins, 2016)

Generating knowledge about nearshore bar behaviour is important, since bars dissipate up to 80% of the incident wave energy and thereby reduce the wave impact on the beach and dunes (Walstra, 2016). This reduction of wave energy causes less erosion and thereby increases the coastal safety.

2.1.1 Bar migration processes

Two main processes are involved in sandbar formation. Generally, wave skewness causes an onshore directed transport at the offshore side of the sandbar, while an undertow current causes offshore sediment transport at the landward side of the sandbar. Due to the combination of these processes, sediments accumulate at the top of the sandbar (Van Der Zanden et al., 2017). This accumulation is limited by gravitational driven transport. A disbalance in the onshore and offshore directed sediment transport can result in sandbar

migration. The magnitude of this on- and offshore directed sediment transport depends on the wave intensity.

When large waves approach the coast, they generally break on the outer (most seaward) bar, creating an onshore current in the upper part of the water column. Moreover, during high waves, wind is generally also strong, creating a shear stress on the upper water column. This also contributes to the onshore current in the upper part of the water column. Since the coast is a closed boundary, the onshore flow in the upper water column must be compensated by a return flow, the undertow current. This offshore directed return flow in the lower part of the water column drives the sand bar offshore (Hoefel & Elgar, 2003).

Under calm wave conditions, waves do generally not break on the (outer) bar and bar migration can be onshore directed. This happens due to the asymmetry of the shoaling non-breaking waves. Sediment transport is often expressed with a simple power function, see Equation (1).

$$q_s = mU^n \qquad (1)$$

In which q_s [m^2/s] is the sediment transport per unit width and U [m/s] the flow velocity. The parameters n and m are both calibration or location specific values, with exponent n normally valued between 3 (Meyer-Peter Müller transport equation) and 5 (Engelund and Hansen) (Kleinhans et al., 2008). The oscillatory velocity under non- or weakly breaking waves is generally skewed, with a high (but short) onshore velocity under the steep wave front and a low (but longer) offshore velocity under the rear face of the wave. In addition, besides velocity skewness there is also acceleration skewness (Elgar et al., 2001). The acceleration under the steep wave front is usually higher. Therefore, the boundary layer under the steep wave front has less time to grow, resulting in relatively large bed shear stress and increased onshore sediment transport (Van Der A et al., 2011).
Albeit the offshore directed transport is generally present over a longer period in one wave cycle, the onshore transport during the steep wave front phase exceeds the total offshore directed sediment transport. Hence, the transport is onshore directed and the sandbar will migrate towards the beach. Under calm wave conditions the undertow current is less dominant, although rip currents can cause local concentrated strong offshore flow under calm wave conditions. The combination of the transport induced by the skewness of the waves and the undertow current determines the net transport.

There is no clear causal relationship between offshore (onshore) migrating bars and erosion (accretion) in the coastal zone (Van Der Spek et al., 2007; Wijnberg, 1995). Along a coast with offshore moving sandbars, there can still be accretion of sediment in the coastal zone. Sediment budget studies indicate that the net sediment transport is generally shoreward along -8m NAP (offshore of zone of decay) for the Holland coast (Van Rijn, 1997). Also along the Danish west-coast at Vejers the offshore moving bars do not result in significant sediment changes in the nearshore region (Aagaard & Kroon, 2007).

The presence of sandbars seems influenced by the steepness of the shoreface. Di Leonardo and Ruggiero (2015) conclude from a large-scale study of 260 km. US north-west Pacific coast that the width of the effective bar zone (the cross-shore locations where bars can be

located) decreases with steeper shoreface slopes. Moreover, steepening of the shoreface was associated with a transition from multiple sandbars to a single sandbar.

2.1.2 Bar behaviour in the Netherlands

For the Dutch coast, the net yearly bar migration is generally offshore directed (van Enckevort & Ruessink, 2003; Wijnberg & Terwindt, 1995). Sandbars move offshore toward a so-called zone of decay. During the offshore movement they grow in height and width. Walstra (2016) found that model results indicate that this growing is due to enhanced sediment stirring on the landward bar slope and trough caused by the breaking wave induced longshore current. The longshore current, particularly affecting the lee slope, causes erosion on the landward slope of the bar, while the sediments settle seaward of the crest. Walstra (2016) found that bar growth does not happen in absence of an alongshore current. However, wave flume experiments show that bar growth can happen in absence of an alongshore current (Van Der Zanden et al., 2017). The bar growth is in this case caused by increased turbulence of waves at the landward slope of the bar, which also stirs up sediment. In both cases, the increased sediment stirring landward of the bar crest and settling on the seaward side of the crest is the cause of the bar growth.

2.1.3 Zone of decay and bar cycle

In the Netherlands, nearshore sandbars often migrate offshore until they reach the zone of decay; often between 400 and 800m from the shoreline (Bruins, 2016). When the sandbars reach the zone of decay they fade away. The decay of one sandbar is generally compensated by the development of a new sandbar close to the shore. Wijnberg (1997) hypothesised that the decay of the outer bar causes less waves to break relatively far offshore. As a consequence of this, more large waves do approach the shore without breaking, creating a relatively large undertow current. This results in an increased offshore migration of the remaining sandbars. An analysis by Aagaard et al. (2010) observed higher waves and an increased undertow current at a Danish coast after a bar decay event, consistent with the theory of Wijnberg (1997).

The time in between two bar decay events is called the bar cycle return period (T_r). This period is usually between 4 and 15 years for the Holland coast (Wijnberg & Terwindt, 1995). For other areas this return period can be significantly different, in Wanganui (New-Zealand) return periods as low as one year are observed (Shand et al., 1999). Shand et al. (1999) found correlation with parameters that indicate that this small bar cycle return period in Wanganui could be due to the high nearshore slope and/or relatively low wave height. This is however in contradiction with more recent literature (van Enckevort & Ruessink, 2003; Walstra, 2016), suggesting offshore transport during high wave events.

Ruessink et al. (2009) found that the migration towards the zone of decay usually happens during extreme wave events. A relatively large undertow current causes further than usual offshore migration of the sandbar. During such wave events sandbars migrate toward a non-breaking- wave regime. In this regime the skewness or wave asymmetry, causes onshore transport during moderate wave events and the undertow current is relatively weak. This onshore transport is associated with bar decay. This might be because the waves action causes

the highest (onshore) sediment transport at the highest bed point (top of the sandbar). As a consequence of this, the bar fades away.

2.1.4 Bar behaviour in Denmark

Besides cross-shore bar behaviour, bars can also migrate alongshore. This is observed along parts of the Danish coast (Kaergaard et al., 2012). The alongshore migration is caused by an alongshore current, which can be induced by wave breaking or an asymmetric tidal current. Along parts of the Danish west coast, southwards migration of sandbars is observed, which corresponds with the net sediment transport direction. Sandbars are generally oblique to the shoreline. At the northern point of sandbars, bars are located very close to the shore. The southernmost point of the sandbar is generally located most offshore, see Figure 2. Kaergaard et al. (2012) determined the southward bar migration by analysing the alongshore position of various irregularities in the cross-shore position of the bar crest. An example of such an irregularity, i.e. deviating from a linear shore-oblique bar-form, is the bar crest between longshore coordinate 7000 and 8000 in the year 2006. Besides southward movement the sandbars also migrate offshore.

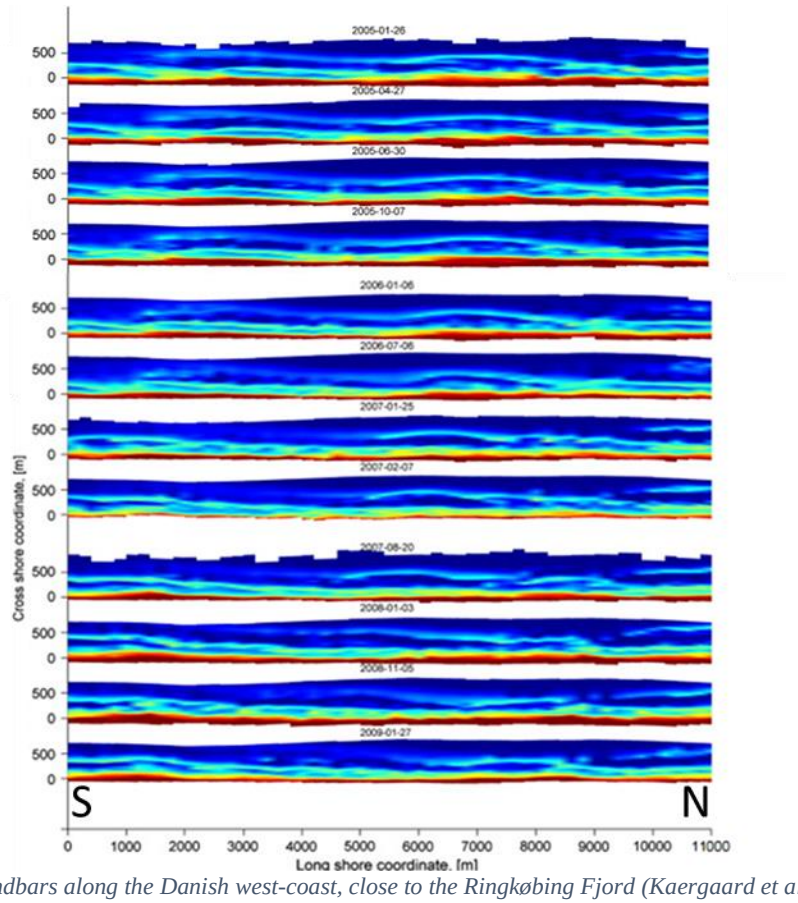

Figure 2: Sandbars along the Danish west-coast, close to the Ringkøbing Fjord (Kaergaard et al., 2012)

2.2 Alongshore variability in bar behaviour

Bars often show consistent behaviour alongshore. Wijnberg and Terwindt (1995) analysed the long-term morphologic behaviour of the Holland coast. The Holland coast is an inlet-free large coastal stretch with a length of approximately 120km. Based on eigenfunction analysis

of yearly cross-shore measurements of the coast (JARKUS data), they characterized five areas with similar large-scale coastal behaviour (LSCB) along this Holland coast.
By using this eigenfunction analysis, Wijnberg and Terwindt (1995) observed differences in bar behaviour. At south and north side of the IJmuiden harbour moles, regions with different bar cycle return periods (respectively 4 and 15 years) were found.

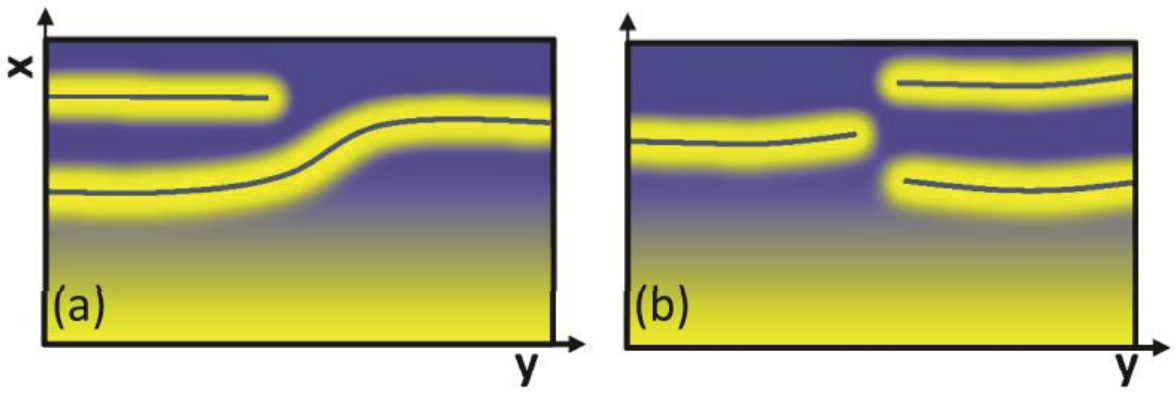

Figure 3: Two different types of bar switches: (a) Inner bar attached to outer bar (b) separated bar switch (Walstra, 2016)

The IJmuiden harbour moles, with 2.5 and 2 km length for the north and south breakwater respectively, function as a sharp boundary regarding the offshore migration of bars. Due to this boundary, bars at both sides can act independently. However, within the north or south side of the breakwaters, bars cannot act independently. The bar movement 5km south of IJmuiden can for example be influenced by the bar movement 10km south of IJmuiden. Wijnberg (1995) hypothesised that coherent bar movement within one 'coastal cell' can play an important role in the sharp boundary that is observed at the IJmuiden moles, since nearshore conditions at the borders of the IJmuiden moles are very similar.

Other parameters, like grain size or hydrodynamics could not explain this sharp change. Directly south of the harbour moles, a small decrease in grain size is observed compared to north of the moles. This could, see equation (2), be a reason for increased sediment mobility. However, further south (km 77-90), larger grain sizes are observed compared to North of the moles.

Besides this difference in bar cycle return period, it was found that within some regions sandbars show similar behaviour regarding return period, but are in a different phase, i.e. an outer bar which is connected to a bar in a different phase (for example an inner bar, see Figure 3a). This lack of alongshore coherence does not mean that different bar behaviour is present, bars are only in a different phase. Bar switches are usually temporal (Walstra et al., 2015).

Shand et al. (2001) show that bar switches usually occur during extreme wave events combined with a high alongshore current. However, not every high wave event does cause a bar switch. The antecedent morphology and local nearshore hydrodynamics are thought to be important too. Local morphologic circumstances (e.g. slight change in slope, different location of the outer bar) can enhance this bar switching.

2.2.1 Parameters related to bar behaviour

Bar migration cannot yet be deduced well from hydro- and morphodynamic characteristics. Various data analysis studies were not able to relate the contribution of parameters like hydrodynamic forcing, sedimentological constraints (grain size, stratigraphy) and morphological constraints (shoreline orientation, shoreface and surf-zone morphology) to characteristics like the bar cycle return period (Walstra, 2016). Dominant physical processes that determine the bar cycle return period in different LSCB regions or sides could not be identified. Walstra (2016) found from model studies that the bar cycle return period is positively correlated with the sediment diameter, the bar spacing and profile slope and negatively correlated with the wave forcing. He determined this from numerical model simulations, wherein he alters conditions, (e.g. shoreface profile, wave climate) of the Egmond and Noordwijk beach and evaluates the resulting bar cycle duration. The correlations he found were consistent with earlier findings from field observations.

The physical explanation of the positive correlation of the sediment size and bar cycle period is intuitive. Sediment mobility reduces when grain sizes increases. A common threshold used to determine if sediment is brought into motion is the Shields parameter (Shields, 1936), see equation (2).

$$\theta = \frac{\tau_b}{\Delta g D} \qquad (2)$$

In which

θ	[-]	Shields parameter
τ_b	[kg/m/s^2]	Bed shear stress
Δ	[kg/m^3]	Delta, density of the sediment minus the density of the water
g	[m/s^2]	Gravitation acceleration
D	[m]	Grain size

If the Shields parameter exceeds a certain value (also mentioned critical Shields value, θ_{cr}), sediment is brought into suspension and sediment transport will occur. This Shields parameter is negatively influenced by the grain size. Decreased sediment mobility results in a longer return cycle period (Walstra, 2016).

Also a positive correlation was observed with the bed steepness. Walstra (2016) found this result counter-intuitive, since increased steepness causes more intense wave breaking, which results in a large undertow current and increased offshore migration of the sandbars. If this large undertow current is dominant, a negative correlation should be present. He found that this increased offshore transport is indeed present, but only for a small section of the shoreface. When the sandbars have migrated into deeper parts of the shoreface, migration velocities are reduced.

In addition, two other effects are observed that contribute to the positive correlation of bar cycle return period with the bed steepness. Firstly, model results show that bars become larger in case of a steeper bed profile. This large size and increased volume of the bars reduces the offshore migration velocity. Secondly, the zone of decay is located relatively deep due to the intense wave breaking and large undertow current. Therefore, the sandbars migrate to a relatively deep section (Walstra, 2016).

2.3 Shoreface Nourishments

2.3.1 Function of shoreface nourishments

Shoreface nourishments are widely applied in the NSR. However, the design of these shoreface nourishments is often highly empirical (Ojeda et al., 2008), i.e. based on behaviour of previous nourishments with similar characteristics. The goal of a shoreface nourishment is to increase the sand volume in the coastal zone, generally shoreward of the nourishment. Shoreface nourishments are increasingly applied over the last decades to counteract coastal erosion. One of the main advantages of shoreface nourishments are its low cost compared to the more traditional beach nourishment (Verwaest et al., 2000). Van Duin et al. (2004) hypothesised two main effects of a shoreface nourishment, based on a lee (also mentioned longshore) and feeder (also mentioned cross-shore) effect.

The feeder effect is straight-forward; the supplied sediments of the nourishment will be transported by the dynamics of the waves to the adjacent beach (Van Duin et al., 2004). The skewness of the waves causes a net shoreward sediment transport, in a similar way as explained in section 2.1 *Bar behaviour*.

Since large waves will break at the seaward side of the nourishments due to the decreased water depth, a calmer wave climate will be present at the lee side of the nourishment. This results in less wave stirring and a decreased wave induced return flow (Van Duin et al., 2004). Hence, the offshore directed transport is reduced due to the decreased offshore return flow while the onshore transport (due to wave asymmetry) is increased because of the decreased depth at the location where the nourishment is placed.

Therefore, the nourishment will migrate toward the beach, see Figure 4b. Another effect of the nourishment is an increased water level shoreward of the nourishment. There is a transport of water over the nourishment, which is caused by (breaking) waves. This water level gradient will induce a flow alongshore to the sides of the nourishment. This can induce erosion shoreward of the nourishment.

The lee or longshore effect is induced by a gradient in the longshore current. A calmer wave climate will be present in the landward (lee) side of the nourishment. Oblique incident waves,

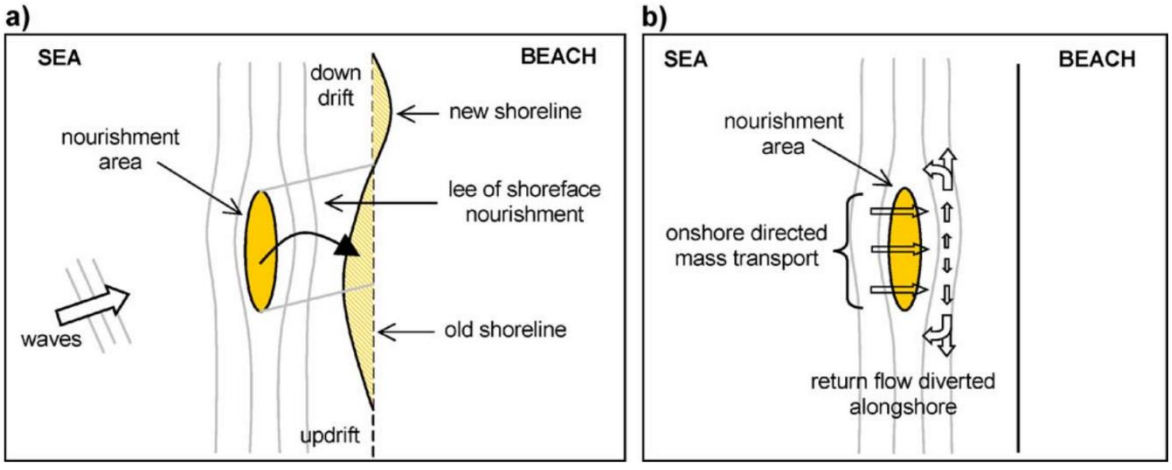

Figure 4: (a) Lee and (b) feeder effect of a shoreface nourishment (Van Duin et al., 2004)

which are generally present along the NSR coast, contribute when they break to the creation of a longshore current in the direction of propagation. The contribution at the lee-side of the nourishment is (due to the calmer wave climate) relatively small. This causes a negative gradient in the longshore (sediment) transport. This gradient causes sedimentation at the lee side of the nourishment. The reduced longshore current also decreases the amount of sediment that is transported alongshore to the border of the lee side. Because wave energy is not decreased after the boundary of the lee side, a positive gradient in the alongshore current is present here. This causes downdrift erosion, see Figure 4a.

2.3.2 Shoreface nourishments practice in the NSR

Netherlands

In the Netherlands shoreface nourishment are common practice, a yearly evaluation of the coast determines where and when nourishments should be applied. On average, 12 million m^3 is yearly supplied in the Netherlands (Deltares, 2017b), of which a large (and growing) part is shoreface nourishments. Shoreface nourishments executed along the Holland coast, which is an approximately 120km long inlet free coast, are illustrated in Figure 5. The thickness of the lines in this figure represents the volume per meter coastline [m^3/m], ranging from 40 to 920 m^3/m.

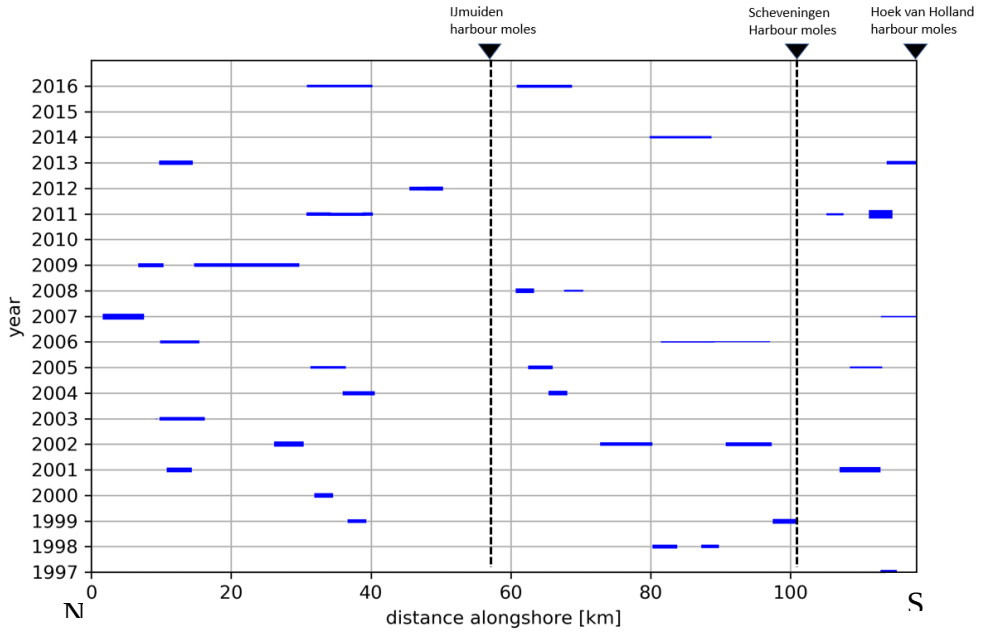

Figure 5: Shoreface nourishments applied along the Holland coast, origin is the Den Helder coast.

When evaluating Figure 5, it becomes clear that most areas along the Holland coast are quite frequently nourished. Especially in the coastal stretches 10-15 km, 30-40 km shoreface nourishments are applied often. At other coastal stretches (e.g. 40-60 km) nourishment are applied less.

Denmark

In Figure 7 the nearshore and bar nourishments along a part of the Danish coast are shown. In a large area (section km 0 – 40) no nearshore or bar nourishments have been applied. The x-axis and further mentioned distances are alongshore distances with respect to Hanstholm, the northern boundary of the analysed coast.

Generally, land-owners at the coast are responsible for coastal protection. However, between Lodbjerg (km. 39) and Nymindegab (km. 149) the state and four municipalises have a special role to protect for floods and to reduce erosion. This agreement has led to many nourishments since it was signed in 1982. Most recent erosion objectives and the calculated retreat of the coastline are presented in Figure 6.

The thickness of the lines in Figure 7 again represents the volume per meter coastline [m^3/m]. Some nourishments are placed on an alongshore very small section and have a very high volume, e.g. the nourishment in 2008 around km. 52. Therefore, the resulting lines are very thick and very short, and therefore seem like vertical lines in Figure 7. The largest shoreface nourishment in terms of volume [m^3/m] which was applied over more than a kilometre was in 1998 at km. 82 and a had nourishment volume of 480 m^3/m.

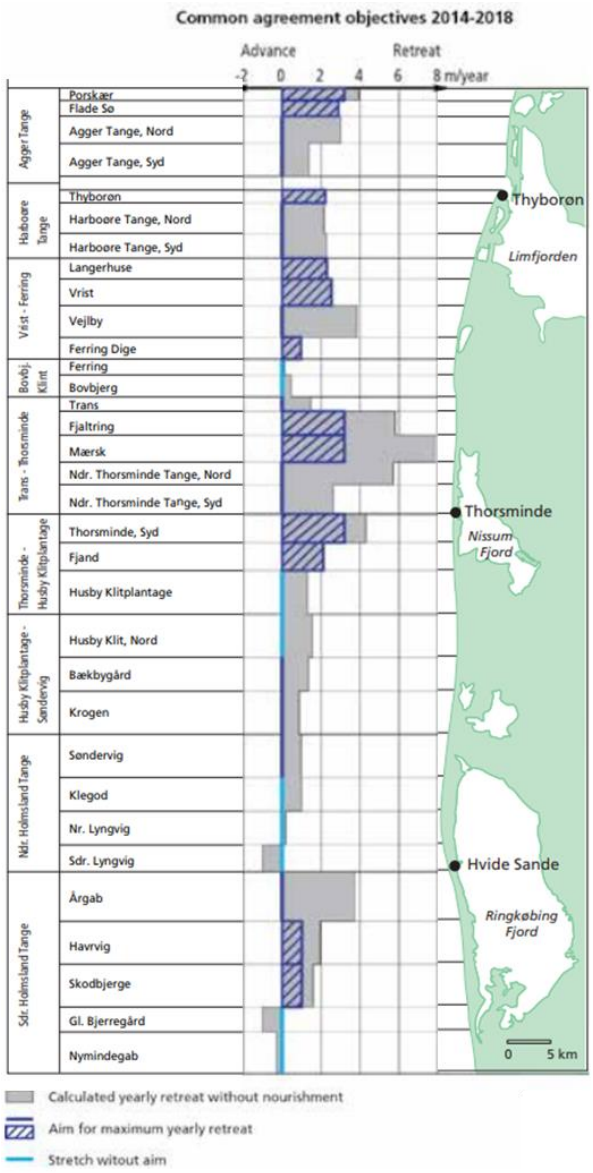

Figure 6: Danish erosion agreement (Thomsen, 2018)

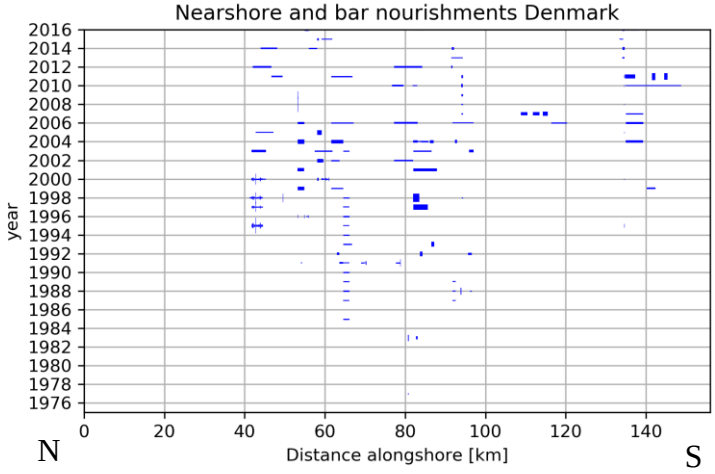

Figure 7: Nearshore and bar nourishments applied in Denmark. The origin in the Hanstholm coast, the distance alongshore is defined positive southwards.

2.3.3 Nourishment migration

In section 2.3.1 *Function of shoreface nourishments* a cause of cross-shore migration of nourishments is explained. However, influenced by an alongshore current, nourishments can also migrate primarily alongshore. Bruins (2016) analysed the post-nourishment migration of 20 shoreface nourishments in the Netherlands and found a relation in original bar behaviour and nourishment behaviour. When the original bar behaviour was cross-shore, the nourishment also migrated cross-shore, while there was little or no alongshore migration in these cases. Bruins (2016) observed that the nourishment moves (cross-shore) to the zone of decay of the natural bar system. If the nourishment is placed offshore of this zone of decay, the nourishment moves landwards. If the nourishment is placed landward of the zone of decay, the nourishment migrates offshore.

Alongshore migration of the nourishment is dominant when no cross-shore bar migration occurred in the original bar system. Generally, nourishments migrate toward the beach in case of no cross-shore bar behaviour.

This finding is in correspondence with a Dutch-Danish comparison of nourishments by Lodder and Sørensen (2015). The nourishment in Denmark primarily migrated alongshore (corresponding with the alongshore and offshore bar migration), while the nourishment migration along the Dutch coast was cross-shore (corresponding to the offshore bar migration). However, the nourishments differed quite in implementation, which could also result in the different migration direction. The nourishments applied in Denmark had higher median grain size (D_{50}) compared to the Dutch nourishments and either a much lower volume per meter or a much lower total volume.

2.3.4 Bar behaviour after nourishment

A shoreface nourishment changes the nearshore (morpho)dynamics, i.e. the idea that the profile only moves seaward after diffusion of the nourished sand is way too simplistic (Van Der Spek et al., 2007). Nature strives to return to the original profile morphology, but this is a long-term process. Directly after the implementation of a nourishment, the nearshore sandbar migration process is affected. Various studies have examined the post-nourishment behaviour of nearshore sandbars. A shoreface nourishment is commonly placed offshore of the outer bar. This nourishment often forms a new outer bar. This process happens mostly within 6 months after implementation (Walstra (2016) and references therein). The former outer bar will then become the middle bar. The nourishment often reverses or delays the bar migration direction for a couple of years. Therefore, the bars at the nourished coast are often not in phase with surrounding bars (Van Der Spek et al., 2007), i.e. shoreface nourishment can cause a bar switch.

Analysis of one of the first shoreface nourishments implemented at an erosion hotspot in the Netherlands near Egmond aan Zee in 1999, showed that the bar behaviour changed from offshore migration to significantly shoreward migration during the two years after the implementation of the nourishment. The nourishment was placed offshore of the outer bar. After these two years, the coast seemed returned to its pre-nourishment dynamic bar system, since the outer bar did migrate offshore (again) and the nourishment started to defuse (Van

Duin et al., 2004). Similar changes in bar behaviour after a shoreface nourishment were observed in other studies. After a nourishment in Noordwijk in 1998, the Netherlands, the offshore migration of sandbars was decreased, see Figure 8 (Ojeda et al., 2008). Reduced velocities in the offshore direction were first observed in the outer bar and later in the inner bar. In this case the offshore migration was reduced for at least 6 years.

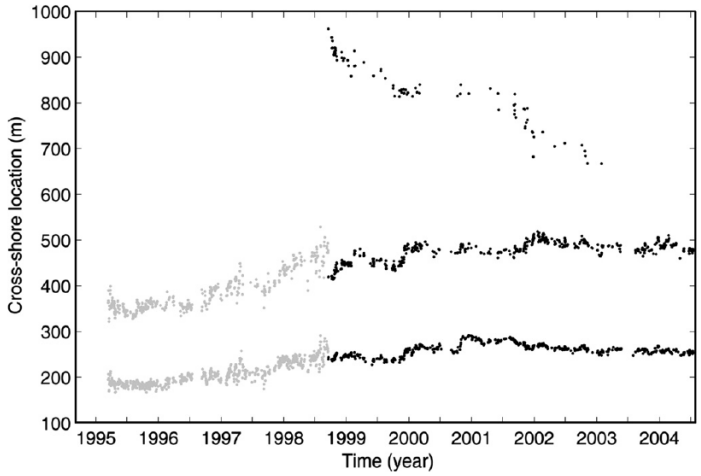

Figure 8: Cross-shore location of inner and outer bar crests. In grey: Pre-nourishment observations.(Ojeda et al., 2008).

Ojeda et al. (2008) suggested that this long period compared to the Egmond aan Zee nourishment could be due to the grain size of the sediment used at the Noordwijk case (D50 ± 400 μm), which was almost twice the grain size used at Egmond aan Zee (D50 ± 208 μm). Also, the nourishment size was larger compared to the Egmond case, while in the Egmond case the observed sandbars were larger. This makes the nourishment even larger compared to the sandbars. Since shoreface nourishments generally start forming a new outer bar, Van Der Spek et al. (2007) advice to nourish approximately the volume [m^3/m] of the original bar. The duration of the effect of the nourishment on the bar migration is then approximately the original bar cycle period. A third possible reason why the nourishment had a longer effect on the bar behaviour could be because the location of the nourishment, at the seaward end of the active profile.

The first shoreface nourishment applied in The Netherlands at Terschelling in 1993 was placed at a coast with 3 bars. Here the nourishment was placed in the trough between the outer and middle bar. This sand eroded from the trough and increased the height of the bars. This caused the offshore migration of the middle bar to stagnate until 1999. The original bar return period was approximately 12 years (Grunnet & Ruessink, 2005).

This nourishment applied in Terschelling migrated alongshore, with approximately 400m per year. This was in the same direction as the net sediment transport. Nearshore sandbars migrated alongshore with a velocity of 800m per year. The shoreline did accrete significantly (from 3 m per year retreat to up to 15m per year accretion) in the years after the placement of the nourishment (Grunnet & Ruessink, 2005).

At the Danish Skodbjerge coast, two nourishments were placed in 2010 and 2011, offshore of the outer bar. Rapidly after the implementation of the nourishments the outer bar started

moving towards the shore, followed by offshore migration in the last year of the observation period, 2014 (Lodder & Sørensen, 2015). Hence, the onshore migration or stabilization of the bars was much shorter compared to above described nourishments. However, it is also possible that the offshore migration could completely be ascribed to the 20-year return period storm in December 2013. The inner bar did not show a clear change in migration after the nourishment.

In summary, along the NSR the bar migration is affected by nourishments. Different nourishment gave a different effect on the bar migration. In all cases the offshore migration of the bars was (temporary) reduced or even turned to onshore migration. The duration of the changes in bar migration differed along the various studied nourishments, from roughly 2-3 to at least 6 years.
An area that is suitable to study the post-nourishment bar migration is the coastal stretch between the IJmuiden and Scheveningen harbour moles (km. 60-95). Along this coastal stretch, the bar cycle return period is 4 years. Hence, if the bar system has returned to its natural pattern, this can be concluded quickly. North of the IJmuiden harbour moles, the bar return period is 15 years. Therefore, it takes much more temporal data to analyse if changes in this return period are present. Since the most shoreface nourishments are applied after 2000 and one pre-nourishment bar cycle takes 15 years, it is difficult to determine if the nearshore morphology acts similar as prior to the nourishment. Moreover, within a 15-year period often other nourishments are executed at the same location along the coast, which likely complicates the analysis of the long-term effect of individual nourishments.

3. Methodology

Within this chapter firstly characteristics of the study area are given, followed a description of the dataset and the used method to analyse the nearshore morphology.

3.1 Study area

The studied area consists of the Dutch and Danish North Sea coast, see Figure 9 and Figure 10. The studied coasts are both straight sandy coasts with few (Denmark) or no (Netherlands) inlets. Constructions along both coastlines are described briefly in this chapter. A more thorough description of waves and currents along the Dutch-Danish North Sea can be found in Appendix B.

3.1.1 Netherlands

The study area consists of the coast from Den Helder to Scheveningen. This coastal stretch has a length of 97km. Due to disturbance due to the influence of the Marsdiep inlet in the North, the northernmost 5 kilometres are not analysed. Alongshore distances mentioned in this report are with respect to Den Helder. The coast consists of two coastal areas ('kustvakken'), the Noord-Holland and Rijnland coast, north and south of the IJmuiden moles respectively.

Figure 9: Analysed Dutch coast

Constructions along the coast

There are a few major constructions along the Holland coast, influencing the coastal morphology.

The northernmost analysed section, km. 5 – 31 (from Den Helder) contains groynes. Between km. 20 and 26, a seawall was present until 2015. In 2015, mega-nourishment of 30 million m^3 sand was placed in front of this seawall, creating the Hondbossche dunes. This changed the nearshore morphology and bathymetry. The groynes and seawall have been constructed in the 19th century (Wijnberg, 1995).

At km 55, the IJmuiden harbour moles are located. These harbour moles reach lengths of 2-2.5 km. The harbour moles have also been constructed in the 19th century and extended between 1962 and 1967 (+1 and +1.5 km).

In the southern part of the study area, at km. 86, the Katwijk discharge sluice is located. This construction has been built in 1807. In 1984, the capacity of the discharge sluice has been increased (Wijnberg, 1997).

At the southern border of the study area, at km. 98 a new section of groins starts. Other significant constructions that might influence the morphology in the study area are the Scheveningen harbour moles (500m length) at km. 102, the 'sand engine' 21m^3 mega-nourishment between km. 108 and 110 in 2011 and the Maasvlakte constructed in 1960's,

extended with Maasvlakte 2 between 2008 and 2013. This Maasvlakte (2) is located south of km. 118.

3.1.2 Denmark

The analysed Danish coast reaches from Hanstholm (km. 0) to the border of Midtjylland and Syddanmark km. 156. This analysed coast is with a length of 156 kilometre larger than the 92-kilometre analysed coast in the Netherlands. The southernmost part of this stretch is not analysed, because less measurements have been performed here.

The coast consists of three coastal areas, the Thy area in the north (km. 0-39), followed by Agger (km 39-53) and the Midtjylland coast (km. 53-156).

Constructions along the coast

The northern part of the coast (km. 0-22) is not a straight coast. Constructions and changes in beach orientation exist near Vorupør (km 22) and Klitmøller (km 9). Although on the large scale the beach orientation remains equal, locally the beach makes a sharp bend. Near Vorupør (km 22), there is also a mole structure of over 400m.

Figure 10: Map of Denmark with the analysed coast © Wikimedia Commons, adjusted

There is a 1km wide inlet at km. 50, the Thyborøn Kanal. This inlet was created after a flood breakthrough in 1862. The inlet connects the North Sea with the Limfjord, which is connected to the east-coast of Denmark (Kattegat). There is an approximately 700m long mole structure at the northern side of the Thyborøn inlet. The Thyborøn inlet acts as a sediment sink. To maintain the coastline, groynes have been constructied between 41-63 and 69-79. The first groynes are built in 1875 (Danish Coastal Authority, 2011). In 1909, the groined section was extended.

At km. 91 and 133-134 two discharge sluices are located. The sluices regulate the water level and salinity in the Nissum and Ringkøbing Fjord respectively (Ringkøbing Fjord Turisme, 2018; Thorsminde Havn, 2018). They do not only discharge water, but also let water from sea flow into the lakes.

3.2 Cross-shore depth profiles dataset

3.2.1 Interreg Building with Nature project

This research is executed within the Interreg Building with Nature project. In this European Union project, multiple partners from Belgium, The Netherlands, Germany, Denmark, Scotland and Sweden work together to improve their understanding regarding nature-based flood protection solutions. As a previous part of this project, a dataset has been put together, consisting of cross-shore transect measurements from Belgium, The Netherlands, Germany and Denmark, see Figure 11. With the help of this dataset, coastal morphology can be studied using a shared methodology. The goal of a part of this project is to reveal links between driving parameters and observed nourishment behaviour (Wilmink et al., 2017). For more information about this project, see http://www.northsearegion.eu/building-with-nature/.

3.2.2 Spatial and temporal data resolution and coverage

The majority of the profiles is located in The Netherlands and Denmark. Typical length of the cross-shore profiles is in the order of 700m to 3 km. In the Netherlands, transects are located 250m from each other. This spacing is larger in Denmark, here the distance between transects is mostly between 600 and 1200m. Cross-shore profile data is provided from 1874 until 2017. However, the measurements done before the 1950 do have large temporal intervals. This makes this data less suitable for the analysis of the bar behaviour. More frequently measured data, with an interval between two measurements of at most two years (incidentally 3 years), is available from 1954, see Table 1. In this table all areas and their measurement periods are listed. The numbers in the first column correspond with the locations shown in Figure 11. Please note that these numbers do not correspond with national numbering of the coastal sections, such as the 'Kustvak' numbers in The Netherlands. Measurements with many intervals larger than 3 years are excluded in this table, since they are less suitable for data analysis than the data with a yearly or biannual interval. In case of a large data gap, the resolution might become to coarse to properly analyse the nearshore morphologic behaviour.

The analysed regions in this study are marked bold in Table 1. These regions are selected based on the temporal availability of data and uniformity of the coastline.

Table 1: Data availability, data with a temporal interval larger than 3 years is ignored in this table. The areas that are used in this research are marked bold.

Number	Region name	County	Yearly or biannual data available		Observed temporal intervals [year]
			From	until	
1	Middelkerke	Belgium	2006	2017	1
2	Zeeuws-Vlaanderen	Netherlands	1965	2016	1
3	Walcheren		1967	2016	1
4	Noord-Beveland		1965	2016	1
5	Schouwen		1965	2016	1
6	Goeree		1965	2016	1
7	Voorne		1965	2016	1
8	Delfland		1965	2016	1
9	**Rijnland**		**1965**	**2016**	**1**
10	**Noord-Holland**		**1965**	**2016**	**1**
11	Texel		1965	2016	1
12	Vlieland		1965	2016	1
13	Terschelling		1965	2016	1
14	Ameland		1965	2016	1
15	Schiermonnikoog		1965	2016	1
16	Baltrum	Germany Lower Saxony	1977	2016	1980-2000: 1, other periods 2-3
17	Langeoog		1980	2000	1
18	Sylt	Germany Schleswig-Holstein	1992	2017	1
19	Vadehavsoer	Denmark	1969	2006	1
21	Midtjylland South		1969	1996	1969-1984 mostly 1, 1984-1996 2
20	Holmsland		2005	2014	1
21	**Midtjylland North**		**1965**	**2016**	**1-2**
22	**Agger**		**1954**	**2016**	**1-2, incidentally 3**
23	**Nationalpark-Thy**		**1957**	**1995**	**1-2**
24	VigsoJammerbugten		1969	1978	1
25	Tannis-Bugt		1970	1978	1

Figure 11: Location of cross-shore profiles available in dataset (Map: © OpenStreetMap)

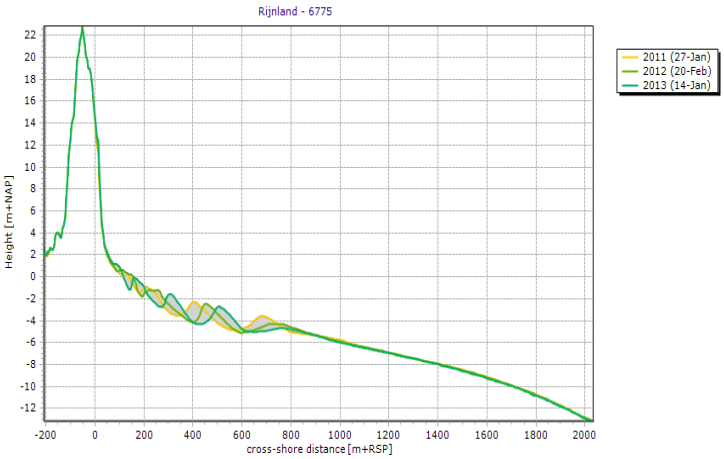

Figure 12: Arbitrary profile in the Rijnland (NL) coastal region, offshore migration of the sandbars is observable

3.2.3 Uncertainties in dataset

The cross-shore profiles contain dry beach measurements as well as underwater bed measurements. Echo sounding from a boat is used to determine the wet profile, while dry beach measurements are obtained by stereo photogrammetry (until 1996) from an airplane and Light Detection and Ranging (LiDAR, from 1996). Ideally, the dry beach profile is measured during ebb and the underwater profile during flood, which results in an overlap of both measurements (De Graaf et al., 2003). However, often measurements are taken several months apart, which complicates combining the 'dry' and 'wet' measurement.

Working with measured data automatically results in uncertainties and measurements errors. Relative errors can be present within one cross-shore profile measurement, whereas systematic errors are constant error for the complete cross-shore profile measurement. Errors in the wet part do mostly result from inaccuracies in the water level and the squat effect; lowered pressure below the moving ship causes the ship to sag further than without movement. To rectify this error of the squat effect, the used ship and skipper (navigation style) should be known. However, for many profile measurements these data are absent. Even if these ship and skipper data are known, it is very difficult to determine the error due to the squat effect. Since 2000 the horizontal position of the ship in the Netherlands is determined with GPS, resulting in higher accuracies (Wiegman et al., 2002).

Inaccuracies of the dry section are mostly formed by the orientation of the measured heights with respect to the reference system. Besides this, both measurement techniques (photogrammetry and LiDAR) are sensitive to (dune) vegetation (De Graaf et al., 2003).

The variable error is neglectable compared with undulations originating from bars in the profile. Since the horizontal migration of bars will be analysed, it is important to realize that a systematic wet error of 0.2m corresponds a horizontal positioning error of 20m in case of a slope of 1:100. Since an extensive (temporal and spatial) dataset is used, it is expected large measurement errors will be outliers compared to neighbouring measurements (in time/space) and will therefore not influence the outcome of the analysis severely. It is however a source of noise in the outcome.

Table 2: Estimates of errors that can be present in the Dutch cross-shore transects

Type of measurement	**Variable error [m]**	**Systematic error [m]**
Wet (before 2000) (Wiegman et al., 2002)	0.09	0.25
Wet (after 2000) (Wiegman et al., 2002)	0.09	0.05
Dry (Veugen, 1984) after (Damsma et al., 2009)	0.06-0.09	0.07

Cross-shore measurement interval

Another factor that influences the accuracy is the measurement interval of the cross-shore profiles. The horizontal grid size is 5m in the Netherlands. Inaccuracies due to linear interpolation can reach up to 0.6 metres at the dune foot (De Graaf et al., 2003). For the underwater bed section, bed profiles are generally smoother and errors due to the interpolation are less significant. The cross-shore resolution of Danish transect measurements is generally less than 10m (beach) to 10-20m (shoreface). However, for old profile measurements, large

cross-shore gaps in transect measurements can be present. In Figure 13 an example of a very coarse profile measurement is shown. The green lines represent measurements for which the measurement interval is short. Measurements with a larger measurement interval are marked with blue dots. An 87m long gap can be observed between 1308m and 1395m. Although this profile is quite an extreme example, smaller gaps from shoreline to ± -2m MSL of 50m are more common.

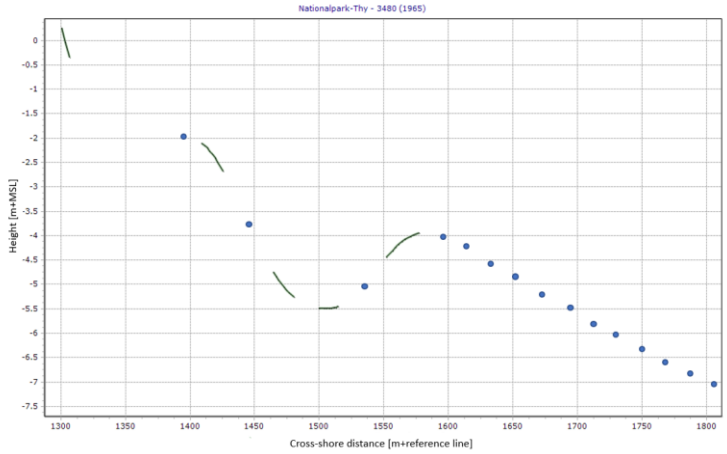

Figure 13: Example of very course cross-shore resolution Denmark.

When such large cross-shore gaps are present, larger errors due to linear interpolation can be expected. Moreover, old transect measurements are performed with undocumented methods with higher measurement inaccuracies than the values mentioned in Table 2.

Seasonality

The transect measurement data is often collected at different times of the year, while seasonality (increased wave activity in winter) does influence the nearshore morphology (Quartel et al., 2008). Since very long time series are analysed, the irregular measurement intervals mainly average out and a trend can be observed. However, this does likely make the resulting year-to-year bar migration less constant.

3.3 Eigenfunction analysis of cross-shore profile data

Eigenfunction analysis can be used to analyse cross-shore depth profiles on bar behaviour. Eigenfunction analysis (also mentioned as empirical orthogonal function (EOF) analysis), is a decomposition of a dataset in orthogonal basis functions. These eigenfunctions are determined by exploiting the properties of matrices to the dataset, so that dominant patterns of variation in the dataset can be identified (Miller & Dean, 2007). The following equation is solved:

$$[\boldsymbol{U}] \cdot [\boldsymbol{E}] = \lambda_k \cdot [\boldsymbol{E}] \tag{3}$$

In which

$[\boldsymbol{U}]$ = Product matrix: Matrix multiplication of the original data with its transpose
$[\boldsymbol{E}]$ = Matrix containing eigenvectors
λ_k= Vector containing eigenvalues corresponding to eigenvectors

Equation (4) states that a dot product of the (adjusted) original data matrix with a matrix containing eigenvectors equals a vector containing eigenvalues multiplied with the eigenvector matrix. Linear algebra is used to determine for which eigenvectors and which eigenvalues equation (4) is true, see Appendix A. The matrix $[\boldsymbol{E}]$ contains (after scaling) the patterns/shapes of variation, corresponding to their eigenvalue λ_k. The latter provides information about variance from the reference datum that can be explained with this eigenfunction (shape/pattern of variation). In this report, the total variance is not the deviation from the mean profile, but the sum of variance from the reference datum (+1 m NAP or MSL line for the Dutch and Danish coast respectively). This is equal to the sums of squares.

With these dominant patterns of variation, the original dataset can be reconstructed using equation (4) (Winant et al., 1975). By examining the first most dominant 'x' eigenfunctions, underlying patterns in noisy datasets can be identified. By using a limited amount of eigenfunctions often a majority of the total variance in a dataset can be explained, e.g. Wijnberg and Terwindt (1995).

$$h(y,p) = \sum_{k=1}^{m} w_k(p) \cdot e_k(y) \tag{4}$$

In equation (4), e is the unscaled eigenfunction and y is the cross-shore position. P is the profile observation, and w is the weighting. The latter can be calculated by solving Equation (3) with the minor product matrix $[\boldsymbol{U}] = [\boldsymbol{D}]^T \cdot [\boldsymbol{D}]$ instead of the major product matrix $[\boldsymbol{U}] = [\boldsymbol{D}] \cdot [\boldsymbol{D}]^T$. By multiplying all m eigenfunctions with their corresponding weightings, the original dataset can be reconstructed. See Appendix A for an elaboration and a calculation example.

The eigenfunctions are ordered in a way that they explain most of the variance in the dataset (i.e. cross-shore profiles) over time and/or space. Eigenfunctions are determined mathematically and do therefore not have a direct inherent physical significance. However, with additional information of physical processes, a physical interpretation can be given (Miller & Dean, 2007).

3.3.1 Interpreting eigenfunction analysis

The outcome of the eigenfunction analysis is a combination of dominant signals or patterns of variation (the eigenfunctions themselves) and their temporal component (the weightings). These weightings provide information about with which magnitude the corresponding eigenfunction loading can reduce most of the variance for a given measurement. In other words, the weightings provide information on how (with which scalar multiplication) the profile measurement can be represented best with the corresponding eigenfunction shape.

In case of eigenfunction analysis of cross-shore depth profiles, the eigenfunction loadings contain dominant patterns of variation of the nearshore morphology, see Figure 14a. These eigenfunction loadings show different amplitudes at different cross-shore positions. The weightings shown in Figure 14b, show the magnitude of the corresponding eigenfunction loading for a given measurement. In other words, the weightings of an individual measurement on the first three eigenfunctions, describe the morphology of this measurement in terms of these three eigenfunctions (Wijnberg, 1995). Based on the eigenfunction loadings and weightings, the nearshore morphologic behaviour can be studied. A physical interpretation of the eigenfunction loadings and the corresponding weightings is given in Figure 16.

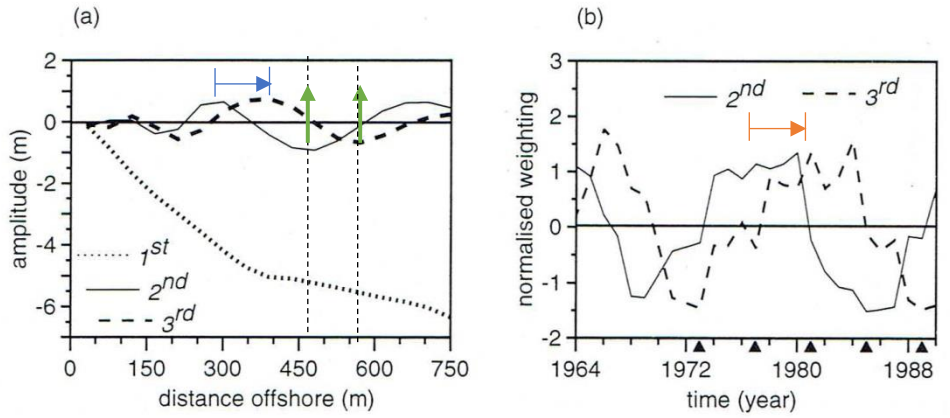

Figure 14: Example of eigenfunction loadings (a) and the corresponding weightings (b) (Wijnberg, 1995).

Typical cross-shore profiles for the Holland coast are given in Figure 15. The first eigenfunction, which explains most of the variance from the reference datum in the dataset, strongly resembles the time-averaged profile shape, see also Figure 14a. Although not exactly the same, in this report, with mean profile shape the shape of the first eigenfunction is meant. The first eigenfunction is the shape that (with changes in its weighting) can explain most of the variance (sums of squares) from the reference datum in the dataset.

The choice to name the first eigenfunction the mean profile is consistent with earlier eigenfunction studies of the nearshore morphology (Miller & Dean, 2007; Wijnberg, 1995; Winant et al., 1975). It is chosen to study the steepness with the weightings of the first eigenfunction since this allows to study a cross-shore change in average steepness over time. Moreover, analysing the steepness with the first eigenfunction is consistent with analysis of the bar behaviour with higher order eigenfunctions.

The weighting of the first eigenfunction gives information on the steepness of the profile. A lower weighting indicates that the observed profile is flatter than the average, while a higher weighting represents a steeper profile.

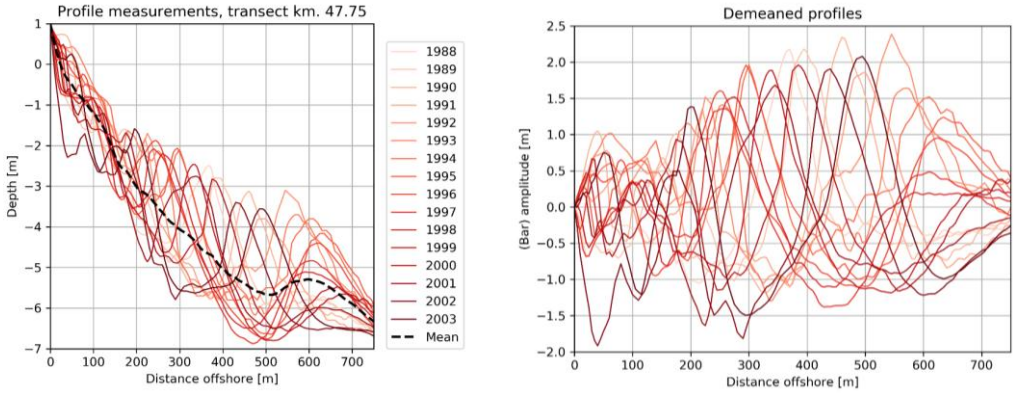

Figure 15:Left: transect measurement data. Right: Bar signal obtained with demeaned profiles. Please note that a demeaned dataset is not the same as a dataset of which the first eigenfunction signal is removed.

The residual variance is all data that cannot be described by the (changes in amplitude of the) shape of the first eigenfunction. In case of a barred coast with migrating sandbars, most of the residual variance which cannot be explained by this first eigenfunction shape is mainly originating from the migrating sandbars, see Figure 15. The residual (bar) signal will be represented in the second and third empirical eigenfunction. These eigenfunctions will have a similar shape as the bars in the profile measurements, see Figure 14a.

Based on the weightings of the second and third eigenfunction the position of bars in the profile can be deduced. A positive weighting on the second eigenfunction means that the topography or bar signal of the second eigenfunction corresponds well with the profile measurement. A negative weighting means that a mirror image of the eigenfunction loading corresponds well with the profile measurement. The second eigenfunction signal should be superimposed with the signal of the first eigenfunction to describe the morphology of this measurement. This also applies to the third eigenfunction, which also generally accounts for bars in the profile.

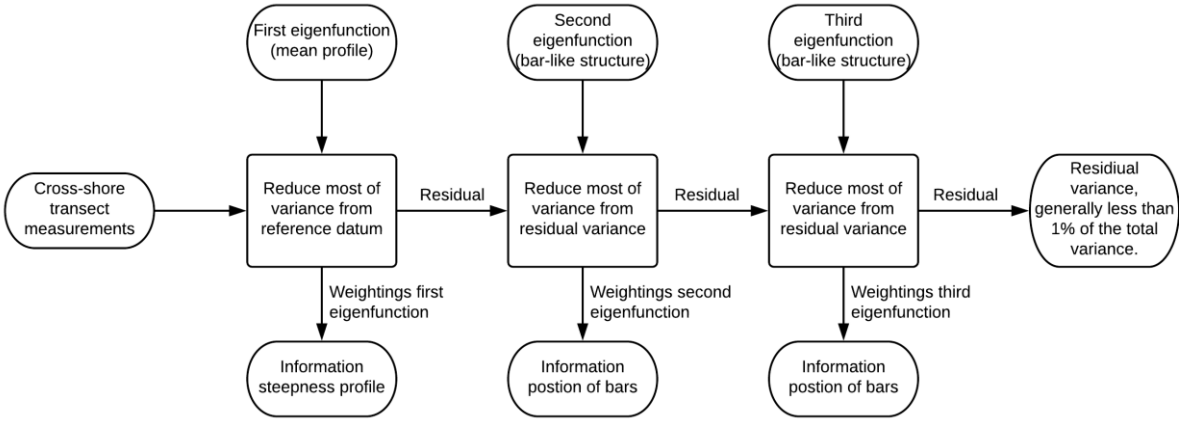

Figure 16: An interpretation of an eigenfunction analysis of the nearshore morphology in case of migrating sandbars

Two eigenfunctions are needed to explain migrating bars, since the second and third eigenfunction can only explain undulations from the mean profile at certain cross-shore positions. The second eigenfunction in Figure 14a can for example not explain/reduce variance at 225, 350 and 575m offshore since is amplitude here is equal to zero. The residual variance mainly originates from the cross-shore location where the second eigenfunction cannot reduce the variance. In order to be able to explain bars at all cross-shore positions, a subsequent eigenfunction is needed to explain the variance at locations where the second eigenfunction amplitude is equal or close to zero. As a consequence of this, the third eigenfunction will have a 90 degrees phase difference with the second eigenfunction.

By evaluating the shapes of eigenfunctions and how their weightings change over time/space, bar processes in the cross-shore profiles can be identified in a consistent and structured way (for example (Miller & Dean, 2007; Wijnberg, 1995)). These bar processes can be disturbed by other processes/noise and may therefore not be directly observable by visual inspection. Eigenfunction analysis is a powerful data analysis technique which enables to 'isolate' this bar signal from other processes.

3.3.2 Bar migration

Based on the weightings and shapes of the second and third eigenfunction, the cross-shore bar migration can be deduced. When the third eigenfunction loading lags 90 degrees behind the second eigenfunction, the top and crests of the third eigenfunction are located seaward from the top and crest of the second eigenfunction, see the purple arrow in Figure 14a. When the third eigenfunction becomes dominant (high weightings, orange arrow Figure 14b) after a period with dominance of the second eigenfunction, bar crest and troughs have moved seaward (blue arrow Figure 14a). Hence, if the temporal density of the measurements is high enough (no aliasing), it can be concluded that bars have moved seaward. The bar profile going from a positively weighted second eigenfunction to a positively weighted third eigenfunction is shown in the top two graphs of Figure 17.

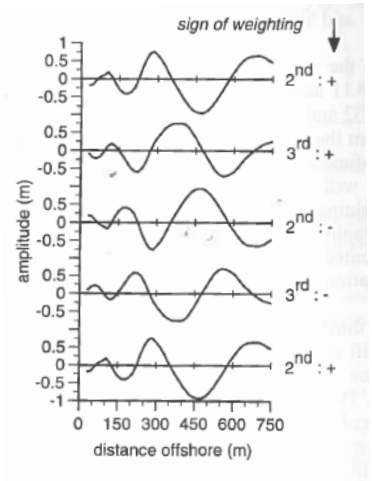

Figure 17: Visualisation of offshore moving bar based on successive dominant eigenfunctions (Wijnberg, 1995)

When bars move further seaward, for example with crest around 460m offshore in Figure 14a, also the third eigenfunction does not correspond anymore with the location of the bars. The bar position now compares well with a mirror image of the second eigenfunction (see left green arrow Figure 14a). Hence, a negative weighting of the second eigenfunction becomes dominant after a period with a high weightings of the third eigenfunction, see Figure 14b year 1985. When bars move even further offshore, with a crest around 600m offshore, a negative weighting of the third eigenfunction compares best with the shape of bars, see Figure 14b year 1989. When bars move further offshore, bars reach the position of the positive second eigenfunction again. At this point, one complete bar has cycle has passed through, i.e. one bar has vanished in the point of decay and a new bar has been created close to the shore.

In this example (Figure 14), loadings are in a 90 degrees phases shift and the lagging eigenfunction weightings constantly follow the leading eigenfunction weightings as well. This eigenfunction pattern can be related to offshore bar migration. When the migration of bars is onshore directed instead of offshore, the above mentioned cycle is gone through in reverse. See also Table 3 for all possible eigenfunction combinations which could be deduced to on- and offshore bar migration. It is also possible that the position of bars is changing but that bars do not go through a complete bar cycle, i.e. onshore and offshore bar migration alternate. This is be observable from the order of successive dominant eigenfunctions.

Table 3: Bar migration based on the shapes and weightings of the eigenfunctions

Second eigenfunction loading	**Third eigenfunction loading**	**Second eigenfunction weighting**	**Third eigenfunction weighting**	**Type of migration**
Leading	Lag 90 degrees	Leading	Following	Offshore
Leading	Lag 90 degrees	Following	Leading	Onshore
Lag 90 degrees	Leading	Leading	Following	Onshore
Lag 90 degrees	Leading	Following	Leading	Offshore

To visually interpret the eigenfunction results, the signal in the eigenfunctions can be reconstructed based on the eigenfunction weighting and loadings, see Equation (4). This is especially helpful to validate and visualize the bar migration in the second and third eigenfunction. Moreover, by reconstructing the bar signal over alongshore large coastal section, the alongshore coherence in the bar migration can be evaluated. Hereby it is assumed that the coastline forms a linear line. An example of such a reconstruction is given in Figure 18.

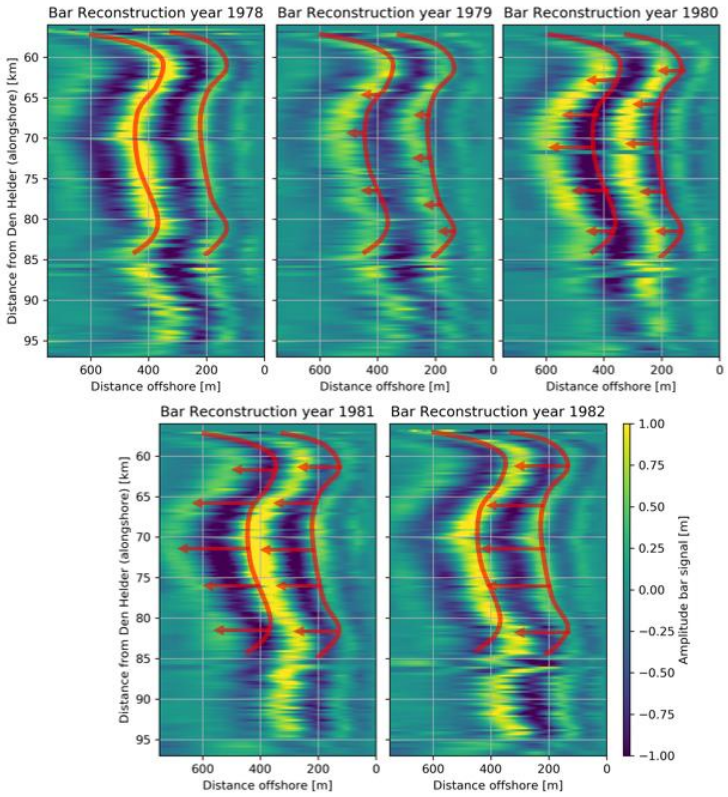

Figure 18: Bar reconstruction km 56-97 between 1978-1982

3.3.3 Analysing eigenfunction results

For areas where a clear rhythmic and constant pattern of migrating bars is observed from the eigenfunctions, results of the eigenfunction analysis are examined to determine the migration direction, bar cycle return period, the bar length and the average bar migration velocity.

Migration direction

To analyse how the bars are migrating (onshore/offshore) based on the order of successive dominant eigenfunction weightings (Table 3), it must first be examined how the second and third eigenfunction weightings are temporally related to each other. This is done by determining the cross-correlation of the second and third eigenfunction weightings (per transect). The cross-correlation is a measure of similarity between two signals, given a certain time difference (lag) between these two signals. Based on the time-lag where the cross-correlation between both eigenfunctions reaches its maximum value, the order of successive dominant eigenfunction weightings is determined.

In case of missing data, the eigenfunctions weightings are interpolated linearly, this is only done if at maximum 6 years of data are missing (in total) in the data. If more data is missing, the cross-correlation is not determined.

Bar cycle return period

The bar cycle return period is obtained by determining the autocorrelation of the eigenfunction weightings. Autocorrelation is a measure of similarity in a signal with a lagged copy of itself. If one bar cycle return period has completed, bars are in a same state as before the bar migration process. Consequently, eigenfunction weightings have similar values before and after a bar cycle. The autocorrelation for a time lag of the bar cycle return period should therefore be high. The time lag where the autocorrelation is the highest represents the bar cycle return period the best.

Bar spacing

To characterise the nearshore morphology the bar spacing and migration velocity of the nearshore sandbars are evaluated. Because the nearshore sandbars have different sizes (The inner bar is generally smaller than the outer bar) and different migration velocities (inner < outer), the results of eigenfunction analysis are used to obtain cross-shore averaged values of these cross-shore processes.

The bar spacing is in this report defined as the (cross-shore, horizontal) wave length of the bar trough and bar crest, see Figure 19.

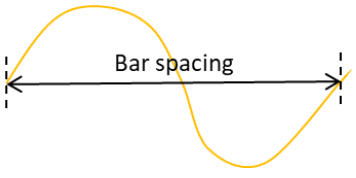

Figure 19: Schematisation of bar spacing.

Since the second and third eigenfunction are approximately 90 degrees apart from each other (see 3.3.1 Interpreting eigenfunction analysis), an estimation of a cross-shore average bar spacing can be calculated with the cross-correlation of the second and third eigenfunction. From the cross-correlation calculation, the lag [m] of the third eigenfunction loading with respect to the second eigenfunction loading can be found, which corresponds with 90 degrees or 1/4th bar. This

length of the 90 degrees or 1/4th bar can be extrapolated to 360 degrees or a full bar wave. However, this can only be done for areas for which the eigenfunctions clearly show a 90 degrees lag. Moreover, eigenfunctions must have a similar shape. To objectively assess the similarity in shape, also the cross-correlation significance is calculated.

Average bar migration velocity

Based on the bar spacing and the bar cycle return period, the migration velocity can be determined for every transect with significant auto- and cross-correlations (i.e. bar cycle return periods and bar spacing) according to equation (5) .

$$C = \frac{\lambda}{T_r} \tag{5}$$

In which:

C Migration speed in [m/year]
λ Bar spacing [m]
T_r Bar cycle return period [year]

It is important to realize that these are rather estimates of the average cross-shore migration velocity. The outcome of equation (5) is one absolute number, however likely year-to-year variations can be observed in the migration velocity.

3.3.4 Data-processing

To perform a proper eigenfunction analysis of the nearshore morphology, all transect measurements should be in a suitable format, ordered correctly, and have an equal spacing and length. Besides this, they also should have the same floating reference line to analyse the same section of the shoreface. The available transects do not have these characteristics yet. Hence, the data should be pre-processed to make them suitable for eigenfunction analysis.

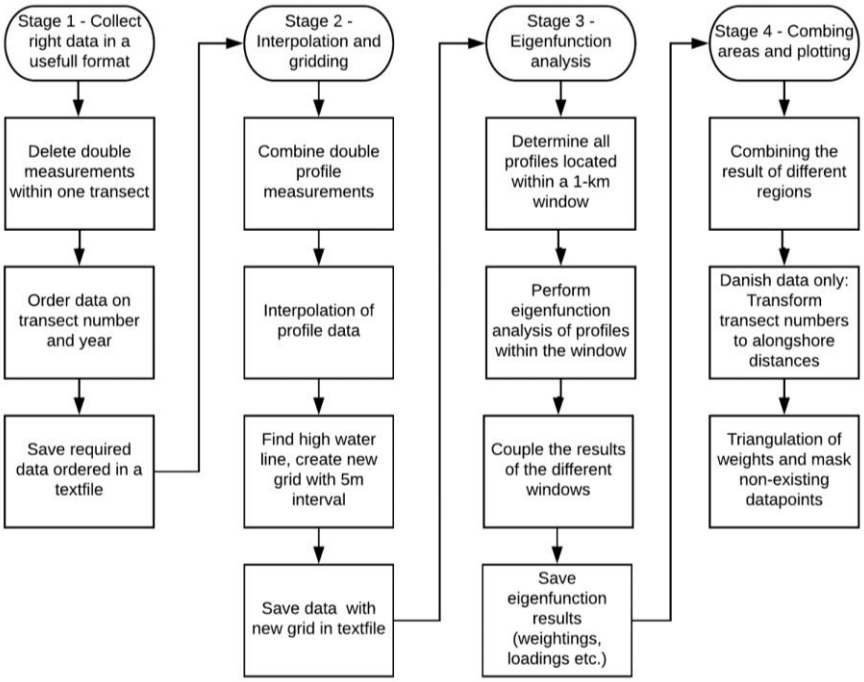

Figure 20: Overview of data-processing

Processing the original transect measurements to useful eigenfunction analysis results is done in four stages, see Figure 20.

Stage 1
This stage contains the extraction of the right data in a useful format and ordering of the data. Here partially a MATLAB file was used, constructed by Naus (2018). Coastal measurements often contain a 'dry' beach measurement during low-tide and a 'wet' measurement during high-tide. As a consequence, a part of the measurements overlaps. In this research, interpolated values of these measurements around the MSL are used, while the separate 'dry' and 'wet' measurement values are ignored. More information this first stage can be found in Appendix C.

Stage 2
In this stage the ordered data is pre-processed so it becomes suitable for eigenfunction analysis. This stage contains the treatment of the double transect measurements as well as the interpolation and gridding of the data. The treatment of double transect measurements is explained in Appendix C. The use of a floating reference line and used grid is explained in the section below.

Floating reference line
To perform an eigenfunction analysis, all profiles within one analysis must have an equal length and grid/interval. In addition, to analyse the shape of the beach profile, the profiles should have the same starting point. This starting point is approximately the high water line (+1m NAP line) for the Holland coast. NAP (Normaal Amsterdams Peil or Amsterdam Ordnance Datum) is the most common vertical datum in the Netherlands. The +1m NAP line was used since it is relatively constant in time. Other refence lines like the mean sea level are more variable, since a swash bar can influence this position significantly. Moreover, this reference line is consistent with the method of Wijnberg and Terwindt (1995), improving the comparability of the results.

For the Danish coast the mean sea level (MSL) was used as reference line. This starting point is different for the Danish coast compared to the Dutch coast because too many profiles did not reach higher than 0.5m above mean sea level. Although swash-bar are generally not present along large parts of the analysed Danish west coast, the year-to-year variability in the used contour line is higher, see Appendix D. Using a different contour line slightly complicates a direct and equal comparison between both countries. For example, no direct comparison between the depth at 750m from the Danish (MSL) and 750m from the Holland (+1m NAP) can be made.

If there are multiple crossings with the contour line within one profile, the most landward profile is chosen as starting point since this most landward crossing is more constant over time. Some profiles include the inner side of the dune in their profile, where also crossings with the +1m or MSL line can be observed. To cover this problem, the starting point is defined as the most landward crossing of the contour line, where the profile seawards of this crossing does not reach higher than one metre above the height the contour line.

Interpolation of profile data

Since the data only contains a measurement every ‘x’ metres cross-shore, the exact position of this +1 or mean sea level contour is not yet determined. Besides this, all measurements handled in the eigenfunction analysis should have the same grid with respect to this contour line. To obtain this, data is interpolated using linear interpolation. Linear interpolation is used since other types of interpolation, like cubic spline interpolation, resulted in erroneous interpolations due the sometimes strongly irregular measurement interval. This was especially the case for the Danish data, where successive intervals can change from 0.2m to almost 10m. See Appendix C for an elaboration on how these errors can occur.

Defining new grid

With the interpolated data the starting point of the transect is defined. From this floating reference starting point, every 5 metres offshore a point (depth value) is extracted from the interpolated values until 750m offshore, see Figure 21. The x-axis at the starting point is set equal to zero. This is the new grid which is constant for all transects.

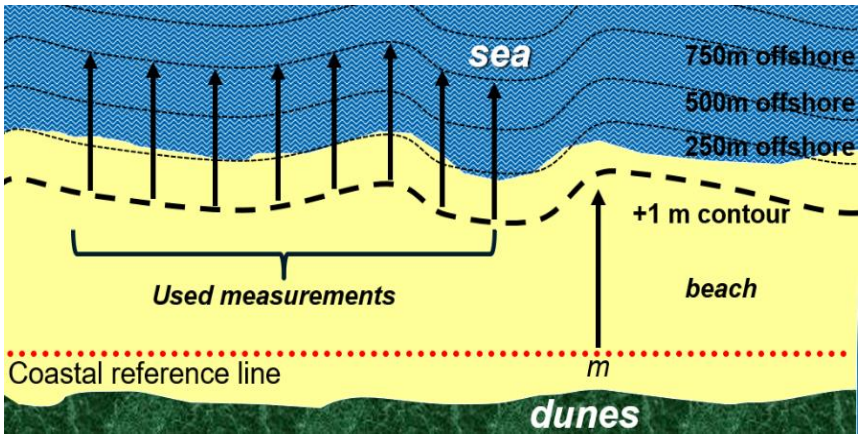

Figure 21: Schematisation of floating reference line and the analysed transects. Please note that this floating reference line is depending on the +1m contour and therefore (slightly) different every year. Source figure: Wijnberg lecture slides, figure is adjusted.

Not all transects can be used in the analysis. When profile measurements do not reach far enough offshore or do not reach near the contour line, profiles are not used. When profile measurements are just too short or when the measurements almost reach the contour line, the missing data is filled according to Figure 22. For further elaboration on the handling of incomplete data, see Appendix C.

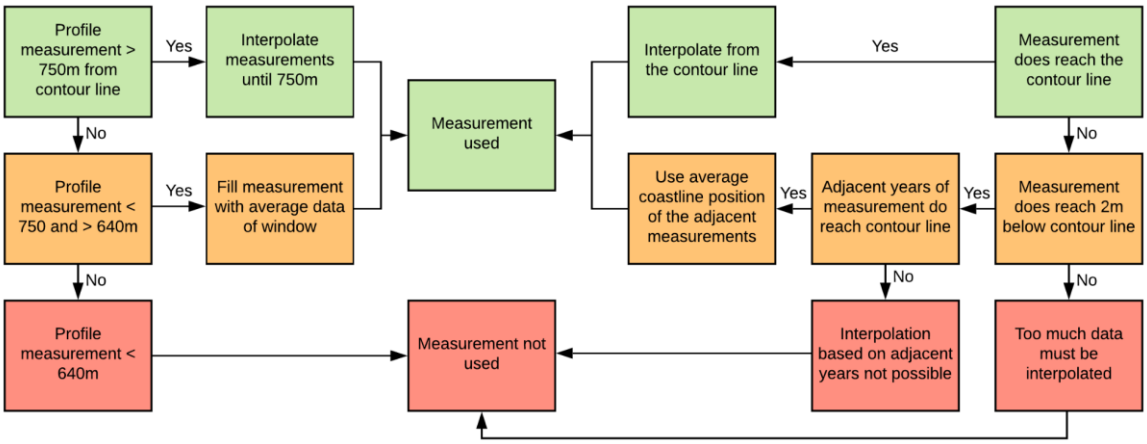

Figure 22: Handling of incomplete data

Stage 3

With the interpolated data and a defined grid the data is ready for the eigenfunction analysis.

Moving window

Since the coast varies significantly along the coast, it is not useful to determine eigenfunction of the whole coast (with various bar systems). Most of the variance in the dataset will then be originating from differences in the (average) transects alongshore instead of the different location of the sandbars. Instead of using a whole coastal section, the coast can better be analysed in alongshore similar sections. In this way, the eigenfunction loadings originate from temporal variability of the profiles instead of alongshore variability. To do so, the coast is divided into small subsets of the coast of 1 km (NL) or 1200-2400m (DE).

If bar changes happen on an alongshore within one window, the lack of alongshore coherence in profiles will show up in the results of the eigenfunction analysis. The alongshore spacing in the Netherlands is usually 250m, so each 'window' of 1km contained 5 locations. Every adjacent window has one cross-shore profile overlap. The alongshore spacing in Denmark varies roughly between 600 and 1200m. Here every alongshore window contains only two profiles, with one cross-shore overlap.

Eigenfunction calculation

Within one window, all transect measurements are put together. Next, eigenfunction analysis of this data is performed with a singular value decomposition (singular value= square root of eigenvalue) command in Python (command: numpy.linalg.svd). Output of this command are eigenvectors/eigenfunctions, their singular values and the weightings. See Appendix A on how these eigenfunctions and eigenvalues can be determined manually with a calculation example. See appendix C for information about scaling of the eigenvectors.

Coupling the windows

The eigenfunctions and their weightings are determined for every window. However, eigenfunctions are derived mathematically and their orientation with respect to the horizontal axis (and their resulting weightings) is arbitrary. This means that an eigenfunction can be,

based on almost equal data, a mirror of the original eigenfunction. This makes interpretation of the results difficult.

Besides this, the variance explained by the second and third eigenfunction can be similar. Because of this, the shape of the second eigenfunction and the third eigenfunction can switch along the different windows. However, to properly analyse the shapes based on eigenfunction weightings and loadings, this shifting of the second and third eigenfunction is undesired. Constant shapes are useful to interpret the data over a long coastal stretch.

To overcome these difficulties, the alongshore windows are coupled based on the overlapping profile. By evaluating the similarity between the weightings of the overlapping profile, it is examined if the eigenfunction in the next window did change in sign and/or order. This similarity is based on the sum of the absolute difference in eigenfunction weightings assigned to the profile in both windows. Also, the difference in case of a sign and/or order switch is calculated. For example, when the absolute difference between the positive second eigenfunction weighting in window one and the negative second eigenfunction weighting in window two is very low, it is concluded that there is a switch in sign between both profiles, see Figure 23. By assessing which combination (bar/sign switch or not) results in the lowest absolute difference, it is determined whether a switch happened between the windows or not.

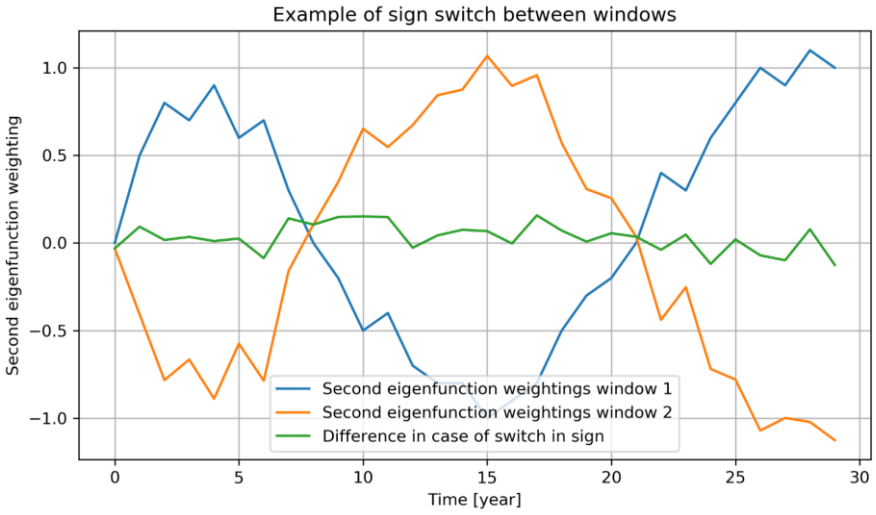

Figure 23: Bar sign switch based on eigenfunction weightings of overlapping profile

If a bar/sign switch happens this is corrected, by simply multiplying the weightings and loadings by -1 or by changing the order of loadings and weightings. In this way, the sign and eigenfunction order are assigned based on correspondence with weightings in the previous window. As a consequence of this approach, the shapes of the eigenfunctions are often consistent alongshore. This does also mean that the second eigenfunction does not always explain more variance than the third eigenfunction, see also Appendix E.

Stage 4

In the last stage, all coastal areas are combined and plotted. The transect numbers of the Danish coast are rescaled to a km. -based scale. Plotting of the eigenfunction weightings is done with the help of Delauney triangulation, which results in a smoother representation of the results, see also appendix C.

4. Results: Pre-nourishment morphologic behaviour

The chapter contains the findings from of the eigenfunction analysis. Eigenfunction results in the chapter only elaborate on data prior to nourishments to specify the pre-nourishment nearshore morphology. There is elaborated on post-nourishment bar behaviour in Chapter 5. In this chapter the first research question will be answered:

1. ***What regions with similar nearshore morphologic behaviour can be characterized along the Dutch and Danish North Sea coast?***

The main interests are:

1. The development of the coastline. Herein the horizontal movement of the coastline is analysed.
2. The loadings of the first eigenfunction, which strongly resemble the average profile.
3. The weightings of the first eigenfunction, which provides information about (changes in) the steepness of the profile.
4. The second and third eigenfunction loadings, which are dominant patterns of variation that explain most of the variance apart from variations in the first eigenfunction. These generally contain the nearshore sandbars.
5. The weightings of the second and third eigenfunction. These give information about changes in bar position. From the combination of the weightings and the loadings, the bar migration can be deduced. Moreover, the bar signal can be reconstructed and the alongshore coherence and migration of the bars can be assessed. Also, based on the eigenfunction loadings and the weightings, cross-shore migration velocities can be calculated.

Firstly, results of the Holland coast are given in Section 4.1. In Section 4.2, results of the Danish coast are given.

4.1 Netherlands

The Dutch coast in analysed from Den Helder (zero on y-axis) southwards, see Figure 9. See 3.1 *Study area* for constructions along this coastline and Appendix B for wave characteristics, (nearshore) currents and tides along this coast.

4.1.1 Development of the coastline

Figure 24 shows the development of the 1m +NAP contour line of the Holland coast with respect to the period the average position in 1989-1991. This reference is used since the in 1990 the 'Basic Coastline' was determined. The task of the Dutch government is to maintain the coastline at the defined positions as defined in the Basic Coastline. The effect of outlying observations (due to storms/measurement errors) in the reference period is minimized by also including 1989 and 1991. The following observations are done based on Figure 24:

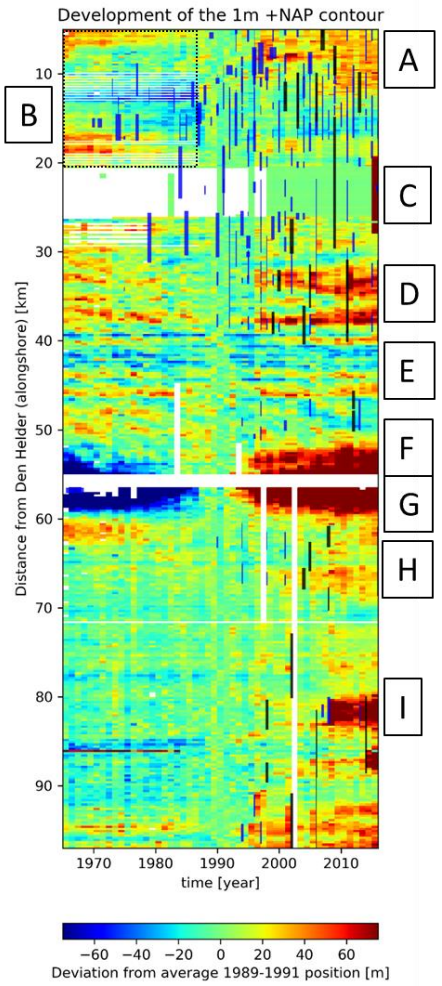

Figure 24:Position of the 1m + NAP contour Black and blue lines represent shoreface- and beach nourishments respectively. Positive values are defined offshore from the reference.

A. Between km. 5 and 15 the shoreline moved offshore up to 60m from 1990. This area is very frequently nourished, as well with beach- as with shoreface nourishments. Km. 15-20 is also nourished frequently. However, in this area no or less progradation of the coast is observed.

B. In section km. 5-20 retreat of the shoreline is visible until roughly 1986, see the dashed box at location B.

C. A mega-nourishment in 2015 in front of the Petten sea dike (km. 20 – 26) changed the nearshore morphology and the position of the +1m NAP contour drastically. The dike was reinforced with 30 million m^3 sand and was renamed as the 'Hondsbossche Dunes'. The shoreline moved seaward after years of stable position due to the sea dike.

D. The region between the former Petten sea dike and IJmuiden (km. 26-55) contains both areas with shoreline retreat and progradation. Between km. 26 and 40 many shoreface- and beach nourishments are applied, especially from 1990. Until 1990, the shoreline retreated, while from 1990 areas with (severe) progradation of the coast is observed, especially at location D.

E. Between km. 40 and 50, nourishment have been applied less. Besides the development close to the IJmuiden harbour moles, the coastline generally stable and sometimes slightly eroding, see location E.

F. The most distinct development in Figure 24 is the progradation of the beach at both sides of the IJmuiden harbour moles. North of the IJmuiden moles, location F, the beach progradation in the period 1965-2016 was just over 200m. Figure 24 shows the development in a range from -75m to +75m, because this corresponds more with the scale of the coastline development at all other locations.

G. At the south side of the moles, the seaward movement of the 1m +NAP contour was significantly larger compared to the north side; 899m since the first measurement in 1965.

H. The area south of IJmuiden (km 60-70) shows local retreat (km 60-63) of the shoreline roughly until 1990. Between km. 63-70 the coast seems stable. From 1990, several shoreface and beach nourishments are applied. In the area where these nourishments are applied coastal progradation can be observed.

I. Between km. 70-97 the coastline is moving seawards gradually, the most offshore positions observed of the contour line are observed in the last 10 years of measurement. After the application of several nourishments seaward movement of the coastline can be observed.

Overall coastal erosion can be observed along the North-Holland coast (km. 5-50) prior to the frequent application of nourishments. South of the IJmuiden harbour moles the coastline is generally stable. The IJmuiden harbour moles stop the northward alongshore sediment current (Van Rijn, 1997), decreasing the supply of sediments north of the harbour moles and causing strong local accretion of the coast close to the moles. Due to the frequent beach and shoreface nourishments the retreat of the coastline has largely stopped.

4.1.2 First eigenfunction, mean profile

In Figure 25 the scaled first eigenfunction, which strongly resembles the mean profile, of the Holland coast in the period 1965-2016 is given.

The influence of large construction works, e.g. Hondsbossche Zeewering (Location A), IJmuiden harbour (Location B) and the Katwijk discharge sluice (C), are visible. Besides these construction works, the average profile is does not change significantly on small alongshore distances. In the north the profile is generally steeper than in the south. This corresponds with results of Naus (2018). He shows that these differences in steepness along this coastal section are primarily present below -2m + MSL.

Around km. 10 to 25 there is an increment visible in the mean profile at 300-600m from the shoreline, just left and north of Location A. This means that bars do show up in the average profile. This indicates that there is generally a bar present at this location. This is in correspondence with other studies, that show a stable bar along km. 10-26, e.g. (de Sonneville & Van der Spek, 2012; Wijnberg, 1995). The bar increment is especially large at the Hondsbossche Zeewering (km. 20-26). A relatively deep trough forms landward of the bar crest. Around 200m from the shoreline, the depth in front of the first eigenfunction reaches -6m below NAP. This is -3m NAP at the boundaries of the coastal defence.

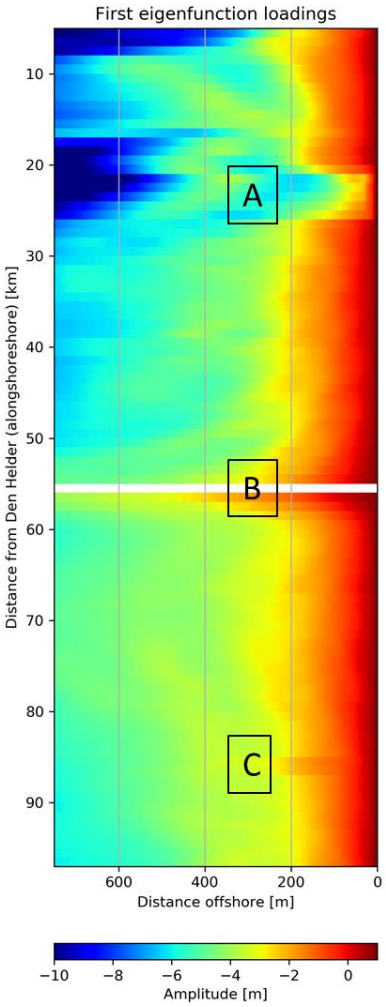

Figure 25: First eigenfunction loadings for the Holland coast

Also around km. 75 a bar shows up in the first eigenfunction profile, see Figure 26. Hence, on average there is a bar present at 500m from the contour line. This bar is also present at km. 80, but at this location rather at 400m from the shoreline. A bar in the first eigenfunction along km. 70-80 is not in correspondence with eigenfunction results of Wijnberg (1995). It is likely that nourishments affected the position of bars, so that bars do show up in the time-averaged profile (first eigenfunction) in the period 1965-2016, but not until in the average profile until 1990. This is investigated more thoroughly with the second and third eigenfunction in section 4.1.4 and 4.1.5.

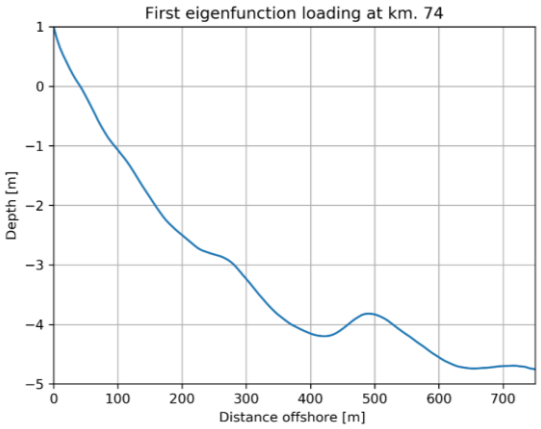

Figure 26: First eigenfunction at km. 74. A bar is visible in the average profile

At most other locations no bars show up in the first eigenfunction. This indicates bars are constantly at different locations and do not have an average position. This benefits the interpretability of the outcome of the eigenfunction analysis since the bar behaviour is then likely captured in the second and third eigenfunction.

The average depth at 750m from the shoreline ranges between almost 12m at the Hondsbossche Zeewering until just over 4m close to the IJmuiden harbour moles.

4.1.3 Development of first eigenfunction weightings

In Figure 27 the weightings of the first eigenfunction for the Holland coast are given. The black vertical lines show shoreface nourishments. The thickness represents the volume of the nourishments in m^3/m, ranging from 100 to 630 m^3/m. Missing data is highlighted green.

Excluding the post-nourishment measurements (which are assessed in Chapter 5), several trends can be observed in the eigenfunction weightings, see Figure 27.

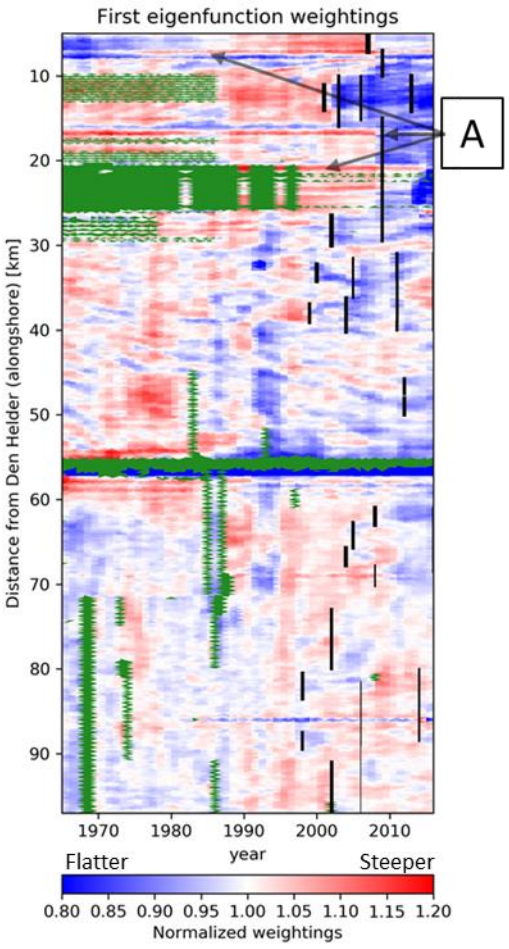

Figure 27: Weightings of the first eigenfunction for the Holland coast

- Between km. 5 and 7, there is severe steepening of the profile. In 1965-1970 weightings ranging as low as 0.85 (relatively flat) are observed. Prior to the nourishment weightings up to 1.12 (steep) are observed in 2006.
- South of this area, between km 7 and 30, the first eigenfunction weightings do not show a clear trend as between km. 5 and 7. Horizontal lines do show up in the eigenfunction weightings, which indicates that the alongshore uniformity of profiles in a window is low (see A). This is often due to the constructions as groynes or the 'Hondsbossche zeewering' coastal defence. These constructions cause a constant difference between the profiles within a window, resulting in constant different eigenfunction weightings.
- Between km 30 and 50, no clear trend in steepness of the profiles is found. The first eigenfunction oscillates around one but is not in an increasing or decreasing trend. From 1990 severe flattening of the profile is observed along this complete section. The profiles return to their average steepness values in the year 1994. It could be that storm events and dune erosion caused an extra supply of sediment to the shoreface, resulting in flattening of the profiles. In 1990 severe dune erosion occurred after a series of storms (Waterloopkundig Laboratorium, 1992). However, the drop in first eigenfunction weightings is primarily observed from 1991 to 1992, see Figure 28.
- South of IJmuiden, between km. 60 and 97 the first eigenfunction weighting increases over time. Between 1967 and 1997 the average weightings increase from 0.96 to 1.00.

The overall increase between 1967 and 1997 in first eigenfunction is small with respect to the fluctuations in average weightings, see also Figure 28. Just as in km. 30 – 50, a decrease of the first eigenfunctions is observed from 1991.

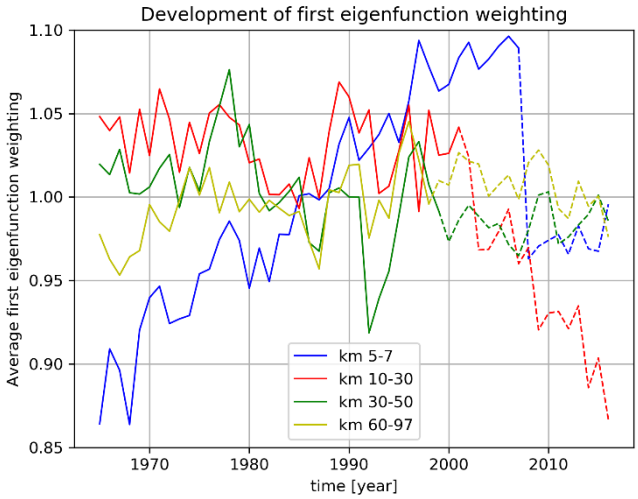

Figure 28:Development of first eigenfunction, dashed lines indicate post-nourishment data

4.1.4 Second and third eigenfunction loadings

For the Holland coast, the second and third eigenfunction generally represent bars in the profile. Please note that weightings corresponding to the eigenfunction loadings can as well be positive as negative. This means that a crest in an eigenfunction loading can also represent a trough, namely in case of a negative weighting.

The eigenfunction loadings of the Holland coast are given in Figure 29. Based on visual inspection of this figure, the coast is divided into the following areas with similar eigenfunctions:

- Area A: Km 5 - 20. In this section, a bar shape shows up in the first eigenfunction. Therefore, the second and third eigenfunction at the cross-shore location of the bar do describe variations in the relative height and position of this bar. The loadings of the eigenfunctions are not consistent alongshore, although they do show similarities. In the first 200m from the shoreline, no significant amplitudes of the second and third

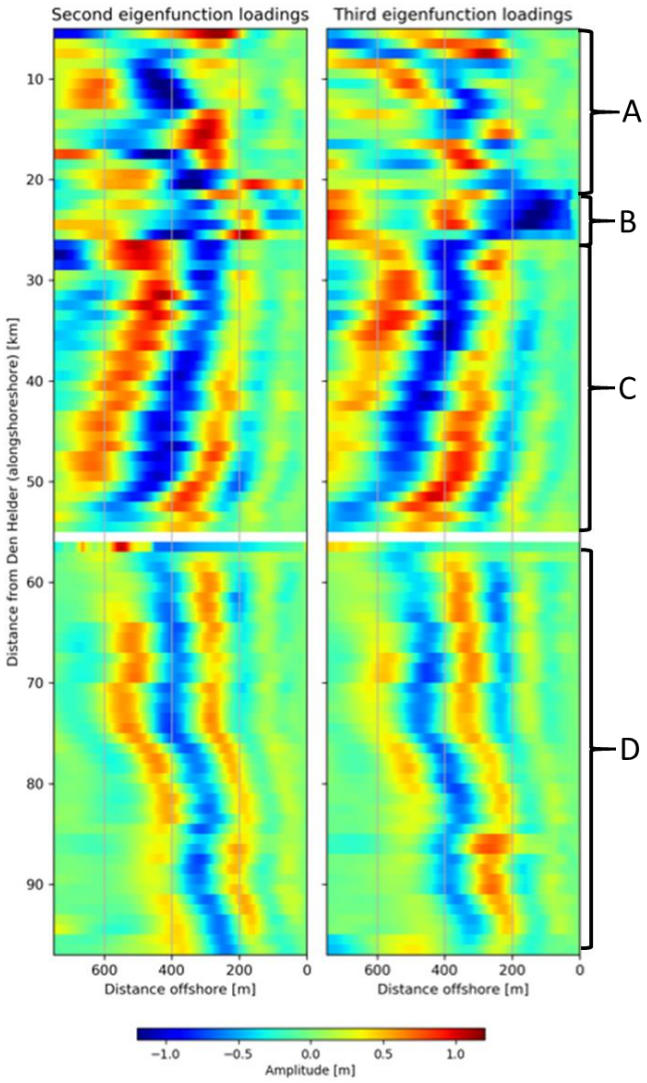

Figure 29: Loadings second and third eigenfunction for the Holland coast

eigenfunctions are observed. There is likely no (or very little) bar activity in this first 200m.

- Area B: Km 20-26. The Hondsbossche Zeewering dyke was located here until 2015. In 2015, this dyke was replaced by a mega-nourishment of 30m^3 sand, creating dunes in front of the dyke. Just as in section 7-20, already a bar shows up in the first eigenfunction.
- Area C: Km 26-55. The eigenfunctions in this section are consistent alongshore. Generally, 3 bars show up in the eigenfunctions. The bars are oblique to the shoreline, extending offshore in the south. This means that if the eigenfunction weightings are consistent alongshore, bars are extending more seawards in the south. However, this shore-obliqueness is very limited taking into account the alongshore length of over 20km. The highest amplitudes of the bars are found between 400 and 600m offshore.
- Area D: Km 56-97. The eigenfunctions in this section are consistent alongshore. Generally, 3 bars show up in the eigenfunction. The highest amplitudes of the bars are found between 300 and 600m offshore. The amplitude of the bars is smaller than the amplitude of the bars in section 26-55.

Bar spacing

Figure 30 shows the average bar spacing based on the cross-correlation in the eigenfunctions. It shows that the bar spacing north of the IJmuiden harbour moles is higher than area south of IJmuiden. North of the IJmuiden harbour the bar spacing fluctuates around 320m, while this is around 240m south of the IJmuiden moles. A low cross-correlation significance as observed between km 27 and 28, indicates that even with the most favourable spatial lag, the second and third eigenfunction still do not overlap well. This is, to a lesser extent, also the case around km. 85, where the Katwijk discharge sluice is located.

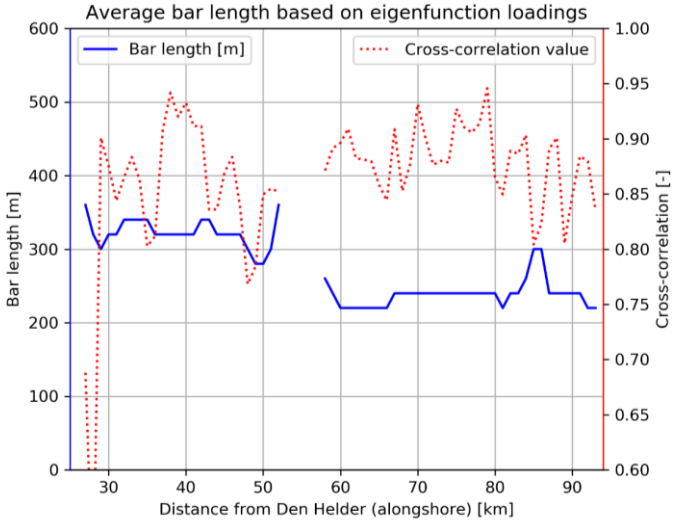

Figure 30: Bar spacing and corresponding maximum cross-correlation. Left: The bar spacing along the Holland coast (blue), right: The cross-correlation significance corresponding to this bar spacing (red)

The found bar spacings correspond well with findings of Short (1991). He observes spacing between bars of 300-400m north of the IJmuiden harbour moles. South of IJmuiden, spacing is around 200-240m.

Using the method of cross-correlation of the eigenfunction loadings, large bars (causing a lot of variance and thereby result in large amplitudes in the loadings) predominate. The predomination of large bars results in a bar spacing of 340m for large part of the Noord-Holland coast, where generally three bars are observed from the eigenfunction loadings in the first 750m offshore. However, these three bars would cover 1020m based on this 'average' bar spacing.

4.1.5 Second and third eigenfunction weightings

The weightings of the second and third eigenfunction are given in Figure 31.
Based on Figure 31, the Holland coast is divided into three areas with similar eigenfunction weightings. These are area A, B and C, respectively km 5-26, 26-55 and 56-97.

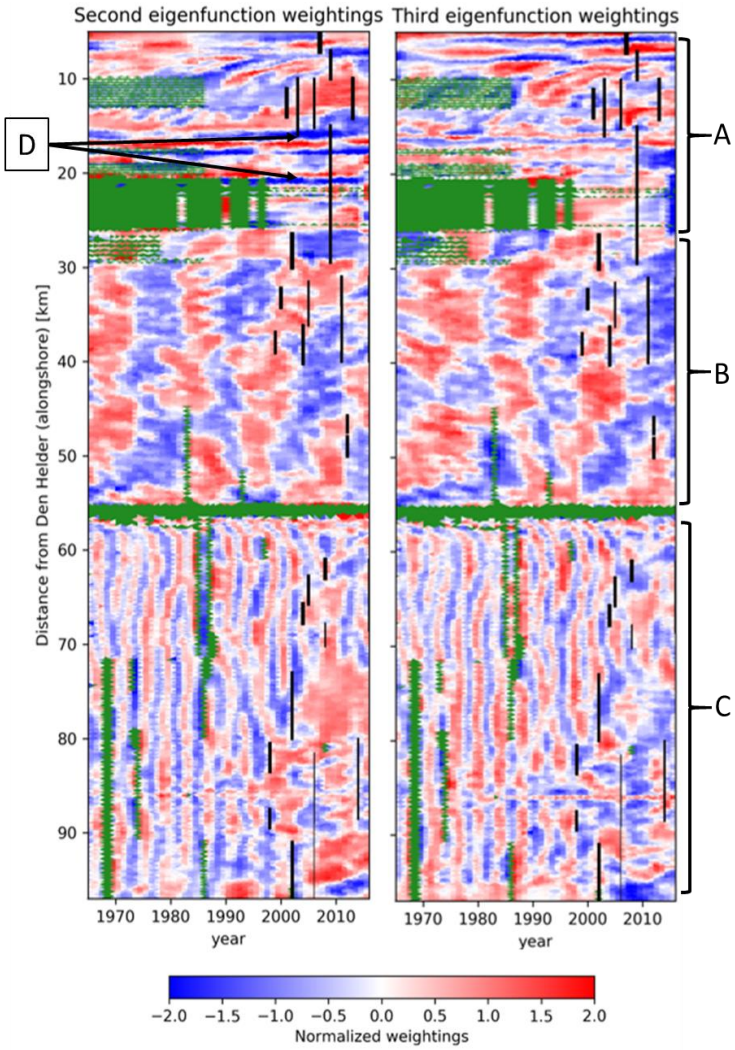

Figure 31: Weightings second and third eigenfunction for the Holland coast

Section km 5-26

No consistent pattern is observed in the eigenfunction weightings in this area. There is some northward movement of the eigenfunction weightings around km. 10, see Figure 32. However, due to the alongshore inconsistent bar loadings, interpretation of this northward movement is difficult. In this area, several horizontal lines show up in the eigenfunction

weightings, see D in Figure 31. This is due to alongshore irregulates within one window. Most of the variance explained in the dataset of the window is caused by the differences in profiles alongshore. Interpreting the temporal developments in the eigenfunction weightings in this area is difficult due to this alongshore variability, large construction works and large data gaps (km 21-26). In areas where the eigenfunctions are not (visibly) affected by alongshore variability, no periodic bar behaviour or clear trend can be observed from the eigenfunction weightings.

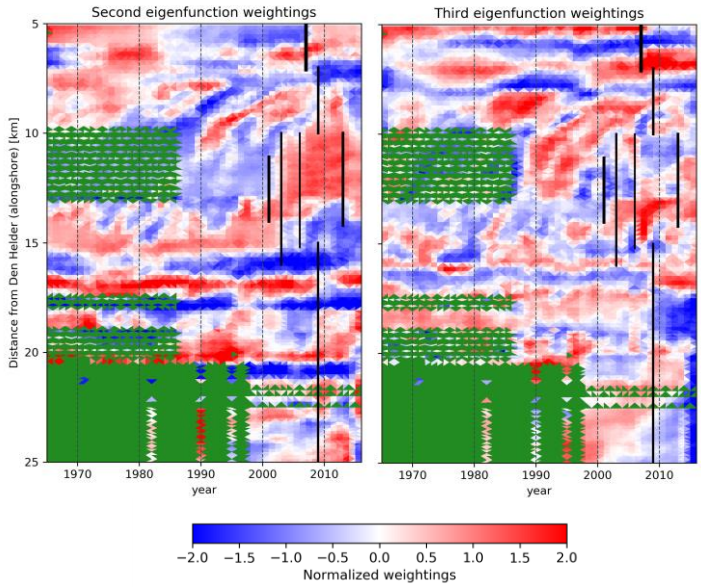

Figure 32: Enlargement of eigenfunction weightings area A, km 5-25

Section km 26-55

Between km 26 and 55 there is clear cyclic bar behaviour, see Figure 33. The alongshore coherence in the eigenfunction weightings is high, although alongshore variations do occur. When the alongshore coherence is high, for example around the year 1985 between section 30-38, the position of the bar is represented well with the shape of the eigenfunction loadings. This means, see Figure 29, that relatively shore parallel bars are present. In case of alongshore variations in the eigenfunction weightings, for example between km. 40 and 55 in the year 2000-2010, the position of the bar alongshore is variable. This alongshore variability and difference in migration can also be observed between 1982 and 1995. This can be observed more clearly based on reconstructions of the bar signal using the weightings and the loadings of the eigenfunction analysis, see Appendix J. Generally, connected bars are located closer to the shore in the north and further offshore in the south. However, this obliqueness is limited taking into account the alongshore length of the bar.

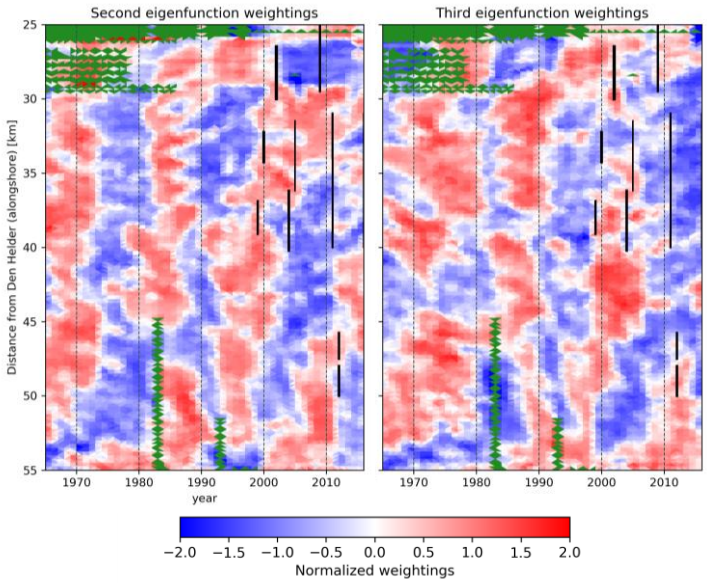

Figure 33: Enlargement of eigenfunction weightings area B, km 25-55

Cross and autocorrelation

To investigate how the weightings of the second and third eigenfunction are temporally related to each other, the cross-correlation between is determined per transect, see Appendix I. The cross-correlation of the second and third eigenfunction weightings in this area reaches a maximum with a time lag of three years. This indicates that the third eigenfunction generally lags 3 years behind the third eigenfunction. Since both the loadings and weightings of the third eigenfunction lag the second eigenfunction, this sequence indicates offshore moving bars. See section 3.3.2 *Bar migration* for an explanation.

For many transects, particularly between km. 30-45, a maximum autocorrelation was found with a time lag of around 15 years, i.e. the bar cycle return period is approximately 15 years. This is in correspondence with the bar cycle return period of around 15 years observed by Wijnberg (1995). Between km. 45 and 50 the autocorrelation is different and insignificant. This is likely the effect of a bar switch and irregular bar return period at this location, see also Figure 33. Because the measurement period prior to nourishments (1965-1997) is short compared to the bar cycle return period, one bar switch can influence the outcome of the autocorrelation significantly. The observation of one bar switch at this location is not enough to conclude that the bar cycle return period is significantly different along km. 45-50 compared to km. 30-45.

Section km 55-90

In this section clear cyclic bar behaviour shows up. The alongshore coherence in eigenfunction weightings is higher than in section 26-55. In case of perfect or very high alongshore coherence in the eigenfunction weightings, bar shapes similar to the shapes of the eigenfunction loadings (Figure 31) are often present. The high alongshore coherence is confirmed by reconstructions of the bar signal based on the eigenfunction results, see Appendix J.

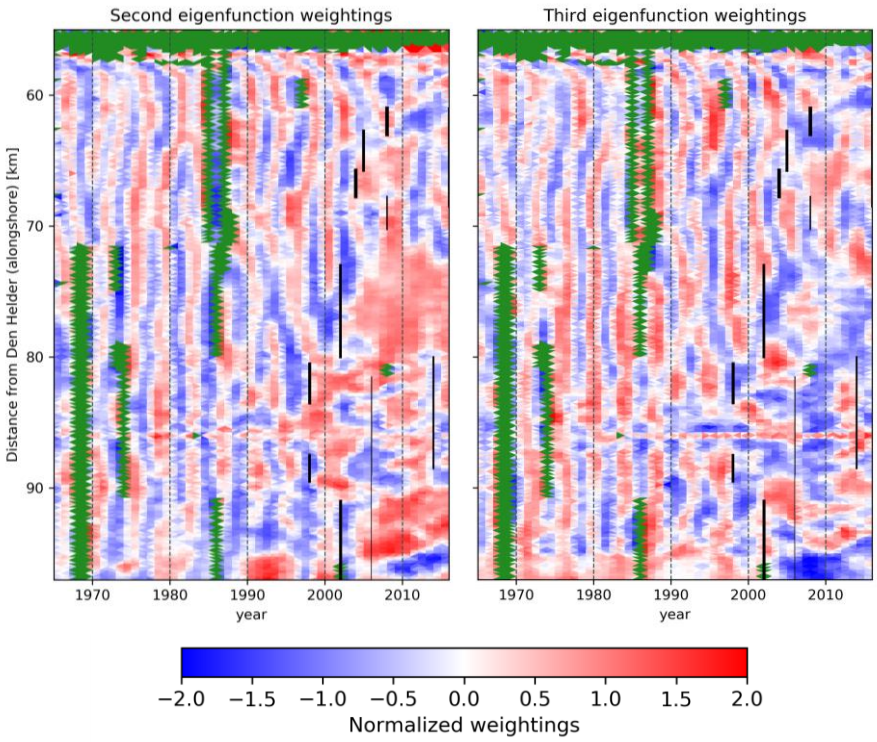

Figure 34: Enlargement of second and third eigenfunction area C, km. 55-97

Cross correlation

The cross-correlation of the second and third eigenfunction weightings reaches a maximum with a time lag of one year, see Appendix I. The second eigenfunction corresponds well with the third eigenfunction weightings one year later. Since both the and weightings of the third eigenfunction lag behind the second eigenfunction, this sequence indicates offshore moving bars.

The autocorrelation between km 70-90 consistently peaks at a four year time lag (4, 8 and 12 years), see Appendix I. However, the autocorrelation between transects km 56 and 70 is less consistent and shows a peak with a time lag 3 years. Peaks for higher time lags occur at 6-7 years and 10 years, which indicates that the bar cycle return period is just over 3 years.

Walstra et al. (2015) hypotheses that because cross-shore processes dominate the bar migration, bar switches may occur when alongshore differences in nearshore morphology are present, e.g. a slightly different slope. However, no significant difference in slope is observed between the areas.

4.1.6 Offshore migration

The bar cycle return period (red, left axis) and the offshore migration velocity (blue, right axis) are given in Figure 35.

The bar cycle return period is determined by searching for the maximum autocorrelation value within a time lag between 8 and 20 years (km. 30 – 50) and between 2 and 6 years (km 60-90). These intervals are set to avoid very small (or zero) time lags to become the most significant. In Figure 35, only values are shown of which the maximum autocorrelation reaches at least 0.2. When the autocorrelation is insignificant or when the second and third eigenfunction show dissimilarities, respectively the bar cycle return period or bar spacing cannot be determined accurately. The offshore migration velocity is not determined for these locations.

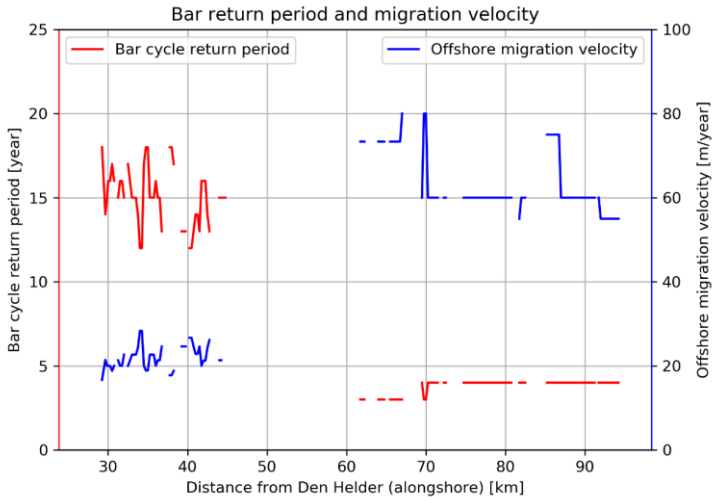

Figure 35: Bar return period and offshore migration velocity for the Holland coast

Km. 26-50

Based on Figure 35, a bar cycle return period fluctuates around 15 years is found for the area North of the IJmuiden harbour moles. This fluctuation is likely caused by the short period (1997-1965=32 years) with respect bar cycle return period (around 15 years). It is expected that the fluctuations, as shown in Figure 35, are therefore not structural. The corresponding offshore migration velocity, taking into account the bar spacing of 320m (Figure 30), is approximately 21m per year. This does not mean that every year a migration of 21m can be observed, but on average the migration is around 21m per year.

Km. 60-95

For the area south of the IJmuiden harbour moles, a bar cycle return period of 3 to 4 years is observed. The offshore migration velocity is around 75 m/year for the area km. 60-70 and further south around 60 m/year. Along km 85 to 87 a higher bar spacing (and consequently higher offshore migration velocity) is observed. However, this higher bar spacing is disputable, because the second and third eigenfunction are less alike in this section, see the eigenfunction loadings Figure 29.

4.1.7 Areas with similar nearshore morphologic behaviour.

Based on the results of this chapter, the following areas with large scale coastal behaviour are defined.

Table 4: Regions with similar nearshore morphologic behaviour along the Holland coast. Values between brackets are average values. The subsequent interval gives the range that is observed.

Area [km from Den Helder]	**7-26**	**26-55**	**55-95**
Slope	1:93 (km 9) 1:59 (km 21)	1:100, close to IJmuiden moles 1:115.	1:115, close to IJmuiden moles, 1:135.
Trends in steepness	Stable steepness	Stable steepness	Slightly increasing steepness
Coastline development	Retreat until 1990, accretion since 1990 (km 7-20)	Variable alongshore, retreat until 1990, accretion since 1990. Significant accretion close to the IJmuiden moles	Stable, accretion since 1990. Severe accretion close to the IJmuiden moles
No. of bars in profile	1 (first eigenfunction)	3	3-4
Bar spacing [m]	-	320	230
Consistency of cross-shore bar position alongshore	Bar position variable alongshore	Bar positions slightly variable alongshore and in time.	Alongshore relatively uniform, bar switches km. (68-70)
Migration	Non-migrating bar	Offshore	Offshore
Bar cycle return period [year]	-	(15) 12-18	(4) 3-4
Average migration velocity [m/year]	-	(21) 18-24	60-75

Km. 7-26.

In the northernmost section of the analysed coast no clear bar migration can be deduced from the second and third eigenfunction. The first eigenfunction does show a bar present in the average profile, corresponding with earlier research (de Sonneville & Van der Spek, 2012; Wijnberg, 1995). This non-migrating bar contains a variable cross-shore position between 300 and 600m from the shoreline. The shoreface in this section is relatively steep. Average slopes vary between roughly 1:60 to 1:90. Although directly north of this section severe steepening is observed, this is not the case in this section.

Km. 26-55.

In this area offshore bar migration is observed. The bar spacing is on average around 320m and the bar cycle return period is about 15 years. This corresponds to an average migration velocity of 21m/year. The bars are often slightly shore-oblique. Northwards they are located relatively close to the shore while at the southern end they reach further seawards. Close to the IJmuiden moles, no clear and constant cyclic bar behaviour is observed. At the southern boundary, next to the IJmuiden harbour moles, the coastline accreted with over 200m. Time-average slopes range between 1:100 and 1:115.

Km. 55-95

Also along this area, offshore migration of nearshore sandbars is observed. The average bar spacing is around 240m and the bar cycle return period is 3-4 years. Close to the harbour moles (km. 55-68) this return period is rather 3 than 4 years. The average offshore migration velocity is between 60 and 75m per year. The alongshore coherence in bar movement is larger than along section km. 26-55. The sandbars are often shore-parallel. For some periods shore oblique bars are observed. In contrary to km. 26-55, the bars are relatively far offshore in the north and close to the coastline in the south.

Time-average slopes are roughly 1:115. Close to the IJmuiden harbour moles this slope decreased to 1:135. Here also severe progradation of the coast is observed, the coastline moved almost 900m seaward.

4.2 Denmark

The analysed Danish coastline is shown in Figure 10. The starting point (zero on y-axis) is just south of Hanstholm, at transect number 3100. Distances in the figures below are with respect to this point. For some areas, data from 1874 is available, see Figure 36. However, in the eigenfunction analysis data from 1957 is used. This is done for two reasons:

- Using different timescales along one coast is inconsistent. Long term steepening trends are observed in the development of the coastline. Therefore, the first eigenfunction describing the average profile, might show alongshore variability due to the difference in timescale. In case of a long-term trend the average profile in the period 1957-2016 is not equal to the average profile between 1874 and 2016. From 1957, data is available along the complete analysed coast.
- The long-term steepening does not happen proportionally, see also *Discussion: eigenfunction analysis*. The variance that is not explained by the first eigenfunction is rather due to changes in the shape of the average profile than due to migrating sandbars. Decreasing the timescale does decrease the variance of this disproportional steepening, since less of this steepening occurs during the shorter period. The variance explained caused by the migrating bars is not affected.

Since data from 1874 gives insight in long-term changes and developments which are missed when analysing data from 1957. Appendix F provides a separate analysis of the Danish coast (km.21-79) from 1900.

4.2.1 Development of the coastline

In contrary to the 1m + NAP line in The Netherlands, the MSL contour line is used as reference for the coastline for the Danish coast. The mean sea level is chosen instead of an approximation of the high-water line because many transect measurements did not reach higher than 0.5 m.

In Figure 36 the development of the MSL contour is shown. In this figure the position of the MSL contour is given with respect to the average measurement in period 1980-1990. Since measurements do not start in the same year, comparison from the first measurement may lead to false interpretation. Moreover, using an average position over 10 years, the effect of outlying observation (due to storms/measurement errors) is minimized. The reference period in Figure 36 is marked with a dashed box. Shoreface and beach nourishments are illustrated with blue and black vertical lines respectively.

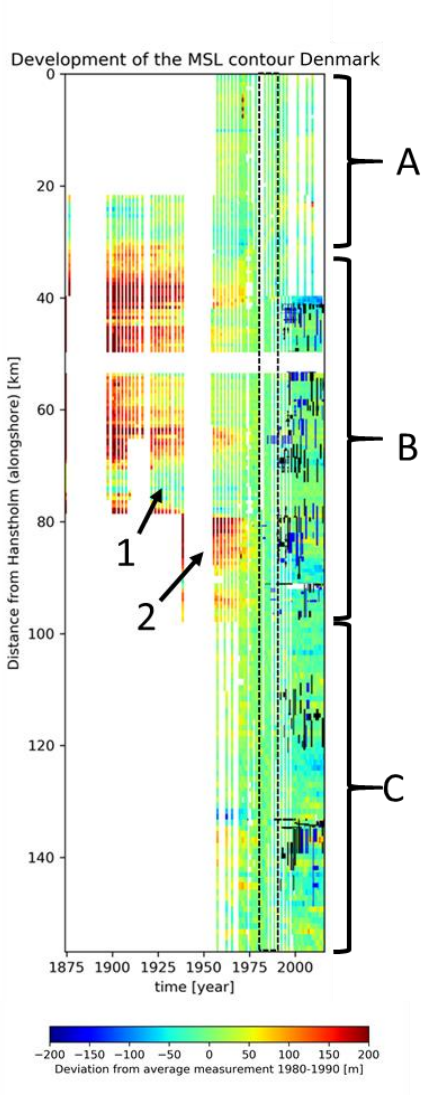

Figure 36: Development of Danish Coastline

In section A, between km. 0 and 30 the shoreline is variable but does not show a clear negative or positive trend. Small progradation can be observed as well as shoreline retreat.

In section B, between km. 30 and 95, significant retreat of the coastline can be observed. Groynes are present between 41-63 and 69-79. Remarkably, this retreat does occur less between km 72 and 76, see arrow 1 in Figure 36. From the year 1990, this retreating trend is less severe, as well areas with accretion as retreat are observed. This goes in harmony with the application of nourishments the in this period.

South of the section with groynes (km 79-95), coastline retreat is the most significant, see arrow 2 in Figure 36. The coastline retreated up to 200m between 1965 and 1985. After the reference period, as well retreat as progradation is observed in this area. These differences and reduced retreat are likely due to the nourishments applied here.

In section C, between location km. 100 and 150 the shoreline retreats, although arguably slowly with respect to region km. 30 and 95. Due to the absence of data, no position of the shoreline before 1957 can be shown.

4.2.2 First eigenfunction, mean profile

The mean profile shape or first eigenfunction loadings of the Danish coast (period: 1957-2016) are given in Figure 37. This figure shows that, over longer alongshore distances, significant alongshore changes in steepness of the average profile are present.

Section A (km 0-21) is not a straight coast. Average depths at 750m from the shoreline contour vary from 7m (km 6) to 10m (km 0 and 10). Around the moles along the coast at km. 21 and km. 9 the lowest steepness values are observed.

South of the mole at km. 21 (Area B) the coast is relatively straight. The steepness gradually increases going southwards. The depth at 750m from the shoreline increases from 9m at km. 22 to 11m at km. 39.

Groynes are located along major parts of section C, between km. 40 and 79. At km. 42, the steepest time-average (1957-2016) profiles are observed (1:54). At km 79 a jump in the steepness of the profiles can be observed. Km. 79 is the end of the groined section.

The southernmost section D (km 79-156) is the flattest section of the analysed coast. Within this section, the steepness gradually decreases going southwards. The mean depth 750m from the MSL contour around km 155 is 6m, while this increases to more than 7.5m around km 80. Locally, decreased steepness is observable around the harbour moles of Hvide Sande (km 133).

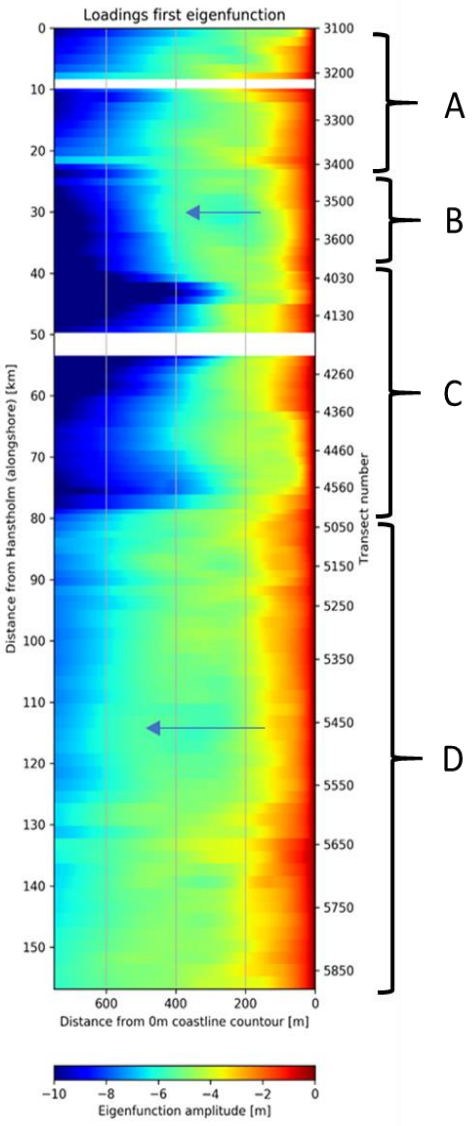

Figure 37:First eigenfunction loadings / average profile

At two locations signs of a bar can be observed in the mean profile. This is between km 28 and 35 and between km 110 and km 120. This is indicated with arrows. The arrows' triangle is located at the crest of the bar, while the line segment of the arrow crosses a section which is slightly deeper than the bar itself. A one-dimensional plot of the first eigenfunction at km. 116 is given in Figure 38. The presence of a bar in the first eigenfunction indicates that there is a bar present in the time-averaged profile.

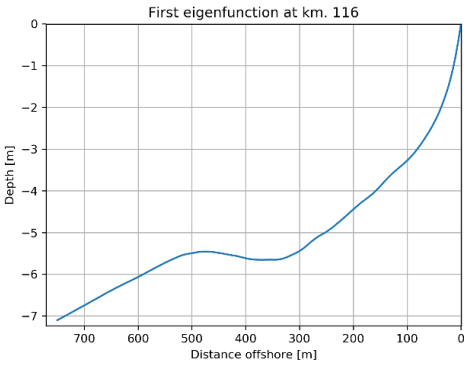

Figure 38: First eigenfunction at km. 116. A bar is visible at 500m from the shoreline.

4.2.3 Development of first eigenfunction weightings

Figure 39 gives an overview of the weightings of the Danish coast, corresponding to the first eigenfunction in Figure 37.

In the northernmost section, km. 0-10, no trend in the first eigenfunction weighting is observed. Between km. 10-22, an increase in the first eigenfunction can be observed from 1970. Figure 40 shows that the position of the shoreline and the first eigenfunction weighting are correlated. In case of a retreated coastline, the profile is relatively flat while in case of a coastline relatively offshore, the profile is relatively steep. This indicates that there is no structural erosion along this coastal stretch. Steeper profiles are rather caused by a coastline which is located further offshore. Along other locations no relation between the shoreline position and first eigenfunction weighting was found.

South of km. 22, a large increase in first eigenfunction weighting is observed. This is especially the case around km. 42 and km. 75. This increase is observed until km. 79. An analysis on a longer timescale (1900-2016), shows that the eigenfunctions weightings gradually increase from (at some locations) 0.8 in the start of the 19th century up to 1.2 in 2016, see Appendix F. This indicates that the average steepness in the shoreface has increased by up to 50 percent. More commonly the eigenfunction weightings increase from 0.85 to approximately 1.15, an increase in steepness of 35%

South of km. 80 changes in steepness over time are less significant and consistent. Between km. 85 and 110 year-to-year changes in steepness are observed, but there is not a clear trend.
Between km. 120 and km. 130 a period of low eigenfunction weightings (flat profile) in the 1960s' is followed by steeper profiles between 1980 and 2000. However, since 2000 profiles are flattening again. From km. 130 to km. 156 the first eigenfunction weightings are variable but do not have a clear trend.

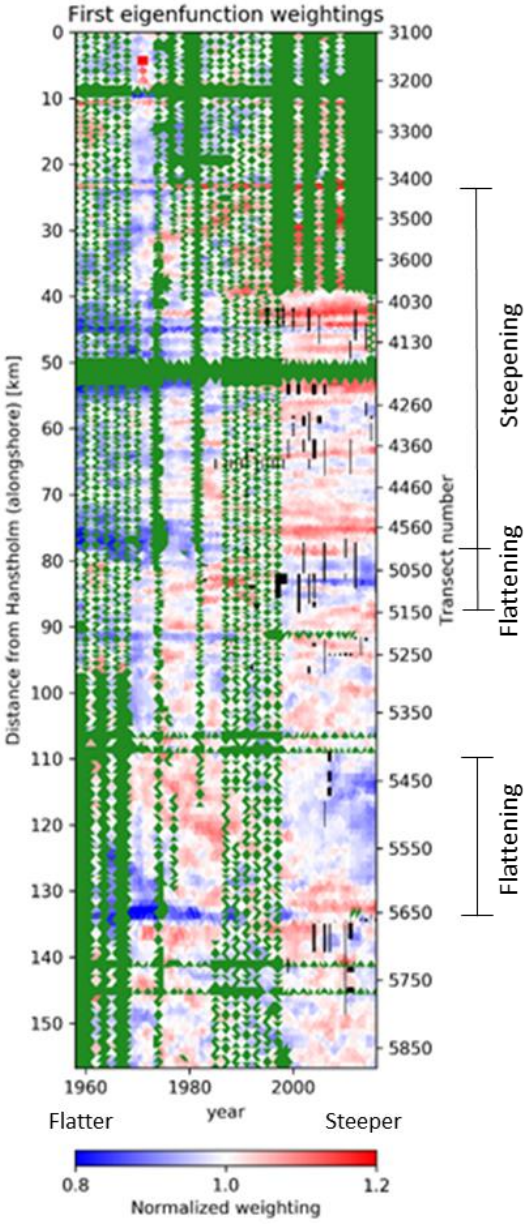

Figure 39: Weightings on first eigenfunctions Denmark

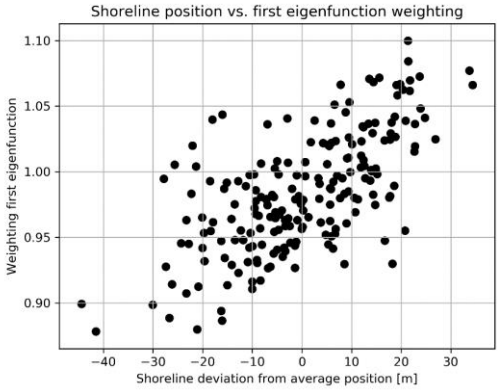

Figure 40: Correlation first eigenfunction weighting between and shoreline position between km. 12 and 21.

4.2.4 Second and third eigenfunction loadings

The loadings of the second and third eigenfunction are shown in Figure 41. These show the dominant patterns of variation in the profiles, apart from variations in the amplitude of the mean profile (first eigenfunction). These eigenfunctions generally explain the variation originating from the changing position of nearshore sandbars.

Based on visual inspection of the loadings of the second and third eigenfunction, the Danish coast is divided into four regions with roughly similar eigenfunction loadings. These regions largely coincide with the coastal regions as defined by the Danish coastal authority.

1. Nationalpark Thy, km 0-39.
2. Agger and Midjylland north, km 39-79.
3. Midtjylland km 79-156

Section A: Nationalpark Thy, km 0-39

This coastal section is not a straight uninterrupted beach. Constructions and changes in beach orientation near Vorupør (km 22) and Klitmøller (km 9) do influence the position of bars in the eigenfunctions. Generally, one bar can be observed from the eigenfunctions. Most significant bar amplitudes can be found between 100 and 400m from the MSL coastline contour. In the northern section (km 0-10) bars are located closest to the coastline in the north. Here the profile is the steepest, see Figure 39. In the south (at km. 8), where the shoreface is the flattest, bars are located further offshore.

Most significant amplitudes can be found between 30 and 300 from the MSL coastline contour. Bathymetry measurements indicate that the large negative third eigenfunction loadings close to the shore are not caused by bar variability, see Appendix J. A bar can be observed in the eigenfunctions between 200 and 300m from the shoreline.

Section C: Agger and Midtjylland North, km 39-79

One bar can be observed in the second eigenfunction between 100 and 300m from the shoreline. The bar signal in the third eigenfunction is less strong and consistent.

Section D: Midtjylland South, km 79-156

The loadings of the eigenfunctions in the southern area (80-156) are, in contrary to the other areas along the Danish coast, consistent alongshore. Two bars show up in the eigenfunctions. Largest amplitudes are observed between 200 and 600m from the contour line.

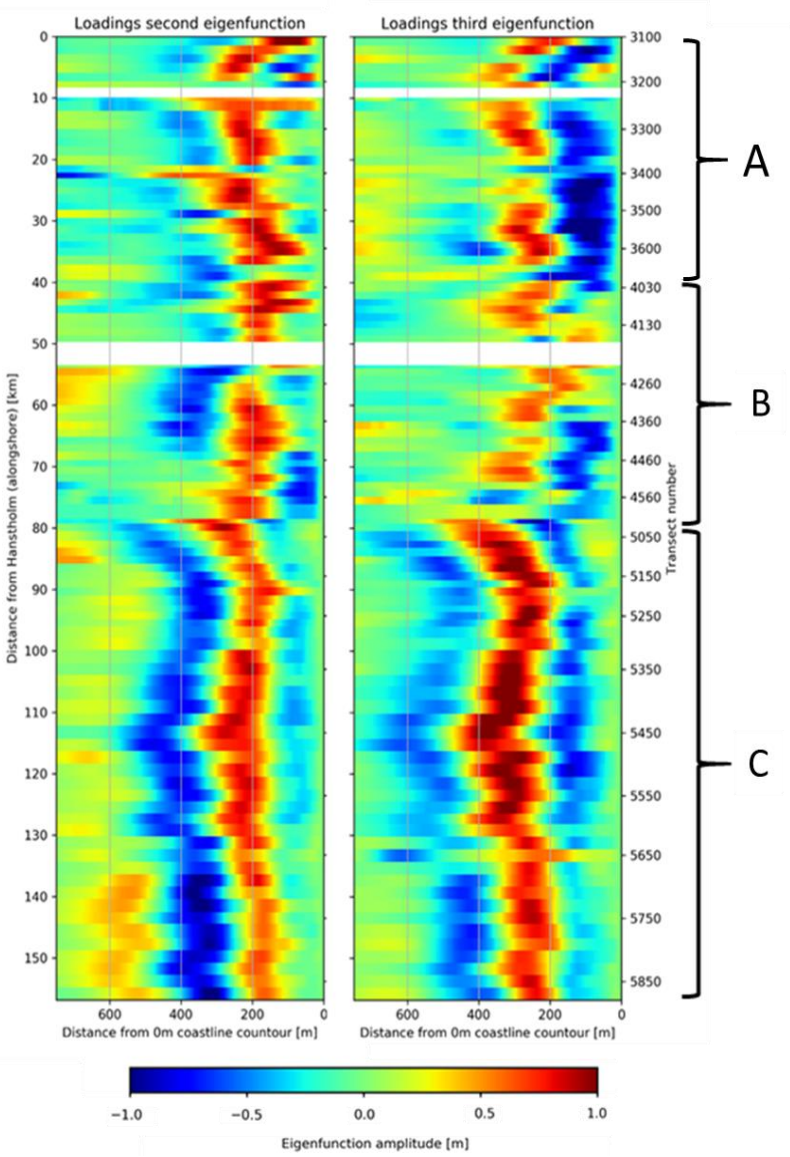

Figure 41: Second and third eigenfunction loadings of the Danish coast

The bar spacing along this southern part of the Danish coast is shown in Figure 42. The bar spacing varies between 300 and 440m. The bars spacing is high compared to the Holland coast. Between km. 131 and 134 no bar spacing is shown since the similarities between the second and third eigenfunction are too low here (max cross correlation < 0.6). Around this location, the Hvide Sande harbour (km 133) moles are located.

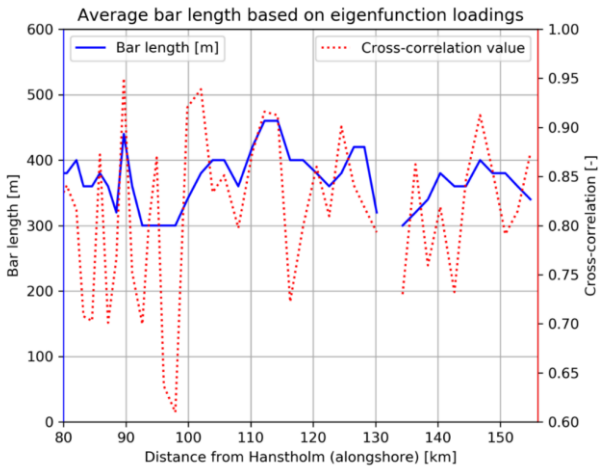

Figure 42: Bar spacing along the Danish coast

4.2.5 Second and third Eigenfunction weightings

The weightings of the second and third eigenfunction are shown in Figure 44. Data that is not available or suitable is highlighted in green. In the northern area, data is not collected yearly which results in gaps in the data. The black lines are shoreface nourishments in the area. The thickness of the lines represents the volume of the nourishment in m^3/m. The weightings of the eigenfunctions are a lot less consistent than the eigenfunctions weightings derived from the Holland coast. However, still regions with similar behaviour show up.

Nationalpark Thy North, km 0-22

No clear pattern or harmonic behaviour can be observed in the eigenfunction weightings in this area. Analysis is complicated by the large measurement interval and the variability of the shoreline (Appendix D). It could be, that the bar is stable but that variability of the reference line causes the bar position to change. If this is the case, the shoreline position and the second or third eigenfunction should be correlated. This is however not the case, see Figure 43. Along other areas this correlation is difficult to assess, since the shoreline is in a long-term retreating trend.

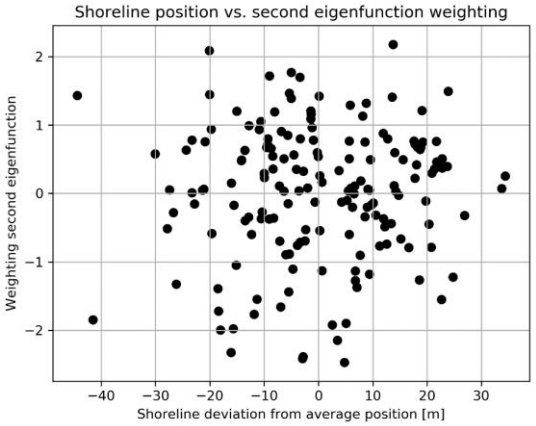

Figure 43: Relation between the position of the shoreline and the second eigenfunction weighting between km. 12 and 21

Nationalpark Thy South, km. 22-39

Just as in Nationalpark Thy North, no clear pattern or harmonic behaviour can be observed in the eigenfunction weightings in this area. However, a long-term increase in the third eigenfunction weighting is visible. By examining the shape of the third eigenfunction (Figure 41), it can be concluded that, superimposed on the steepness change of the first eigenfunction, close to the shore (0-200m) the coast steepened, while a bar became increasingly present around 250m from the shoreline.

Agger and Midjylland North, km. 39-79

North of the Thyborøn harbour moles (km. 39-50), the eigenfunction weightings do not show a clear trend or pattern. Over time, especially after the application of nourishments, both eigenfunction weightings become more positively weighted. Based on the eigenfunction loadings, this indicates an increased presence of a bar between 200 and 300m from the shoreline.

South of the Thyborøn harbour moles (km 50), eigenfunction weightings are relatively constant. Between km. 55 and 70, the second eigenfunction is positively weighted while the third eigenfunction is generally negatively weighted. This inverses after the application of shoreface nourishments. Based on the eigenfunction loadings, this indicates that the bar is located more offshore, rather around 300-400m instead of 200m. However, profile inspections show that this bar is not present in every measurement, this is also visible in the irregularity in the third eigenfunction weighting.

Between km. 70 and 79, the second and third eigenfunction are generally negatively weighted and become positively weighted over time. Based on the eigenfunction loadings, this

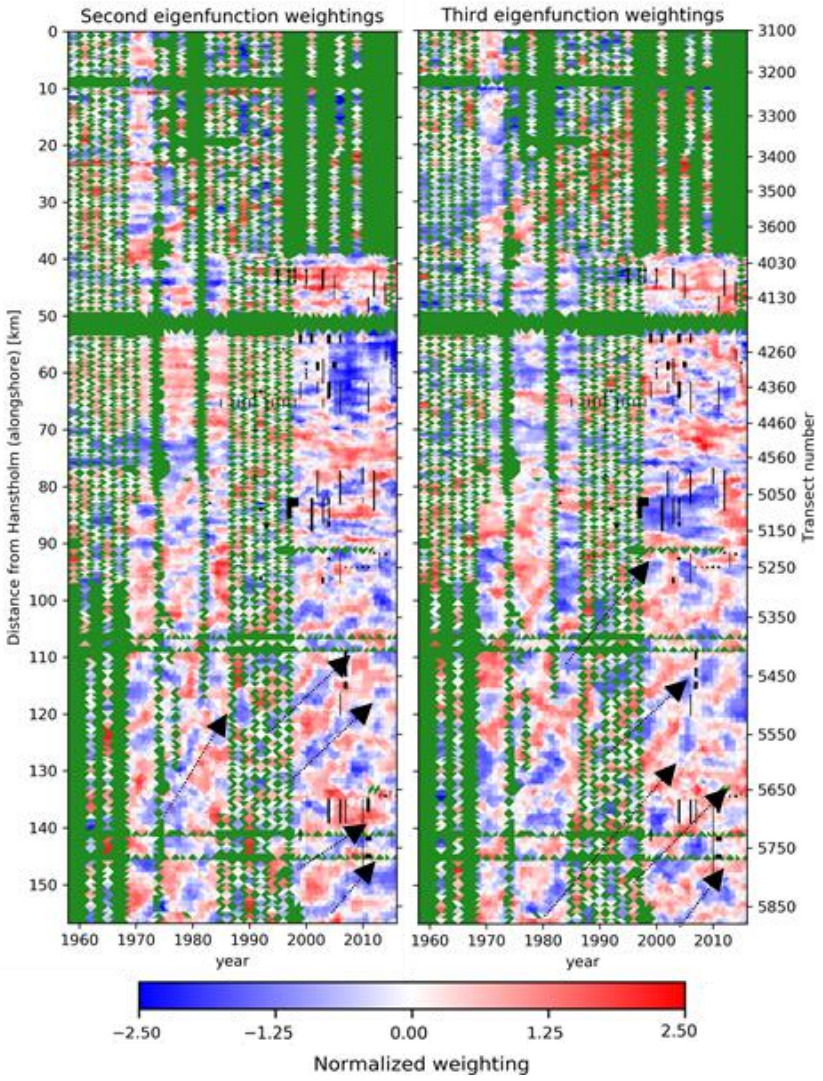

Figure 44: Second and third eigenfunction weightings of the Danish coast

generally also corresponds with the positions of a bar further offshore. South of km. 75 the third eigenfunction does not form a consistent bar alongshore. A bathymetry plot in Appendix J confirms that the sandbars are located further from the shoreline between km. 54 and 75.

Midtjylland, km 80-156

In the northern area, km 80-100, this northward movement of similar eigenfunctions weightings does not happen. No clear trend can be observed from the eigenfunction weightings. A long-term development in bar position and shape seems absent. For some periods, reconstructions of the bar signal show offshore migrating bars, see Appendix J.

In this region weightings of the eigenfunctions seem to move northward in time along km. 100-156, this is indicated with arrows in Figure 44. This indicates that deviations with the shape of the corresponding eigenfunction move northward in time. The alongshore consistency in the eigenfunction weightings and therefore in the position of the bars is very limited. Hence the bars are not uniform alongshore.

Reconstructions of the bar signal show that bars are indeed not uniform alongshore, see Appendix J, Figure 103. The bars are generally shore oblique, the sandbars do have lengths of approximately 6-10 km and are generally attached to the shore in the north and extend seawards in the south. The bars seemingly migrate northward over time. However, bar

migration is far from a uniform and clear trend. Shapes of bars are unsteady. For some periods the bar signal is noisy, and no clear migration can be observed. This northward movement of the eigenfunction weightings in Figure 44 can have two causes:

I. The bars migrate northward, i.e. sand on the bar migrates northward, causing northward transport of the nearshore sandbar.
II. The bars migrate offshore. Due to the oblique orientation with respect to the shoreline, offshore migration does also result in ostensibly northward migration. At the most offshore part, the bar fades away in the zone of decay while a new bar develops close to the shore, see also Figure 45. Therefore, the bar remains in its shape.

The northward movement in this area is against the direction of residual sand transport mentioned by Lodder and Sørensen (2015) and against the direction of bar movement reported by Kaergaard et al. (2012) in this area. A more detailed inspection (with a higher temporal resolution) of the nearshore bathymetry shows that bar migration as indicated in Figure 45 is indeed present along the Danish coast, see Figure 2. Offshore migration of the shore oblique bars, combined with fading out of the bar relatively far offshore and development of new bars close to the shore, ostensibly results in northward migration of the bar shape when analysing the bar migration on a coarse resolution.

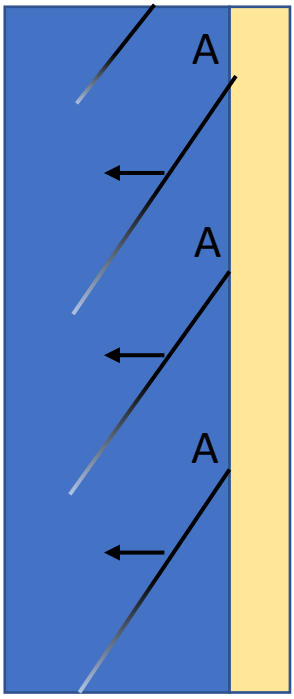

Figure 45: Schematisation of bar migration along the Midtjylland coast. Arrows indicate the migration of the nearshore sandbars (black lines). White ends indicate the fading out of the bar offshore. The 'A's represent development of a new bar close to the shore.

Moreover, based on the movement of irregularities in the shape of the shore-oblique bars, Kaergaard et al. (2012) conclude that bars actually migrate southward. This analysis indicates that the ostensibly northward migration due to offshore migration is larger than the actual southward migration of the bar itself. Therefore, the net migration of the bar shape is northward.

Based on the autocorrelation of a coastal section with a relatively constant pattern in the eigenfunction (km 122 – 129), positive autocorrelations are observed for a time lag between 8 and 12 years, see Appendix I. However, the significance of the autocorrelation is quite low. A best estimate of a bar cycle return period is 8-12 years. This corresponds with findings of Aagaard and Kroon (2007). They observe offshore bar migration just south (approx. at km. 160) of the study area with a return period of 8 years. Since they analyse singe cross-shore transects (not two-dimensional), they do not observe alongshore migration.

The cross correlation shows that the third eigenfunction generally lags 2 years behind the second eigenfunction, which corresponds with a 90 degrees phase lag in case of a bar cycle return period of 8 years and offshore migrating sandbars. However, also the spread in the cross-correlation is high while the significance is low. Because of the insignificant auto- and cross correlations, no offshore migration velocity is determined per transect. An estimation for the offshore migration velocity is $\frac{\lambda}{T_r} = \frac{360m}{10y} = 36\frac{m}{y}$

4.2.6 Areas with similar nearshore morphologic behaviour.

Compared to the Holland coast, the observed bar signal from the eigenfunctions is less consistent in Denmark. This complicates the interpretation of the eigenfunction analysis.

Table 5: Summary of areas with similar nearshore morphologic behaviour along the Danish North Sea coast

Section	**0-21**	**21-79**	**79-156**
Slope	1:107 - 1:75	1:94 - 1:54	1:115-1:100
Trends in steepness	No clear trend in steepness	Severe steepening of the profile, primarily between km. 40 and 79	No clear trend in steepness
Coastline development	No significant changes	North of km. 30: No significant changes. South of km. 30: Significant coastline retreat	Km 80-95, severe coastline retreat
No. of bars in profile	1	1	2
Length of bars [m]	-	-	300-440 m
Consistency of bars alongshore	Low	Low	Low, Oblique sandbars
Bar cycle return period [year]	-	-	8-12
Bar migration	-	-	Offshore, approx. 36 m/year

The area most comparable with the Holland coast is the Midtjylland (km. 80-156) coast. This coast also contains multiple offshore migrating bars and has a similar slope. In contrary to the Holland coast, the nearshore sandbars are shore-oblique.

Along km. 21-80 no bar migration pattern can be observed with the eigenfunction analysis. Along this coastal section there is erosion of the coastline. Between km. 21-30, this is limited to steepening of the shoreface (i.e. the coastline is stable), south of km. 30 there is besides steepening also severe retreat of the coastline. The Thyborøn inlet, located at km. 50, functions as a sediment sink. Around 0.5 million m^3 sand flows into the Limfjords trough the Thyborøn inlet annually (Niemann et al., 2011).

The groynes placed along km. 41-63 and 69-79 stabilize the coast to some extent, but also induce extra steepening of the shoreface. Especially south of the groined section (km. 80-95), the coastline retreated significantly more compared section with groynes. However, this section did steepen less compared to they groined section.

5. Results: Post-nourishment morphologic behaviour

In this chapter the second research question will be answered:

How do shoreface nourishments influence the nearshore morphologic behaviour?

This question was built up in 3 sub-questions, namely:

a) ***How do shoreface nourishments influence the steepness of the shoreface?***
b) ***How do shoreface nourishments influence the migration of nearshore sandbars?***
c) ***Is the post-nourishment nearshore morphologic behaviour region-specific or do nourishment implementation characteristics govern this morphologic behaviour?***

The first sub question will be answered by examining the weighting of the first eigenfunction, representing the average steepness of the profile. To answer the second sub question, the post-nourishment bar migration velocity will be compared with the pre-nourishment migration velocity based on the findings in Chapter 4. Finally, the post-nourishment morphologic behaviour at the nourished sections (answers sub-question a and b) will be evaluated based on the pre-nourishment morphologic behaviour and implementation criteria, such as volume [m^3/m], total volume and location of placement within the profile.

5.1 Netherlands

5.1.1 First eigenfunction weighting after nourishment

In Figure 46 the first eigenfunction weightings of the Holland coast are shown. After the application of nourishments, the first eigenfunction weighting generally decreases. The lowering of the first eigenfunction weightings is most severe between km 8 and 30 along the Holland coast and does not seem to decrease fast in the years after a nourishment. Since the first eigenfunction describes the average profile, a lower weighting indicates a flatter profile.

The lowering of the first eigenfunction weighting is a logical result of the decreased depth due to the placement of a nourishment. However, this decreased depth does not have to present along the whole coastal profile. The weightings on the first eigenfunction is determined mathematically, based on how the eigenfunction can reduce most of the variance from the reference datum. The decrease in the weighting of the eigenfunction can be completely caused by the reduction of variance from the reference datum at the cross-shore position of the nourishment (See also, Discussion: Eigenfunction analysis).

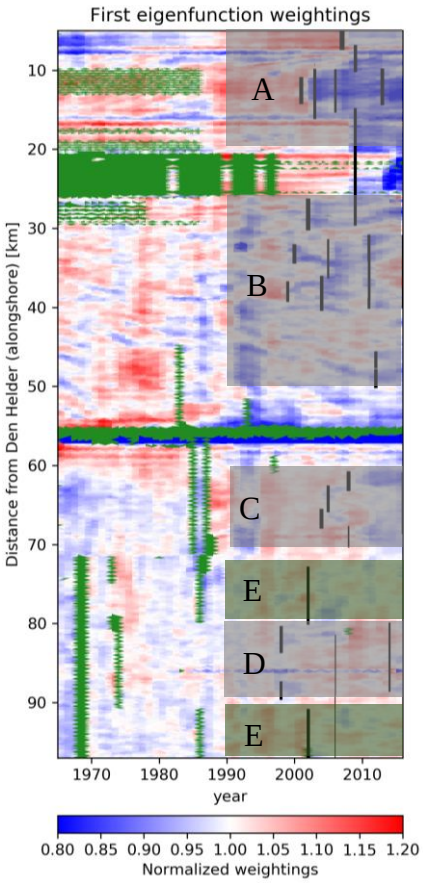

Figure 46: Weightings of the first eigenfunction for the Holland coast

The nourishments are divided into subsection A until E. Subsections are based on nourishments that are close to each-other. Subsection E consist of two nourishments with very similar implementation characteristics (year, volume, grain size, and location between -6 and -8m MSL). However, these two nourishments are not located very close to each-other.

In Figure 47, the development of the average first eigenfunction weightings are shown. The vertical dashed black line (year 0) represents the last measurement prior to nourishment application. This last measurement year prior to the nourishment is provided in the legend of Figure 47. The eigenfunctions weightings are normalized with the help of the average last eigenfunction weighting prior to the application of the nourishment (year 0). Therefore, eigenfunction weightings do always have a value of 1 just prior to the nourishment.

Location A

In the area shown in Figure 46, three nourishments are evaluated in Figure 47a. Nourishments between km. 10 to 13 are excluded since it consists of four nourishments which are applied in a short period.

A clear drop in the first eigenfunction weighting can be observed after the application of the nourishments. This first eigenfunction weightings do not recover to its pre-nourishment value. This indicates that the changes in nearshore morphology due to the nourishment are relatively structural (> 8 years).

Location B

Similar to location A, the first eigenfunction weightings in section B show a drop after the application of shoreface nourishments. The weighting decreases with approximately 7.5% for the nourishments applied in 1999 and 2002, while this is less for the nourishment applied in 2011. The gradual decrease of the eigenfunction weighting in 2011 is likely due to the placement just offshore of the 750m contour line.

The nourishment in section km 32.25 – 34.25 in the year 1999 shows a recovery to pre-nourishment values in six years. After six years, another nourishment is applied in this area, after which the eigenfunction weighting decreases again. This nourishment and first eigenfunction weighting decrease happens again 11 years after application of the nourishment. The effect of the nourishment seems less structural compared to the nourishments at location A. It could be that the coast is more dynamic here, causing quicker redistribution or erosion of the nourishment.

After the nourishments in the year 1999 the coastline accretes significantly, with 40 and 25m in the first two years for the nourishment along km. 32.35-34.25 and km. 36.9-39.1 respectively. However, this accretion is not observed for the other two nourishment evaluated in area B, see appendix H.

Location C

Nourishments applied in this region show a different direct response than the evaluated nourishments in location A and B. Whereas the evaluated nourishment result in location A and B in a decrease of one year, after which (limited) recovery takes place, the nourishments applied in 2008 in location C show a gradual decrease in the 5 years after the nourishment. This does not happen for the nourishment applied in 2004. Here only a small decrease is observed after the application of a nourishment.

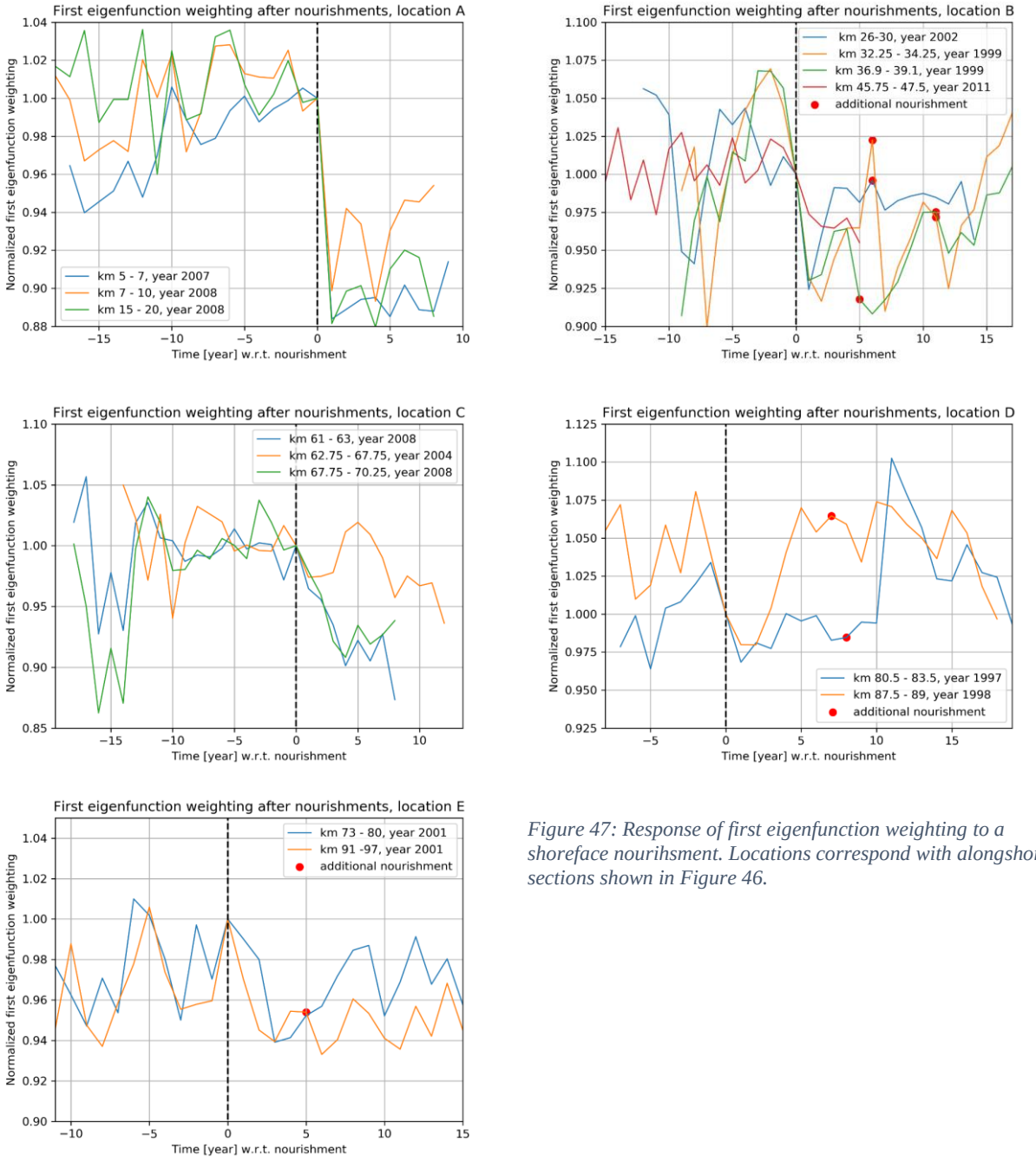

Figure 47: Response of first eigenfunction weighting to a shoreface nourihsment. Locations correspond with alongshore sections shown in Figure 46.

Observation of the Jarkus data shows that the nourishments are applied further than 750m from the +1m contour, and after this migrate towards the shore. This does explain the gradual decrease of the first eigenfunction (or gradual flattening of the first 750m offshore). Since the

nourishments are applied partly outside the analysed cross-shore section, examining the effect on the steepness is difficult.

Location D

The evaluated nourishments applied in location D do not show a large response of the first eigenfunction. Coincidentally, the first eigenfunction shows a drop already before the application of a nourishment. Nourishments executed later, do neither result in a visible change in the first eigenfunction. Inspection of the original transect measurements shows that the measurements only reach around 700m from the shoreline. In these profiles, no nourishment is observed. 10 years after the nourishment along km. 80.5 – 83.5 the first eigenfunction weighting increases to 1.1. This coincides with the placement of a large beach nourishment along this coastal stretch.

Location E

Both nourishments show initially a decrease of 6 percent in the first eigenfunction weighting, which is reached approximately two years after the application of the nourishment. This delayed response is also caused by the application of the nourishment on the border of the 750m contour line. After the placement, the bars slowly migrate shoreward. Along the coastal stretch km. 91-97, another nourishment is applied in 2006. After the application of this second nourishment the eigenfunction weighting decreases in the section km. 91-97, whereas it increases in the coastal stretch km. 73-80, where no nourishment was applied.

Similar to the eigenfunction weightings prior to the nourishment, the first eigenfunction weightings do show up- and downward movement simultaneously. The gap created between the eigenfunction weightings by the additional nourishment in 2006 seems to decrease over the years, although the first eigenfunction weightings in the nourished area remain below the unnourished coastal stretch.

Natural variability

The average first eigenfunction weighting over the coastal stretches where nourishments are applied fluctuates, see Figure 47. Hence, the decrease in the eigenfunction weighting can be caused or adjusted by these year-to-year fluctuations. This complicates the analysis of the influence of the nourishment, especially when the decrease in eigenfunction weighting is small with respect to the year-to-year fluctuations (Figure 47c, d and e).

5.1.2 Second and third eigenfunction

Reconstruction bar signal North-Holland

In Figure 48 the reconstructed bar signal from the second and third eigenfunction for the North-Holland coast is shown. All nourishments are shown together within one page, because only in this way the influence of nourishments on the complete bar system (in time and space) can be shown. The reaction of the bar system to a nourishment might be dependent on the adjacent movement of bars and the application of nearby nourishments. Red lines indicate the placement location of nourishments.

In Table 6 the migration of nearshore sandbars after nourishments is summarized, based on the results in Figure 48 and the migration of the coastline, see Appendix H. Generally, very low migration velocities very close to 0m/year are observed after the nourishments, while this was on average 21m/year in the pre-nourishment situation.

Table 6: Migration of nearshore sandbars after the application of nourishments. Year (start-end) gives the period over which the bar migration analysed. The position of the bar at the year start and year end is given in the bar position column. The average migration of the coastline (reference line) during the period year(start-end) along the area where the nourishments is applied is provided in the coastline migration column. With these characteristics the net average migration is determined ($\frac{bar\ migration + coastline\ migration}{period}$).

Location (starting year)	**Tran-sects**	**Year Start-end**	**Bar position Start-End [m]**	**Coastline migration [m]**	**Net migration [m/year]**	**Remarks**
A: Egmond (1999)	36.9-39.1	2001-2003	300-340	-16	12	
B: Bergen aan Zee (2000)	32.25-34.25	2001-2004	380-420	-26	5	
C: Camperduin (2002)	26.5-30.0	2003-2008	300-300	-2	0	Bar position along km. 26.5-28
D: Egmond aan Zee (2004)	36.2-40.2	2005-2009	380-380	-2	0	
E: Bergen (2005)	31.5-36.2	2007-2010	400-450 400-500	10	3,20	Offshore migration northern boundary
F: HPZ (2008)	15-29.5	2009-2014	290-290-400	0	-1, 21	Bar position along km. 25-29.5. Offshore migration southern boundary
G: Bergen-Egmond (2010)	31-39	2012-2015	400-400	3	1	
H: Egmond (2011)	39-40	2012-2015	400-400	29	10	South offshore mig. north onshore. Mig-ration to 450-500 between 2015-2016
I: Heemskerk (2011)	45.75-47.5 & 48-50	2014-2016	400-530 530-600	-2	66-36	Bar switch after nourishment. Bar position from 2014

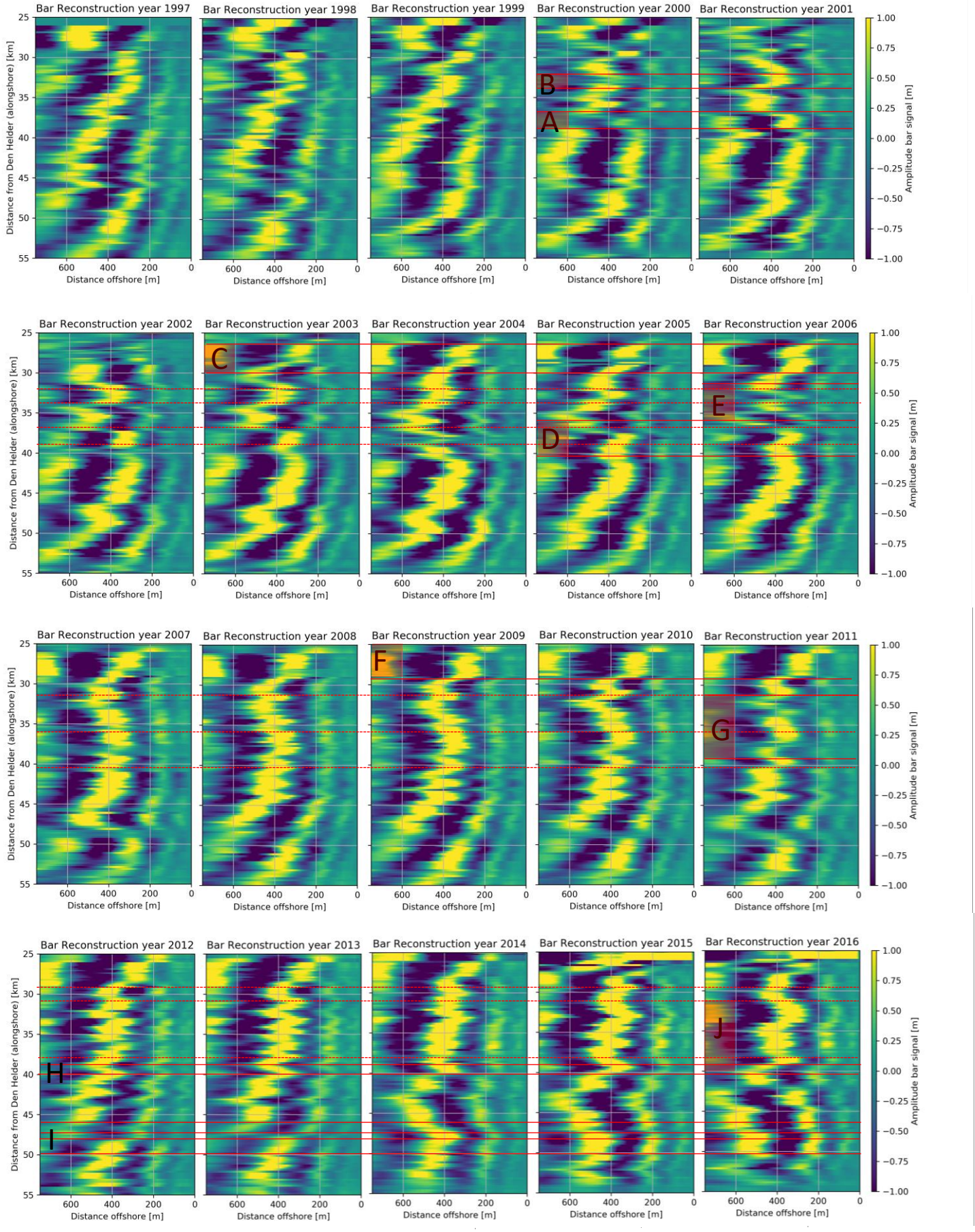

Figure 48: Reconstruction Noord-Holland coast, post-nourishment

After the application of many nourishments (A-E) in the northern section (km 26.5-40), only a small coastal stretch within this section remains unnourished (km. 30-32.25). Along this whole northern section a non/barely-migrating and alongshore relatively uniform sandbar is observed from 2007. Likely, the non-migrating bars in the unnourished section are caused by the stagnation of surrounding bars. This bar remained stable until and also after the execution of the subsequent nourishments in the area (nourishment F, G, H and K). Hence, from 2007, no net migration was observed along this northern stretch from 2007 until 2016.

The coastal stretch between km. 40 and 45 remains unnourished. In contrary to the small unnourished section (km. 30-32.25), offshore migration is observed along this coastal stretch. Along km. 42-45, bars are located at 400 to 500m from the +1m contour line in 2007. In 2016, this was rather 600-750m from the shoreline. This corresponds with the average bar migration of around 21m/year. The net average migration of the shoreline between 2007 and 2016 was very close to zero (-0.4m).

Close to the frequently nourished northern section, bars migrated from 400m to 500m from the shoreline in the same period (2007-2016). Although no nourishments are applied here, this is approximately half of the original migration velocity.

The non-migration along km. 30.25-32.25 and the reduced offshore migration along km. 40-42 indicate that there is an effect of shoreface nourishments on the migration velocity also at unnourished adjacent sections. This effect is in the order of several kilometres. However, the bar behaviour along the whole coastal cell is not affected.

Discussion

There is not always a clear bar signal or bar migration, therefore only periods with a traceable bar migration are listed in Table 6 and Table 7. For example, the bar signal after the nourishment in Egmond in 1999 is only analysed from 2001-2003 since the measurement in 2000 does not show a clear bars. By excluding this measurement, some information might be missed which can be found by investigating on a more detailed (temporal) scale. According to Van Duin et al. (2004), the nourishment in Egmond initially caused onshore migration of the bars. The nourishment became the new outer bar in 2001. After the new situation has formed, the bars migrate slowly offshore. Only this latter process can also be observed from the eigenfunction reconstruction. Also (Walstra, 2016) writes that the bar migration is generally reversed for a short time when a nourishment is placed at the outer bar.

This onshore migration is not observed from the eigenfunctions. The first years after the application of a nourishment, the bar position based on the eigenfunctions is often disputable. It is hypothesized that this is because the shape of the profiles just after the nourishment application cannot be explained well by the eigenfunctions. Moreover, the temporal resolution of 1 year is coarse to observe this fast onshore migration. Therefore, the migration of the bars in Table 6 and Table 7 is mostly determined when the nourishment is absorbed in the nearshore morphology.

In contrary to all other nourishments, a large migration velocity is observed after the completion of the nourishment in Heemskerk in 2011. This might be due to a bar switch with

an outer bar after the nourishment is completed. Analysing this nourishment requires a more detailed approach.

Reconstruction bar signal Rijnland

In Table 7 the offshore migration velocities after nourishments for the Rijnland coastal stretch are given. Besides the nourishment executed at Zandvoort-Zuid in 2008, all post-nourishment measurements show a decrease in offshore migration, stagnation or even (temporal) onshore migration of the nearshore sandbars. The original bar migration was between 60-75m/year.

Table 7: Bar migration after nourishment along Rijnland coast

Location (starting year)	**Tran-sects**	**Year Start-end**	**Bar position End [m]**	**Coastline migration**	**Net migration [m/year]**	**Remarks**
A: Noordwijk (1998)	80.5 – 83.5	1998-2004	360 420	7	11	
B: Katwijk (1998)	87.5 – 89.5	2000-2006	360-360	5	1	First years offshore, later onshore.
C: Noordwijk-erhout (2002)	73-80	2003-2016	400 [400-600]	12	1-16	Two bar switches in the north (2004-2006 & 2011-2013). Little off-shore migration in the north.
D: Wassenaar (2002	91 - 97	2007-2016	380 380	15	3	Weak bar signal until 2006. After additional nourishment landward migration in south
E: Zandvoort Zuid & Noord (2004)	62.75-67.75	2005-2010	500 500	16	3	2010-2014 offshore migration with pre-nourishment migration velocity
F: Noordwijk-Wassenaar (2006)	81.5-97	2007-2014	390-500	24	19	Values of bar position of km. 81.5-90. First stable bar, 2011-2014 offshore migration. 2014 new nourishment
G: Bloemendaal (2008)	61-63.25	2010-2015	400 400	23	5	Likely a bar switch occurs in the north between 2011 and 2013.
H: Zandvoort Zuid (2008)	67.75-70.25	2009-2011	520 620	-2	49	2009-2010 stagnation, later offshore. One bar cycle gone through in 2014

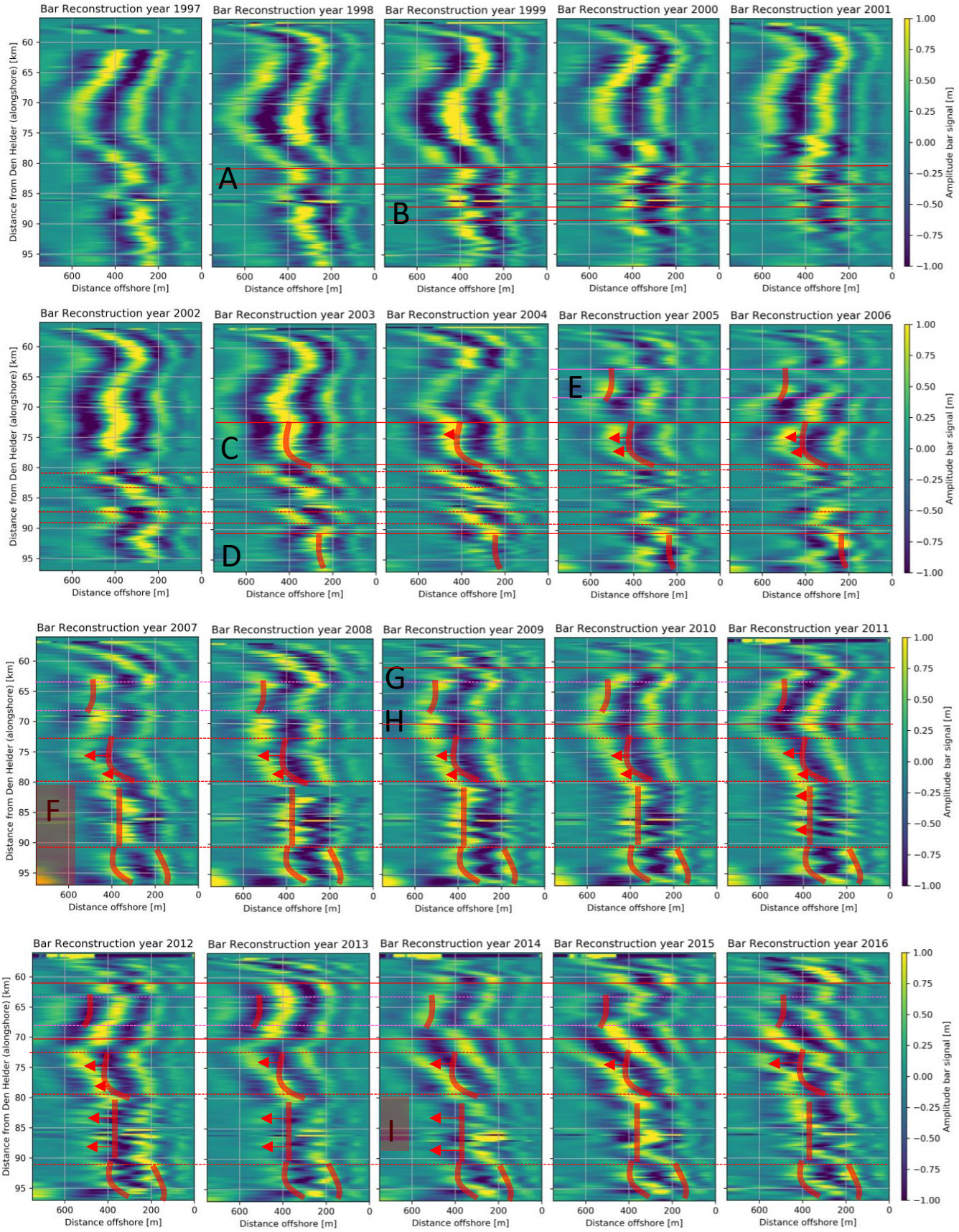

Figure 49: Reconstruction Rijnland

Especially large nourishments seem to have affected the bar migration. Along the coastal stretch where the Noordwijkerhout nourishment (Nourishment C) was applied in 2002, 13 years of very little bar migration is observed from 2003. This period of bar stagnation is significantly longer compared to other studies of bar migration along the Holland coast after nourishments (Grunnet & Ruessink, 2005; Ojeda et al., 2008; Van Duin et al., 2004). Moreover, it is also significantly longer than the original bar cycle return period of 4 years.
From 2008, the bar starts migrating onshore in the south (km. 76 and 80). This might be caused by the nourishment that is applied at the southern boundary (Nourishment F). In the north, (little) offshore migration is observed.

Also in the southernmost area (km 90-97) there is a long period (2007-2016) with stagnated bars, likely due to nourishment D and F. North of this section, where only nourishment F is applied, offshore migration resumes from 2011.

Just as along the north Holland coast, the nourishments do not seem to affect the bar behaviour over large alongshore distances. Mostly, bar switches occur directly north or south of the area where the nourishment is applied. Along the unnourished section (km. 67.75 – 73) between nourishment C and E, offshore bar migration is observed between 2005 and 2008.

For some nourishments it is observed that offshore migration reduction is temporarily and that after a nourishment the original offshore migration velocity returns to pre-nourishment values. After 5 years of bar stagnation after the nourishment in Zandvoort Zuid & Noord (nourishment E), offshore bar migration is observed with a return period of 4 years. However, there are also areas (km. 73-80 and 91-97) where bars barely migrate, despite the fact that the last nourishment were completed respectively 14 and 11 years ago.

5.1.3 Nearshore morphologic behaviour after first nourishment

To investigate if the post-nourishment morphologic behaviour can be linked to pre-nourishment morphologic behaviour and/or implementation characteristics of the nourishment, the influence of first nourishment on a coastal section on the bar behaviour is summarized in Table 8. Only the first nourishments along a coastal stretch are summarized, because these are the only nourishments where there is no influence of prior nourishments. Besides differences in post-nourishment steepness between the areas with and without migrating bars, no consistent relations have been observed.

A comparison based on the impact of the nourishment on the nearshore morphology is difficult. Often a nourishment is carried out in years following the nourishment. All nourishments of with a '*' in the last column of Table 8 indicate that after this period another nourishment was applied, so that the later observed bar behaviour cannot be attributed to the prior nourishment. Therefore, it could be that the change in bar behaviour would be longer than noted in this column if no second nourishment was applied. If these nourishments would be excluded from the analysis, only four nourishments remain.

Difference can be observed between the different regions of bar behaviour. In the area where no pre-nourishment cyclic migration of the bars is observed (blue) the first eigenfunction is decreased the most after the completion of nourishments. Moreover, this first eigenfunction

does not recover fast to pre-nourishment values. This shows that in the area where no migrating sandbars are observed (between Den Helder and the former Pettemer Zeewering), the nourishments cause significant and long term (> 8 years) flattening of the shoreface.

In the region north of the IJmuiden harbour moles, relatively large bars with a return period of 15 years are present in the pre-nourishment situation. Nourishment in these areas are highlighted orange in Table 8. In this area, the first eigenfunction is affected less than in the area where no bar migration is observed. As well in decrease of the first eigenfunction as its duration of decrease is less. After nourishments, reduced bar migration and stagnation of the nearshore sandbars is observed in this area. Due to the application of subsequent nourishments this duration can only be investigated for a short time period. The nourishments in the area affected the bar migration for at least 4 to 6 years.

In the region south of the IJmuiden moles, smaller bars with a short 3-4-year return period are present. Nourishments in this area are highlighted green. The effect of nourishment in this area ranged from a 2 percent decrease to a 10 percent decrease in eigenfunction weighting. The recovery time of the ranged from 3 to more than 8 years. However, analysing nourishments in this area is difficult since the nourishment are often applied on the border of just outside of the analysed cross-shore section.

In this area, as well onshore migration, stagnation as reduced offshore migration is observed after nourishments. The duration of the affected bar migration ranges from 1 to 13 years. The nourishment with only one year of changed bar behaviour was the smallest in volume per metre [m^3/m] and in total volume[m^3] of the nourishment. However, this relation between nourishment volume and changed bar behaviour does not hold, since the second smallest nourishment causes (at least) 8 years of stagnation of the nearshore sandbars.

Discussion

The obtained values of affected bar behaviour are rather qualitative, i.e. based on visual interpretation of the reconstructions and replacement of the coastline. Because the first eigenfunction weighting (Figure 46) fluctuates, also the duration of steepness change (recovery time first eigenfunction) is disputable. This duration is based on the interpretation of the first eigenfunction weightings in Figure 46. When the first eigenfunction weighting has largely recovered after a decrease due to the nourishment, this is seen as the end of affected steepness. The nourishment along km. 26-30 in the year 2002 for example did show an initial decrease of 7.5 percent. After 3 years, this reduced to a decrease to of 2 percent, after which the first eigenfunction weighting /average steepness remains relatively constant. This period of 3 years is seen as the recovery time of the steepness.

Table 8: Summary of nourishments and their influence on the nearshore morphology. Volumes are based on Rijkswaterstaat nourishment database. Other sources Sources: 1= Rijkswaterstaat nourishment database, 2= (Bruins, 2016), 3= (Deltares, 2013), 4= (Quartel & Grasmeijer, 2007),5=(Holzhauer et al., 2009), 6=(Rijkswaterstaat, 2003) 7=(Lodder & Sørensen, 2015), 8=(Ojeda et al., 2008), 9= Visual inspection Jarkus data

Section km	**Area**	**Volume [m3/m]**	**Total volume [million m3]**	**Grain size [µm]**	**Placement depth [m + MSL]**	**First eigenfunction decrease [%]**	**Recovery time first eigenfunction [year]**	**Observed bar migration**	**Duration of observed bar migration [year]**
2-7.1	Julianadorp	635	3.2	-	[-5, -8] [9]	12	>8	-	-
7-10	Julianadorp	434	1.3	-	[-5, -8] [9]	10	>8	-	-
15-29.5	H&P Zeewering	393	5.7	-	[-5, -10] [9]	12	>8	-	-
26.5-30	Camperduin	564	2.0	207 [1]	[-5.5 and -8.5] [2]	7	3	Stagnation	6 *
32.25-34.25	Bergen aan Zee	497	1.0	250 [1]	[-5.5 and -6.5] [2]	8	5-6	Reduced migration	4 *
36.9-39.1	Egmond	400	0.9	228 [1,8]	[-5, -8] [5]	7	-	Stagnation	4 *
45.75-47.5 & 48-50	Heemskerk	410-440	1.6	-	-	3-4	-	Increased/Bar switch	-
61-63	Bloemendaal	501	1	250-300 [7]	[-5, -7] [9]	10	>8	Onshore	5
62.75-67.75	Zandvoort (Zuid&Noord)	441	2.2	250-300 [7]	[-5.5 and -7] [2]	2.5	3-4	Stagnation	6
67.75-70.25	Zandvoort Zuid	204	0.5	250-300 [7]	[-5, -7] [9]	9	>8	Stagnation	1
73-80	Noordwijkerhout	378	2.6	250-350 [6]	[-6, -8] [2]	6	+- 7	Stagnation	> 13
80.5-83.5	Noordwijk	422	1.3	400 [8]	[-5, -8] [4] [-5, -7] [5]	3	4	Reduced migration	6 *
87.5-89.5	Katwijk	377	0.8	-	[-5, -7] [5]	2	3	Stagnation	8 *
91-97	Wassenaar	418	2.5	250-350 [6]	[-6, -8] [6]	6	>5	Stagnation	-

5.2 Denmark

5.2.1 First eigenfunction response after nourishments

In Denmark, shoreface nourishments are generally smaller and are applied more frequently, see Figure 52. This makes it harder to assess the influence of a single nourishment.

To assess the influence of nourishments on the average steepness (first eigenfunction) the average first eigenfunction of frequently nourished areas is plotted against the average first eigenfunction of adjacent areas that are not nourished, see Figure 53. This is helpful since the Danish coast is in a steepening trend. Therefore, it is difficult to determine whether increase of the first eigenfunction is due to the natural steepening or due to migration/erosion of the nourishment.

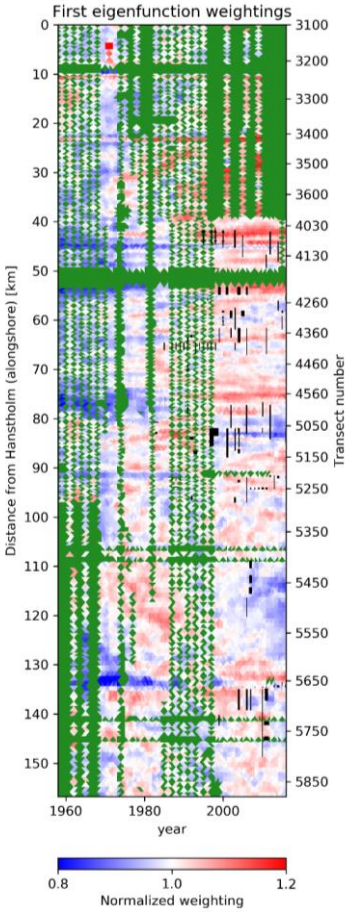

Figure 50: Weightings on first eigenfunctions Denmark

Areas that will be compared are listed in Table 9. The evaluated areas are the areas that received most sand [m^3/m] over time, based on Figure 51. Reference areas are not or to less extent nourished. The Danish Coastal Authority discriminates between two types of shoreface nourishments:

1. Nearshore nourishments. Sand is nourished under water close to the shore with the help of rainbowing. This type of nourishment is indicated in red in Figure 52.
2. Bar nourishments. These nourishments are generally placed outside of the outer bar. This type is indicated in blue in Figure 52.

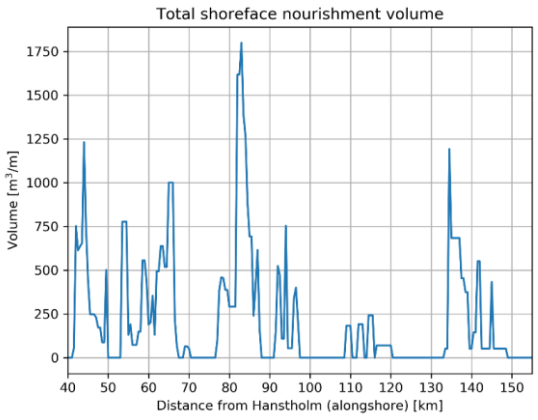

Figure 51: Total volume of shoreface nourishments along the Danish coast (until 2016)

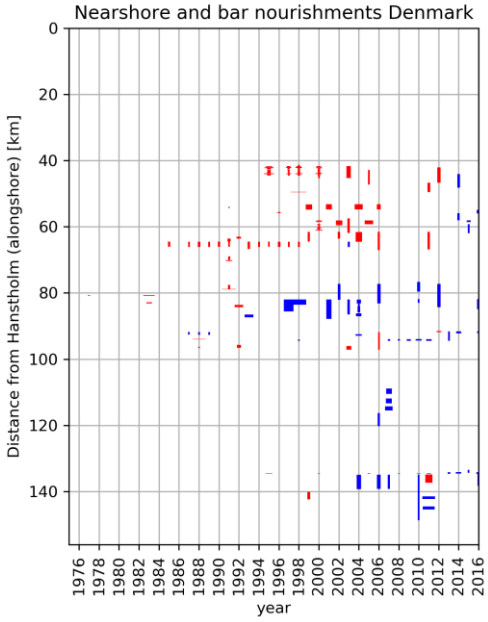

Figure 52: Nearshore (red) and bar (blue) nourishments in Denmark.

The weighting of the first eigenfunction is determined mathematically, based on how the eigenfunction can reduce most of the variance from the reference datum. After application of both types of nourishments, the variance from the reference datum decreases. Hence, for both types of nourishments cases a decrease in eigenfunction weighting can be expected. Nearshore nourishments are still applied under the reference datum and do therefore not directly affect the position of the coastline.

Table 9: Nourishment and reference areas

Area km.	**Nourished [m^3/m]**	**Reference area km.**	**Nourished in reference area [m^3/m]**	**Remarks**
42-44.7	610-1230	45.5-49	90-250	Reference area is located close to Thyborøn inlet. Nourishments are all nearshore nourishments, rainbowing.
62-66	490-1000	68-72	0-65	Nourishments applied since 1984. Nourishments are generally nearshore nourishments, rainbowing.
82-85.5	690-1800	1. 72-76 2. 88-91	1. 0 2. 0	Bar nourishments
108.5-120	0-240	1. 102-106 2. 121-125	1. 0 2. 0	Bar nourishments
134.5-137	680-1190	129-133	0	Bar nourishments

Km. 42-44.7

As visible from Figure 53, there is no significant effect visible on the first eigenfunction. Eigenfunctions in the nourished section and in the reference area are both in an increasing trend, although this trend is slightly less compared to pre-nourishment data. Steepening after completion of the nourishment was not caused by offshore movement of the reference line, see Appendix H.

Km. 62-66.

In this many nearshore nourishments are applied after the first nourishment in 1985. The first eigenfunction weighting in the very little (max 65 m^3/m) nourished area decreases more than the frequently nourished area. Besides this, also beach nourishments are applied in the reference area, see Figure 24. Eigenfunction weightings indicate that the (shoreface) nourished area became steeper than the reference area. However, in this reference area the coastline retreated up to 33m until 1992 (despite beach nourishments), while in the shoreface nourished area there was progradation of the coastline of over 20m in 1992, see Appendix H. Hence, it could be that the nourishment close to the shore migrated and caused progradation of the coastline. By changing the position of the coastline (refence line), the relative steepness is increased. This did not happen in the reference area, where the coastline kept retreating.

Km. 82-85.5

After the application of the nourishments in 1997-2004, a flattening of the shoreface can be observed; the first eigenfunction remains at approximately 0.95 times the pre-nourishment

level. This level remains until 2012, in a period when no shoreface nourishment are applied. After a nourishment in 2012 the first eigenfunction further decreased further. In the reference areas, the first eigenfunction weighting increased in this period to 1.03 and 1.07.

Moreover, there was coastal progradation in the nourished area (up to 33m), while in the reference area the coastline retreated up to 23m, see Appendix H. As explained above, progradation of the coastline reference results in a relative steepening of the shoreface. The combined progradation of the coastline in combination with (structural) flattening of the shoreface show that the nourishment did significantly strengthen the coast.

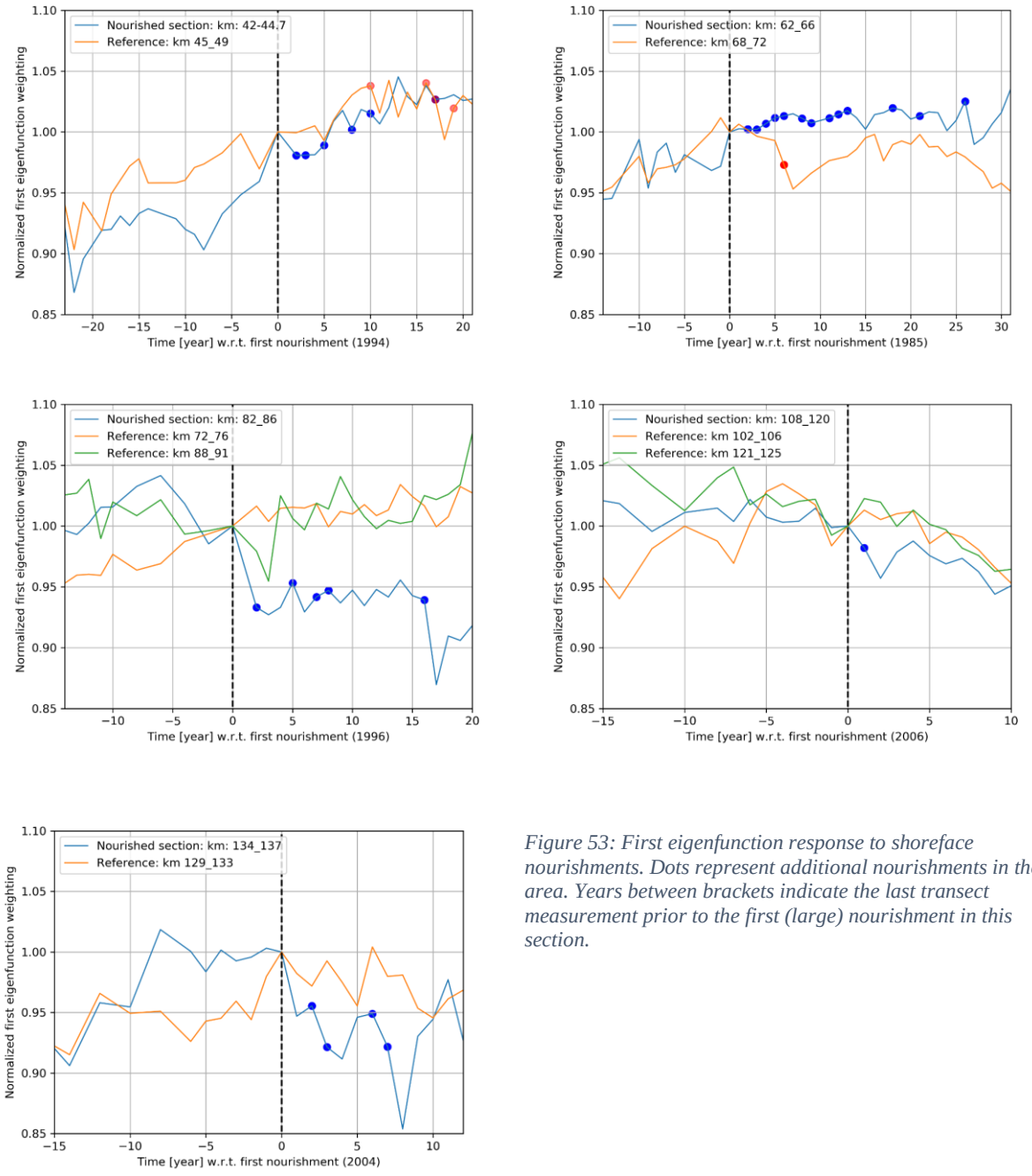

Figure 53: First eigenfunction response to shoreface nourishments. Dots represent additional nourishments in the area. Years between brackets indicate the last transect measurement prior to the first (large) nourishment in this section.

Km. 108.5-120

Although the nourishment volume in this area is small (up to 250 m^3/m), the alongshore component of the nourished section is with 12km large. Also, the reference areas are large alongshore sections without any shoreface nourishments, improving the comparability of the areas.

In the years following the nourishment, the first eigenfunction decreases to 0.96 times the original (pre-nourishment) eigenfunction weighting, i.e. the profile flattens. The reference areas did show a small increase in eigenfunction weighting. However, the difference between both areas gradually decreases. After 10 years, the difference in steepness compared to the pre-nourishment steepness is very small. However, the coastline did accrete 11m in the nourished section while the coastline reference areas retreated with 5m (102-106) and 20m (km. 121-125). This suggests that the nourished sediments do cause (a delayed) progradation of the coast.

Km. 134.5-137

After the application of the nourishment, the first eigenfunction weighting decreases to 0.95 times the original weighting. Several nourishments are applied after the first nourishment in 2004. Every subsequent nourishment initially results in a (sometimes large) decrease of the first eigenfunction weighting. In the following years, eigenfunction weightings increase again.

Due to this fast increase after the nourishment and the decrease of eigenfunction weightings in the reference areas no significant long-term difference is observed in the first eigenfunction weightings 12 years after the first nourishment. In this 12-year period the coastline retreated with 12m in the reference section, while it retreated with 5.5m along the nourished section, see appendix H. Before the application of shoreface nourishment in this area, the area was frequently supplied by sand nourishments, see Figure 24.

Conclusion

Results indicate that the cross-shore placement of the nourishment is an important factor in the morphologic development after a nourishment. Bar nourishments generally decrease the nearshore steepness, while nearshore nourishments do not seem to have a decreasing effect on the steepness. In the latter case, the observed flattening due to the nourishment is usually temporary. After a couple of years, the differences in steepness between the nourished and reference areas decrease. In both cases where the steepness after the nourishments became roughly equal (After 10 years area D and After 12 years area E) did coastline did suffer less erosion (or even accretion) compared to the reference area.

Between km. 82-86 the nourishments seem to have a more constant effect on the nearshore steepness. The first eigenfunction does not increase as quickly as in the other areas. This might be due to the high total nourishment volume, which reaches up 1800 m^3/m.

5.2.2 Reconstruction Denmark

In the northernmost analysed nourishment section, km. 42-44.7, no clear bar signal can be deduced from the eigenfunctions. This is likely because the first eigenfunction already explains 99.5% of the total variance, see Appendix E. In areas where migrating bars are observed this is generally around 97%. The second and third eigenfunction explain in this case around 1.5-2% of the total variance. In this area, the second and third eigenfunction only explain 0.3% of the total variance. For this reason, they are not analysed in detail.

Although the second and third eigenfunction explain a little bit more variance in section km. 62-66, this is still only around 0.6-0.7% of the total variance. In the period until 2004, reconstructions often did not show a clear bar signal, see also Figure 54. From 2005, a clear bar with a crest at 400m and a trough around 200m offshore do show in the reconstruction.

Nourishment area A

The first large nourishment in this area was carried out in 1997. After this nourishment, a local two bar system develops, with an outer bar at 500m from the shoreline and an inner bar at 180-200m. Until 2004 this area is nourished frequently, see also Figure 52. Until 2007, bar roughly remain in their cross-shore position. In the 2009 measurement offshore migration is visible. Bars continue to migrate offshore, in 2016 the prior inner bar has almost reached the cross-shore position of the prior outer bar. In other words, almost one complete bar cycle has been fulfilled.

Nourishment area B

Nourishments are executed in 2006 and 2007. No clear bar signal is reconstructed. This might be due to the irregular placement of the nourishments, see Figure 51. In 2009 and more clearly in 2011, a bar crest forms at 250m from the shoreline. This bar migrates offshore in the following years.

Nourishment area C

The nourishments are primarily executed between 2004 and 2011. Just as in nourishment area B, no clear bar signal is reconstructed. Between 2004 and 2007, a bar can be observed around 200m from the shoreline. From 2009, no bar can be observed at all.

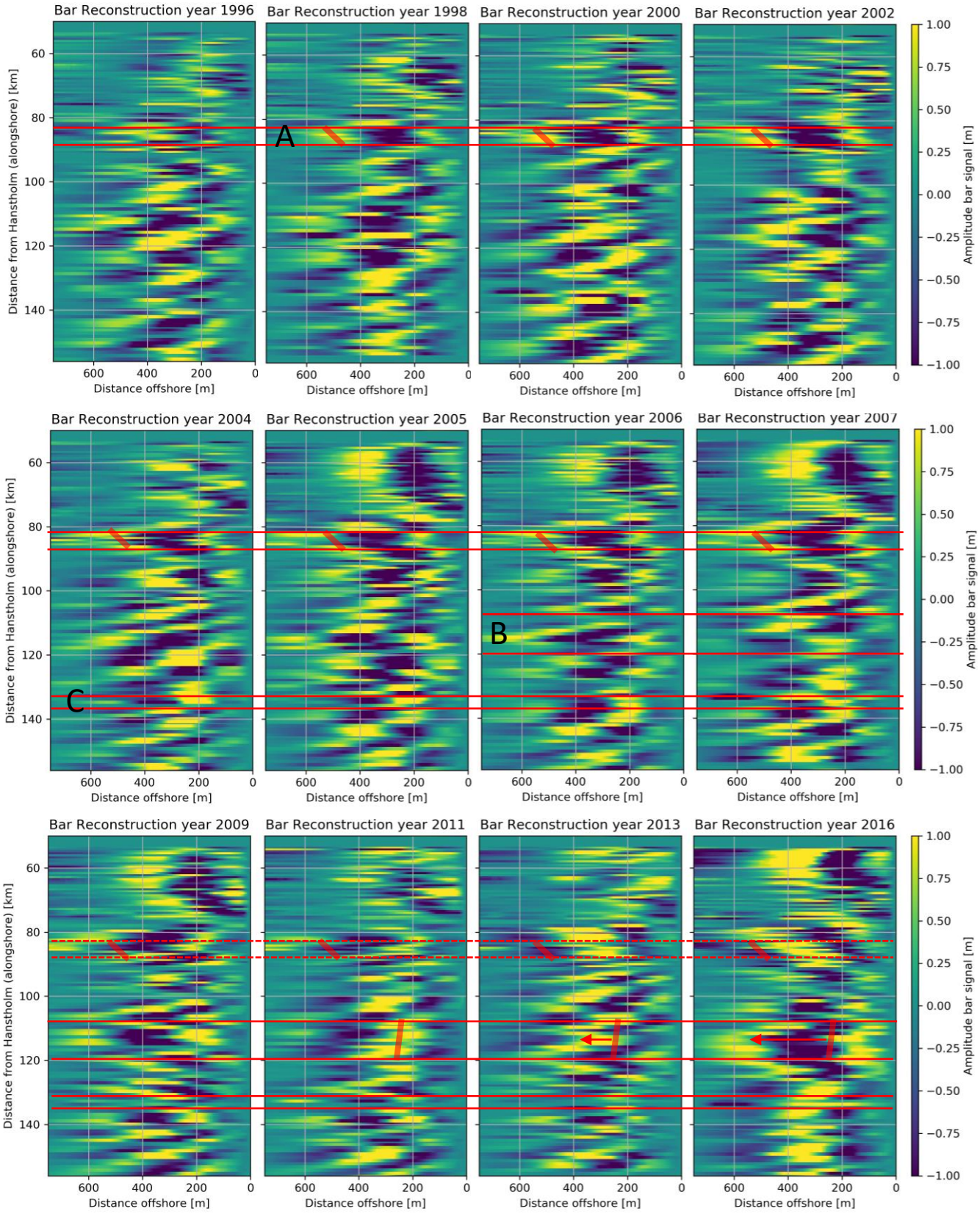

Figure 54: Reconstruction of bar signal, post-nourishment

6. Discussion

This chapter contains a critical reflection on the interpretation of the findings in this research. The role of (uncertainties in) the dataset on the outcome of this research is evaluated and the outcome of the eigenfunction analysis is discussed.

Data accuracy, availability and interpolation

Measurement errors and interpolation of data over large cross-shore distances do influence the accuracy of input profiles of the eigenfunction analysis. Especially for old measurements along the Danish coast, there has been interpolated over large cross-shore distances (20-80m). Linear interpolation over such long distances can influence the shape of the profile measurement significantly. Moreover, old measurement methods are undocumented and have probably high measurement errors. Also, the temporal and spatial (i.e. the distance between transects) interval is large along the Danish coast. The errors occurring due to measurement inaccuracy and interpolation over large cross-shore distances, combined with low alongshore coherence due to the large distance between transects, probably contributed to the irregular and noisy bar signal observed along the Danish coast.

Since the eigenfunction analysis requires a highly consistent dataset, transect measurements that reach between 640 and 750m from the shoreline have been extrapolated up to 750m with data of the time-averaged profile. Therefore, no or little sandbars are present in the extrapolated sections generally. Along km. 70-90 of the Holland coast, this extrapolation occurred for a significant part (over 35%) of the total data, see Appendix G. This extrapolation can have affected the shape of the second and third eigenfunction loadings, resulting in flattening of the eigenfunction shape from 640m offshore. Along other coastal stretches, the percentage of extrapolated profiles is much lower.

Floating reference line

Because a floating reference line has been used, bars are analysed relative to this line. This approach is useful to analyse the same section of the coast over a long time period, even if the coastline is in a retreating trend. In case of movement of this reference line, there is an error in the calculation of the absolute bar migration. In a long-term analysis, the errors due to variability of the coastline average out since the net migration of the coast over multiple years is low and insignificant compared to the offshore moving bars (20-60m/year). For shorter time spans (e.g. the year-to-year evaluation after nourishments), these errors due to variability of the coastline can be significant compared to the bar migration. Therefore, the average movement of the coastline is evaluated to obtain the actual bar migration.

The alongshore uniformity of bars is also based on the position with respect to the floating reference line. It is thereby assumed that the floating reference is a straight line. However, this is not necessarily true, especially in the case of constructions (moles, groynes, dykes). Based on a bathymetry plot of the Noord-Holland coast, different conclusions can be drawn on the obliqueness of the bar observed here, see Appendix J. Moreover, the axes used in the eigenfunction figures do not have the same scale (100m cross-shore is equal to 4700m/5700m alongshore for the Dutch/Danish coast respectively), therefore obliquity of the bars is distortedly illustrated.

Eigenfunction analysis

Eigenfunction analysis has shown to be a useful tool to analyse nearshore morphologic processes. However, by analysing the coast with only the most three dominant patterns of variation (eigenfunctions), one should be careful interpreting the eigenfunction results.

First eigenfunction

The first eigenfunction is very closely related to the mean profile. Per observation, the weighting of the first eigenfunction is determined, based on how it can reduce most of the variance in the dataset. When (large) disproportional changes happen in the steepness of the profile (for example after a nourishment or after disproportional steepening in the profile), the shape of the eigenfunction does not correspond well with the shape of the profile. After a nourishment the weighting of the first eigenfunction generally decreases. This indicates a flatter profile, but this does not have to be the case along the whole profile. A change in depth at the most offshore part already causes the eigenfunction weighting to decrease, see the fourth observation in Figure 55. The dashed black line shows a too flat profile for the first 400m offshore, while the depth from 500m offshore is overestimated by the first eigenfunction.

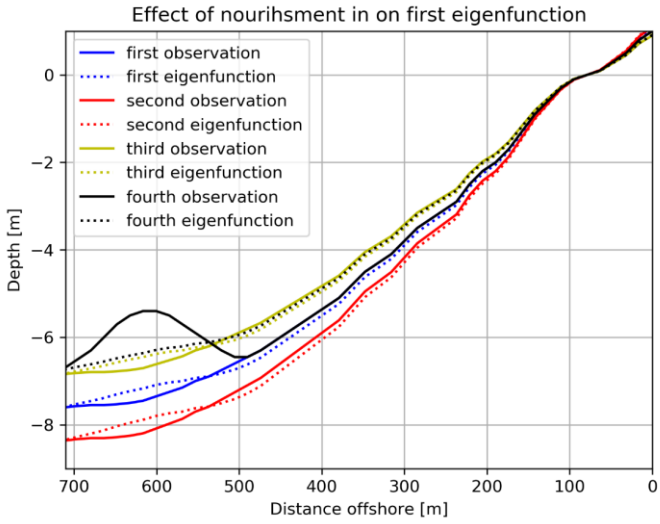

Figure 55: Example of misinterpretation of the first eigenfunction. Solid lines are actual (fictitious) measurement. Dashed lines are there representation by the first eigenfunction.

This mismatch of the first eigenfunction with profile measurements (after steepening/nourishments) results in increased residual variance for the second and third eigenfunction. Consequently, the eigenfunction loadings might become a mixture of bar processes and variance due to steepness changes. This is particularly observed in the long-term (1900-2016) analysis of the Danish coast, see Appendix F. However, also without influencing the eigenfunction loadings, the application of a nourishment can influence the weightings of the second and third eigenfunction. Along the Holland coast, generally a weak and vague bar signal is observed in the first year(s) after the application of a nourishment. This weak signal might be caused by the extra residual variance originating from the above described mismatch between first eigenfunction and the profile observation.

Second and third eigenfunction

Similar erroneous conclusions on nearshore morphology can also be drawn based on a second or third eigenfunction. These eigenfunctions generally describe bars. If an eigenfunction consists of a small bar close to the shore and a large bar further offshore, the former contains due to its size more variance compared to the latter. If in a specific observation, this small bar is absent, and the large offshore bar is present, the small bar will still be generated by the

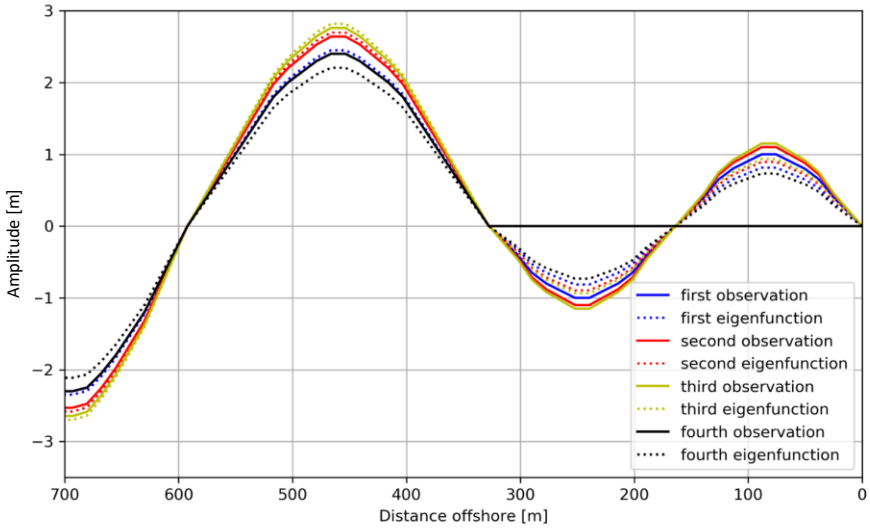

Figure 56: False bar signal in second eigenfunction

eigenfunction. This is shown in Figure 56. Although no significant mismatches have been found, this should be kept in mind when interpreting the results. It could be that an inner bar is reconstructed though it is not actually present.

Migration velocity

The migration velocity is based on the bar spacing and the bar cycle return period. Since the large (outer) bars predominate in the average bar spacing, the migration velocity mostly resembles the migration velocity of the largest outer bar. Moreover, this bar cycle return period is determined by calculating the autocorrelation of the second eigenfunction weightings. This autocorrelation is insignificant however along some coastal stretches, for example north of the IJmuiden harbour moles. This illustrates that the bar cycle return period is not constant, i.e. periods with faster and slower migrating bars are present. Therefore, visual inspection of the eigenfunction weightings is needed to interpret the bar cycle return period based on the autocorrelation. This also demonstrates that obtained values of bar cycle return period and offshore migration velocities are average values which change from year to year.

7. Conclusions

This first section (7.1) answers the first research question regarding the pre-nourishment morphologic behaviour. The second section (7.2) answers the second research question regarding the post-nourishment behaviour.

7.1 Research Question 1

What regions with similar nearshore morphologic behaviour can be characterized along the Dutch and Danish North Sea coast?

Various regions with similar nearshore morphologic behaviour can be observed along the Dutch and Danish analysed coasts. These regions are based on (trends in) steepness, development of the coastline, presence of nearshore sandbars and their migration. These regions are stated below.

Area 1: Holland coast, km. 7-26.

- Time-averaged slopes 1:60 to 1:90.
- Constant slope. Severe steepening along northern boundary (km. 5-7) part, close to the Marsdiep inlet.
- Retreat of the coastline (without nourishments)
- 1 bar in the shoreface
- Nearshore sandbar does not show net cross-shore migration.

Figure 57: Regions with similar nearshore morphologic behaviour along the Holland coast

Area 2: Holland coast, km. 26-55

- Time-averaged slopes between 1:100 and 1:115 (close to IJmuiden).
- No long-term steepening or flattening trend, only small year-to-year variations.
- Retreat of the coastline (without nourishments)
- Close to the IJmuiden moles, accretion of the coast
- Offshore bar migration with a bar cycle return period of 15 years, with a range of 12-18 years.
- The bars are often slightly shore oblique, close to the shore in the north and further offshore in the south.
- 3 bars in the shoreface
- Bar spacing of 320m and offshore migration velocity of around 21m/year (range 18-24 m/year).

Area 3: Holland coast, km. 55-97

- Time-averaged slopes between 1:115 and 1:135 (close to IJmuiden)
- Slightly steepening and stable position of the coastline (without nourishments)
- Severe (900m) progradation of the coast close to the IJmuiden moles.
- Offshore bar migration with a bar cycle return period of 3-4 years in the between km. 60-70 and 4 years south of km. 70
- 3-4 bars in the shoreface
- Bar spacing roughly 230m and the offshore migration velocity is around 60-75 m/year.

Area 1: Danish coast, km. 0-22

- Time-averaged slopes between 1:75 and 1:105, influenced by constructions and changes in orientation of the coastline.
- No significant steepening or flattening of the shoreface and a stable position of the coastline.
- Generally, one nearshore bar in the profile, between 100 and 400m from the shoreline.
- With the eigenfunction analysis no bar migration pattern has been found.

Area 2: Danish coast, km. 22-79

- Time-averaged slopes between 1:55 and 1:95 (period 1957-2016).
- Severe steepening of the shoreface. Along km. 40-79 the steepness has increased 30-50 percent since 1900.
- Between km. 30-79 there is severe erosion of the coastline.
- Generally, one bar is present in the nearshore region, commonly present between 150 and 400m from the shoreline.
- With the used eigenfunction analysis no bar migration pattern has been found.

Figure 58: Regions with similar nearshore morphologic behaviour along the Danish coast

Area 3: Danish coast, km 79-156

- Time-averaged slopes between 1:100 and 1:115
- Variations in steepness, as well areas with flattening as steepening are observed.
- Erosion of the coastline, especially between km. 79-100 severe erosion of the coastline.
- Two bars in the nearshore region, commonly present between 100 and 600m from the shoreline. These bars are generally shore oblique and migrate offshore. The alongshore uniformity and consistency in bar migration and bar position is low.
- The bar cycle return period is estimated between eight and twelve years.
- The bar spacings range from 300-440m and the average offshore migration velocity is between 25-55m per year.

7.2 Research Question 2

This question contains three sub-questions:

7.2.1 Sub-question 1

How do shoreface nourishments influence the steepness of the shoreface?

In all cases of bar nourishment, the steepness is initially reduced. The decreased steepness is a logical result of the decreased depth due to the nourishment. Based on the results from the first eigenfunction is not possible to conclude whether this flatter profile is caused by decreased depth at the cross-shore placement location of the nourishment or due to cross-shore spreading over the shoreface. The magnitude of the decrease in steepness and its temporal component varies for different nourishments.

Along the analysed Dutch coast without cross-shore migrating sandbars, the post-nourishment profiles largely remained their flatter shape for a long period, namely at least 8 years. Along

the Dutch and Danish coast with migrating sandbars the nearshore steepness also flattens, but generally returns quick (3-10 years) to pre-nourishment conditions. Some of the nourishments in the Netherlands have been applied partly outside of the analysed cross-shore section, which complicates equal comparison between the nourishments.

In Denmark, there have been apart from bar nourishments (with the above described effect) also nearshore nourishments applied. In case of a nearshore nourishment, sediment is supplied close to the shore just below water level by rainbowing. No decrease of steepness has been observed for this type of nourishment.

7.2.2 Sub-question 2

How do shoreface nourishments influence the migration of nearshore sandbars?

As confirmed by many other authors investigating individual nourishments along the Dutch coast, nourishments along the Holland coast temporally stop the offshore migration of nearshore sandbars, at least 3-6 years. This research shows that the duration of affected bar migration after a single nourishment is significantly longer. The period of affected migration can be up to 13 years along the Holland coast according to this research.

Along km. 30-55, where bars migrate offshore with a return period of 15 years, it is difficult to assess the influence of a single nourishment. Often, several nourishments are executed along a coastal stretch within this return period. Several nourishments together cause stagnation of the nearshore bars. From 2007 until 2016 the sandbar present along km. 30-40 shows little to no net offshore migration. It is not expected that the bar migration along km. 30-40 will return to pre-nourishment conditions quickly, since a new nourishment has been applied here in 2016. Hence, the current nourishment practice causes stagnation of the offshore moving bars at this location. The interval between the nourishments is not large enough to make offshore migration of the sandbars possible.

South of the IJmuiden harbour moles, the duration of affected offshore migration after a nourishment is highly variable, between one and thirteen years. For some nourishments the reduction of offshore migration is temporarily, and offshore bar migration is observed with pre-nourishment velocities. However, there exist also areas (e.g. km. 73-80, 91-97) where bars barely migrate, even though the last nourishment was completed 14 and 11 years ago respectively.

Results of this research show that along the Holland coast (repeated) nourishments influence the offshore bar migration up to 2km alongshore from the borders of the nourished section. However, bar switches often occur directly at the borders of the nourished section. This means that alongshore effects of the repeated nourishments is found to be very small.

Due to the inconsistent pre-nourishment bar migration, no significant effect of nourishments on bar migration has been found for the Danish coast. Only along km. 82-85.5 the influence of nourishments on the nearshore morphology is clearly visible. Here, the largest nourishments in terms of volume per metre are applied. Since the first large nourishment in 1997, a two-bar system had developed which did not migrate until 2007. From 2007, the bar started to migrate offshore, three years after the last major nourishment in the area.

7.2.3 Sub-question 3

Is the post-nourishment nearshore morphologic behaviour region-specific or do nourishment implementation characteristics govern this morphologic behaviour?

This question remains largely unanswered. No consistent relation between implementation characteristics and effect on the bar system has been observed. On average, a larger nourishment volume has a larger and longer effect on the bar system, but this does not necessarily have to be the case. In the northern area of the Netherlands (km- 5-26) nourishments have a long-term effect on the steepness of the average profile. Nourishments do not seem to erode quickly here. In other areas, where offshore moving bars were observed, the effect on the nearshore slope is less and shorter.

7.3 Suggestions for further research

To obtain a more thorough understanding of differences in the nearshore morphology of the complete NSR coast, also other parts of the Interreg Building with Nature dataset can be studied using eigenfunction analysis. A more detailed or focussed approach is then needed, since these areas often not cover large (inlet free) coastal stretches or not have a large history of shoreface measurements. By investigating also other parts of the NSR, a more complete picture of nearshore morphologic behaviour and variability herein can be obtained. With this more complete picture, general relations can be investigated between nearshore characteristics (e.g. wave-activity, tide/tidal current, grain sizes) and morphologic behaviour.

If an eigenfunction analysis would be repeated for some of the same stretches, one eigenfunction window can be used for an area with similar bar behaviour. This simplifies eigenfunction results because there is only one (first/second/third) eigenfunction shape for a coastal stretch instead of many. Analysing new stretches requires however the same moving window approach as in this report, since the variability in sandbars is often unknown.

Many studies, including this study, have analysed bar migration both pre- and post-nourishment. Bars migrate towards a zone of decay as well as nourishments after depletion. There is still a lack of knowledge on how hydrodynamic and wave characteristics affect mobilization of the sediments in this zone of decay and how these sediments are redistributed. It is likely that the duration of stagnated bar migration depends on the decay of the nourishment. This study has shown that this duration can be significantly longer than the original bar cycle. It is still unclear what causes this large difference, both in between nourishments as well as compared to the original bar cycle. Causal relationships are difficult to determine due to the many variables (e.g. sediment diameter size and distribution, nourished volume per running metre, total nourished volume, wave-variability (storm-events), placement depth and the pre-nourishment morphologic behaviour). Moreover, the nourished grain size is often given with a wide range or without a range, if available at all.

To thoroughly understand the influence of shoreface nourishments, more research is needed to understand the hydrodynamics near the seabed in the zone of decay. Measuring grain sizes and nearshore hydrodynamics, combined with morphologic simulation model studies such as Delft3D could provide insight why the effect of these shoreface nourishments is so different after depletion.

8. References

Aagaard, T., & Kroon, A. (2007). Mesoscale behaviour of longshore bars—net onshore or net offshore migration. *Coastal Sediments' 07*, 2124-2136. doi:10.1061/40926(239)167

Aagaard, T., Kroon, A., Greenwood, B., & Hughes, M. G. (2010). Observations of offshore bar decay: Sediment budgets and the role of lower shoreface processes. *Continental Shelf Research, 30*(14), 1497-1510. doi:https://doi.org/10.1016/j.csr.2010.05.010

Ahrendt, K. (2001). Expected effect of climate change on Sylt island: results from a multidisciplinary German project. *Climate Research, 18*(1/2), 141-146. doi:10.3354/cr018141

Bockelmann, F.-D., Puls, W., Kleeberg, U., Müller, D., & Emeis, K.-C. (2018). Mapping mud content and median grain-size of North Sea sediments – A geostatistical approach. *Marine Geology, 397*, 60-71. doi:https://doi.org/10.1016/j.margeo.2017.11.003

Brettschneider, G. (1967). *Anwendung des hydrodynamisch-numerischen Verfahrens zur Ermittlung der M2-Mitschwingungsgezeit der Nordsee*, 65.

Bruins, R. J. (2016). *Morphological behaviour of shoreface nourishments along the Dutch coast.* (MSc thesis), TU Delft, Delft. Retrieved from https://repository.tudelft.nl/islandora/object/uuid:e7585706-571d-4b97-8b89-d7c7abd9730c/datastream/OBJ/download

Damsma, T., Aarninkhof, S. G. J., Van Koningsveld, M., Walstra, D. J. R., De Vries, S., Geleynse, N., & Stive, M. J. F. (2009). *Dune growth on natural and nourished beaches.* (Master Thesis), Delft University of Technology, Delft. Retrieved from https://repository.tudelft.nl/islandora/object/uuid%3A96c401cb-fa67-407b-ab0d-8429452ba50b

Danish Coastal Authority. (2011). Kystbeskyttelse ved Ferring Sø og Vejlby Klit. Retrieved from http://omkystdirektoratet.kyst.dk/pages/webside.asp?articleGuid=61785

Dashtgard, S. E., MacEachern, J. A., Frey, S. E., & Gingras, M. K. (2012). Tidal effects on the shoreface: towards a conceptual framework. *Sedimentary Geology, 279*, 42-61. doi:https://doi.org/10.1016/j.sedgeo.2010.09.006

De Graaf, H. J. C., Oude Elberink, S. J., Bollweg, A. E., Brügelmann, R., & Richardson, L. R. A. (2003). *Inwinning "Droge" Jarkus Profielen Langs Nederlandse Kust*. Rijkswaterstaat Retrieved from https://publicwiki.deltares.nl/download/attachments/73434331/AGI-GAM-2003-40.pdf?version=1&modificationDate=1329221465000.

De Hauwere, N. (2016). Bathymetry of the North Sea. Retrieved from http://www.marineregions.org/maps.php?album=3747&pic=115811

de Sonneville, B., & Van der Spek, A. (2012). Sediment-and morphodynamics of shoreface nourishments along the North-Holland coast. *Coastal Engineering Proceedings, 1*(33), 44.

Deltares. (2013). *Ontwikkeling suppletie tussen Den Helder en Julianadorp 2007* Delft http://publications.deltares.nl/1206171_000a.pdf

Deltares. (2017a). *Morphan User Manual*. Delft https://content.oss.deltares.nl/delft3d/manuals/MorphAn_User_Manual.pdf

Deltares. (2017b). *Ontwikkeling suppletie Heemskerk 2011-2016* (1230043-001). Delft

Di Leonardo, D., & Ruggiero, P. (2015). Regional scale sandbar variability: Observations from the U.S. Pacific Northwest. *Continental Shelf Research, 95*, 74-88. doi:https://doi.org/10.1016/j.csr.2014.12.012

Egbert, G. D., Erofeeva, S. Y., & Ray, R. D. (2010). Assimilation of altimetry data for nonlinear shallow-water tides: Quarter-diurnal tides of the Northwest European Shelf. *Continental Shelf Research, 30*(6), 668-679. doi:https://doi.org/10.1016/j.csr.2009.10.011

Elgar, S., Gallagher, E. L., & Guza, R. T. (2001). Nearshore sandbar migration. *Journal of Geophysical Research: Oceans, 106*(C6), 11623-11627. doi:doi:10.1029/2000JC000389

Grunnet, N. M., & Ruessink, B. G. (2005). Morphodynamic response of nearshore bars to a shoreface nourishment. *Coastal Engineering, 52*(2), 119-137. doi:https://doi.org/10.1016/j.coastaleng.2004.09.006

Hoefel, F., & Elgar, S. (2003). Wave-Induced Sediment Transport and Sandbar Migration. *Science, 299*, 1885. doi:10.1126/science.1081448

Holzhauer, H., Valk, B. v. d., Tonnon, P. K., & Baptist, M. J. (2009). *Megasuppleties langs de Nederlandse kust*. IJmuiden [etc.] http://edepot.wur.nl/8939

Kaergaard, K., Fredsoe, J., & Knudsen, S. B. (2012). Coastline undulations on the West Coast of Denmark: Offshore extent, relation to breaker bars and transported sediment volume. *Coastal Engineering, 60*, 109-122. doi:https://doi.org/10.1016/j.coastaleng.2011.09.002

Kleinhans, M., Jagers, H., Mosselman, E., & Sloff, C. (2008). Bifurcation dynamics and avulsion duration in meandering rivers by one-dimensional and three-dimensional models. *Water resources research, 44*(8). doi:https://doi.org/10.1029/2007WR005912

Langenberg, H. (1997). Interactions of wind and density driven currents in North Sea ROFIs—a model study. *Journal of Marine Systems, 12*(1), 157-170. doi:https://doi.org/10.1016/S0924-7963(96)00095-4
Lodder, Q. J., & Sørensen, P. (2015). Comparing the morphological behaviour of Dutch-Danish shoreface nourishments. In A. Baptiste (Ed.), *Coastal Management: Changing coast, changing climate, changing mind*.
McGlade, J. M. (2002). 12 The North Sea Large Marine Ecosystem. In K. Sherman & H. R. Skjoldal (Eds.), *Large Marine Ecosystems* (Vol. 10, pp. 339-412): Elsevier.
Miller, J. K., & Dean, R. G. (2007). Shoreline variability via empirical orthogonal function analysis: Part I temporal and spatial characteristics. *Coastal Engineering, 54*(2), 111-131. doi:https://doi.org/10.1016/j.coastaleng.2006.08.013
Naus, I. M. (2018). *Quantification of coastal morphological characteristics for transect profiles along the North Sea coast* (MSc Intership report). Rijkswaterstaat
Nauw, J., de Haas, H., & Rehder, G. (2015). A review of oceanographic and meteorological controls on the North Sea circulation and hydrodynamics with a view to the fate of North Sea methane from well site 22/4b and other seabed sources. *Marine and Petroleum Geology, 68*, 861-882. doi:https://doi.org/10.1016/j.marpetgeo.2015.08.007
Niemann, S., Sloth, P., Buhl, J., Deigaard, R., & Brøker, I. (2011). THYBORØN HARBOUR–STUDY OF WAVE AGITATION AND SEDIMENTATION. *Coastal Engineering Proceedings, 1*(32), 41.
Ojeda, E., Ruessink, B. G., & Guillen, J. (2008). Morphodynamic response of a two-barred beach to a shoreface nourishment. *Coastal Engineering, 55*(12), 1185-1196. doi:https://doi.org/10.1016/j.coastaleng.2008.05.006
OSPAR. (2000). *Quality Status Report 2000, Region II Greater North Sea*. London: OSPAR Commission.
Quartel, S., & Grasmeijer, B. (2007). Dynamiek van het strand bij Noordwijk aan Zee en Egmond aan Zee en het effect van suppleties. *Rijksinstituut voor Kust en Zee (RIKZ). Opdracht RKZ-1667*.
Quartel, S., Kroon, A., & Ruessink, B. (2008). Seasonal accretion and erosion patterns of a microtidal sandy beach. *Marine Geology, 250*(1-2), 19-33.
Rijkswaterstaat. (2003). *Technische evaluatie onderwatersuppleties Noordwijkerhout & Wassenaar*. https://publicwiki.deltares.nl/display/KPP/Rapporten+Rijkswaterstaat
Ringkøbing Fjord Turisme. (2018). The water lock in Hvide Sande. Retrieved from https://www.hvidesande.com/ln-int/hvide-sande/water-lock-hvide-sande
Ruessink, B. G., Pape, L., & Turner, I. L. (2009). Daily to interannual cross-shore sandbar migration: Observations from a multiple sandbar system. *Continental Shelf Research, 29*(14), 1663-1677. doi:https://doi.org/10.1016/j.csr.2009.05.011
Schloen, J., Stanev, E. V., & Grashorn, S. (2017). Wave-current interactions in the southern North Sea: The impact on salinity. *Ocean Modelling, 111*, 19-37. doi:https://doi.org/10.1016/j.ocemod.2017.01.003
Shand, R. D., Bailey, D. G., & Shephard, M. J. (1999). An inter-site comparison of net offshore bar migration characteristics and environmental conditions. *Journal of Coastal Research, 15*, 750-765.
Shand, R. D., Bailey, D. G., & Shepherd, M. J. (2001). Longshore realignment of shore-parallel sand-bars at Wanganui, New Zealand. *Marine Geology, 179*(3), 147-161. doi:https://doi.org/10.1016/S0025-3227(01)00223-7
Shields, A. (1936). Anwendung der Aehnlichkeitsmechanik und der Turbulenzforschung auf die Geschiebebewegung. *PhD Thesis Technical University Berlin*.
Short, A. (1991). Macro-meso tidal beach morphodynamics: an overview. *Journal of Coastal Research*, 417-436.
Sündermann, J. (2003). The changing North Sea: Knowledge, speculation and new challenges. *Oceanologia, 45*(2), 247-259.
Sündermann, J., & Pohlmann, T. (2011). A brief analysis of North Sea physics. *Oceanologia, 53*(3), 663-689. doi:https://doi.org/10.5697/oc.53-3.663
Thomsen, M. A., S.K.
Lassen, A. (2018). *Building with Nature: Systems Description of Krogen*. Lemvig
http://www.masterpiece.dk/UploadetFiles/10852/36/SystemdescriptionofKrogen_10.08.18_web.pdf
Thorsminde Havn. (2018). Slusen. Retrieved from http://www.thorsmindehavn.dk/slusen.html
Turrell, W. R., Henderson, E. W., Slesser, G., Payne, R., & Adams, R. D. (1992). Seasonal changes in the circulation of the northern North Sea. *Continental Shelf Research, 12*(2), 257-286. doi:https://doi.org/10.1016/0278-4343(92)90032-F
Van Der A, D. A., O'Donoghue, T., Davies, A. G., & Ribberink, J. S. (2011). Experimental study of the turbulent boundary layer in acceleration-skewed oscillatory flow. *Journal of fluid mechanics, 684*, 251-283. doi:DOI: 10.1017/jfm.2011.300

Van Der Spek, A. J. F., De Kruif, A. C., & Spanhoff, R. (2007). *Richtlijnen onderwatersuppleties (Dutch)*. https://repository.tudelft.nl/islandora/object/uuid%3Af310d329-c75a-409a-8422-f8041601d95a?collection=research
Van Der Zanden, J., Hurther, D., Caceres, I., O'Donoghue, T., Hulscher, S. J., & Ribberink, J. S. (2017). Bedload and suspended load contributions to breaker bar morphodynamics. *Coastal Engineering, 129*, 74-92. doi:10.1016/j.coastaleng.2017.09.005
Van Dijk, T. A., & Kleinhans, M. G. (2005). Processes controlling the dynamics of compound sand waves in the North Sea, Netherlands. *Journal of Geophysical Research: Earth Surface, 110*(F4). doi:https://doi.org/10.1029/2004JF000173
Van Duin, M. J. P., Wiersma, N. R., Walstra, D. J. R., van Rijn, L. C., & Stive, M. J. F. (2004). Nourishing the shoreface: observations and hindcasting of the Egmond case, The Netherlands. *Coastal Engineering, 51*(8), 813-837. doi:https://doi.org/10.1016/j.coastaleng.2004.07.011
van Enckevort, I. M. J., & Ruessink, B. G. (2003). Video observations of nearshore bar behaviour. Part 1: alongshore uniform variability. *Continental Shelf Research, 23*(5), 501-512. doi:https://doi.org/10.1016/S0278-4343(02)00234-0
Van Rijn, L. C. (1997). Sediment transport and budget of the central coastal zone of Holland. *Coastal Engineering, 32*(1), 61-90.
Verwaest, T., Laustrup, C., Madsen, H. T., Allen-Williams, P., Hofstede, J., & Roeise, P. (2000). *Nourishment Practice in the North Sea Countries*. http://www.kfki.de/files/nscmg-publikationen/0/Nourishment_practices_in_the_North_Sea_Countries_may_2000.pdf
Veugen, L. (1984). De nauwkeurigheid van strandpro fielen, fotogrammetrische data-acquisitie. Report. Rijkswaterstaat, Delft, 20 pp: Dutch.
Walstra, D. J. R. (2016). *On the anatomy of nearshore sandbars.* (PhD Thesis), Delft University of Technology, Delft. Retrieved from https://repository.tudelft.nl/islandora/object/uuid%3A3f86bf04-c6af-486f-b972-bd228d84ebed
Walstra, D. J. R., Ruessink, B. G., Reniers, A. J. H. M., & Ranasinghe, R. W. M. R. J. (2015). Process-based modeling of kilometer-scale alongshore sandbar variability. *Earth surface processes and landforms, 40*(8), 995-1005. doi:https://doi.org/10.1002/esp.3676
Waterloopkundig Laboratorium. (1992). *Krokus-stormen, duinafslag voorjaarstormen 1990*. Emmeloord http://publicaties.minienm.nl/documenten/krokus-stormen-duinafslag-voorjaarsstormen-1990-toetsing-durosta
Wiegman, N., Perluka, R., & Boogaard, K. (2002). *Onderzoek naar efficiency verbetering kustlodingen (Dutch)*. Rijkswaterstaat Retrieved from https://repository.tudelft.nl/islandora/object/uuid%3A33ef8d2f-dcb3-4656-8536-66bee2902cd8.
Wijnberg, K. M. (1995). *Morphologic Behaviour of a Barred Coast Over a Period of Decades*. Utrecht: Koninklijk Nederlands Aardrijkskundig Genootschap.
Wijnberg, K. M. (1997). On the systematic offshore decay of breaker bars *Coastal Engineering 1996* (pp. 3600-3613).
Wijnberg, K. M., & Terwindt, J. H. J. (1995). Extracting decadal morphological behaviour from high-resolution, long-term bathymetric surveys along the Holland coast using eigenfunction analysis. *Marine Geology, 126*(1-4), 301-330. doi:https://doi.org/10.1016/0025-3227(95)00084-C
Wilmink, R. J. A., Lodder, Q. J., & Sørensen, P. (2017). *Assessment of the design and behaviour of nourishments in the North Sea Region.* Paper presented at the Coastal Dynamics.
Winant, C. D., Inman, D. L., & Nordstrom, C. E. (1975). Description of seasonal beach changes using empirical eigenfunctions. *Journal of Geophysical Research, 80*(15), 1979-1986. doi:https://doi.org/10.1029/JC080i015p01979
Wright, L., & Short, A. D. (1984). Morphodynamic variability of surf zones and beaches: a synthesis. *Marine Geology, 56*(1-4), 93-118. doi:https://doi.org/10.1016/0025-3227(84)90008-2

Appendix A: Mathematical derivation of eigenfunctions

The eigenfunction analysis based on singular value decomposition (SVD) of the dataset. Using SVD, a rectangular matrix $[\boldsymbol{D}]$ can be factorized or decomposed into three other matrixes.

$$[\boldsymbol{D}] = [\boldsymbol{E}] \cdot [\boldsymbol{S}] \cdot [\boldsymbol{V}]^T \tag{6}$$

In which

$[\boldsymbol{E}]$ Matrix with eigenfunctions of the major product matrix: $[\boldsymbol{D}] \cdot [\boldsymbol{D}]^T$

$[\boldsymbol{V^T}]$ Transpose of matrix with eigenfunctions of the minor product matrix: $[\boldsymbol{D}]^T \cdot [\boldsymbol{D}]$

$[\boldsymbol{S}]$ Matrix with square roots of eigenvalues (singular values) corresponding to major and minor product matrix

The matrix $[\boldsymbol{E}]$ can be obtained by solving:

$$[\boldsymbol{U}] \cdot [\boldsymbol{E}] = \lambda_k \cdot [\boldsymbol{E}] \tag{7}$$

In which

$[\boldsymbol{U}]$ Major product matrix: $[\boldsymbol{D}] \cdot [\boldsymbol{D}]^T$

$[\boldsymbol{E}]$ Eigenvectors corresponding to the product matrix

λ_k Eigenvalues corresponding to the eigenvectors in matrix $[\boldsymbol{E}]$

Equation (7) can be solved using the characteristic that the determinant of matrix $[\boldsymbol{U}]$ must be zero. Eigenvalues λ_k can be found for which the determinant of the matrix $[\boldsymbol{U}]$ is zero. These eigenvalues, or more exactly their square roots, form matrix $[\boldsymbol{S}]$. With $[\boldsymbol{U}]$ and λ_k known, matrix $[\boldsymbol{E}]$ containing the eigenfunctions can be derived.

Since the eigenvalues λ_k give information about the extent to which this eigenvector applies to the data, matrix $[\boldsymbol{E}]$ will be ranked on the corresponding eigenvalues. In this way, eigenvectors explaining most of the variance in the dataset will come out as a first eigenfunction. Also, the eigenvectors are normalized so that the sum of the squares in a vector will be equal to one. This is convenient since in this way the length of all eigenvectors is one. Since the eigenfunctions are normalized, the eigenfunctions do not give information about the amplitude of the process. This is accounted for in the corresponding eigenvalue. Matrix $[\boldsymbol{E}]$ can be scaled with the matrix with the eigenvalues $[\boldsymbol{S}]$.

The matrix $[\boldsymbol{V^T}]$ can be solved similar as equation (7), only now with a minor instead of major product matrix.

$$[\boldsymbol{U}] \cdot [\boldsymbol{V}] = \lambda_k \cdot [\boldsymbol{V}] \tag{8}$$

In which

$[\boldsymbol{U}]$ Minor product matrix $[\boldsymbol{D}]^T \cdot [\boldsymbol{D}]$

$[\boldsymbol{V}]$ Eigenvectors corresponding to the product matrix

λ_k Eigenvalues corresponding to the eigenvectors in matrix $[\boldsymbol{V}]$

Appendix A1: Example calculation

In this example calculation is based on a calculation example of the University of Minnesota (http://www.d.umn.edu/~mhampton/m4326svd_example.pdf).

As a representation of profile data, a very simplified data matrix $[\boldsymbol{D}]$ is assumed. In this data matrix each column is a very simplified (and unrealistic) representation of a profile measurement with two cross shore measurement points.

$$[\boldsymbol{D}] = \begin{bmatrix} 3 & 2 & 2 \\ 2 & 3 & -2 \end{bmatrix} \tag{9}$$

From this data matrix, measures of correlation were calculated, from which eigenvectors are determined. Wijnberg (1995) determined the measure of correlation by calculating the uncorrected sum of products matrix, given by:

$$[\boldsymbol{U}] = [\boldsymbol{D}] \cdot [\boldsymbol{D}]^T \tag{10}$$

In which:

$[\boldsymbol{U}]$ Uncorrected sum of products matrix
$[\boldsymbol{D}]$ Matrix of depth values
$[\boldsymbol{D}]^T$ Matrix of transposed depth values

$$[\boldsymbol{D}]^T = \begin{bmatrix} 3 & 2 \\ 2 & 3 \\ 2 & -2 \end{bmatrix} \tag{11}$$

$$[\boldsymbol{U}] = \begin{bmatrix} 3 & 2 & 2 \\ 2 & 3 & -2 \end{bmatrix} \cdot \begin{bmatrix} 3 & 2 \\ 2 & 3 \\ 2 & -2 \end{bmatrix} \tag{12}$$

The dot product of the matrixes gives:

$$[\boldsymbol{U}] = \begin{bmatrix} 17 & 8 \\ 8 & 17 \end{bmatrix} \tag{13}$$

The eigenfunctions are calculated by:

$$[\boldsymbol{U}] \cdot [\boldsymbol{E}] = \lambda_k \cdot [\boldsymbol{E}] \tag{14}$$

In which $[\boldsymbol{E}]$ contains the m eigenvectors of matrix $[\boldsymbol{U}]$. λ_k contains the m eigenvalues (corresponding to the eigenvectors) that are used to rank the m eigenvectors. The m eigenvectors form the m unscaled eigenfunctions (Wijnberg, 1995). Substituting $[\boldsymbol{U}]$ in this equation yields:

$$\begin{bmatrix} 17 & 8 \\ 8 & 17 \end{bmatrix} \cdot \begin{bmatrix} x_1 \\ x_2 \end{bmatrix} = \lambda_k \cdot \begin{bmatrix} x_1 \\ x_2 \end{bmatrix} \tag{15}$$

This is equivalent to the equations (16) and (17)

$$17x_1 + 8x_2 = \lambda x_1 \tag{16}$$

$$8x_1 + 17x_2 = \lambda x_2 \tag{17}$$

Rewriting equation (16) and (17) gives respectively:

$$(17 - \lambda)x_1 + 8x_2 = 0 \tag{18}$$

$$8x_1 + (17 - \lambda)x_2 = 0 \tag{19}$$

In matrix form

$$\begin{bmatrix} 17 - \lambda & 8 \\ 8 & 17 - \lambda \end{bmatrix} = 0 \tag{20}$$

The determinant of the matrix should have a zero solution, therefore:

$$(17 - \lambda) * (17 - \lambda) - (8 * 8) = 0 \tag{21}$$

$$\lambda^2 - 34\lambda + 225 = 0 \tag{22}$$

Solving this gives two solutions which are called the eigenvalues $\lambda_1 = 25$ and $\lambda_2 = 9$. Substitution these eigenvalues in the original [numbers] equations yields the following eigenvectors:

$$(17 - 25\ )x_1 + 8x_2 = 0 \tag{23}$$

$$8x_1 = 8x_2 \tag{24}$$

$$x_1 = x_2 \tag{25}$$

Which yields eigenvector 1. $e_1 = [1\ ,1]$, corresponding to eigenvalue $\lambda_1 = 25$
The other solution, $\lambda_2 = 9$, gives:

$$8x_1 + (17 - 9)x_2 = 0 \tag{26}$$

$$8x_1 = -8x_2 \tag{27}$$

Which yields eigenvector 2. $e_2 = [1\ , -1]$, corresponding to eigenvalue $\lambda_2 = 9$
The eigenfunction matrix is ranked on the values of the eigenvectors, therefore the matrix $[\boldsymbol{E}]$ containing the eigenvectors is:

$$[\boldsymbol{E}] = \begin{bmatrix} 1 & 1 \\ 1 & -1 \end{bmatrix} \tag{28}$$

With $\lambda_1 = 25$ and $\lambda_2 = 9$
This matrix needs to be normalized:

$$\overrightarrow{u_1} = \frac{\overrightarrow{v_1}}{|\overrightarrow{v_1}|} = \frac{[1\ , 1]}{\sqrt{1^2 + 1^2}} = \frac{[1\ , 1]}{\sqrt{2}} \tag{29}$$

$$\overrightarrow{u_1} = \left[\frac{1}{\sqrt{2}}, \frac{1}{\sqrt{2}}\right] \approx [0.707, 0.707] \tag{30}$$

The vector $\overrightarrow{u_2}$ can be determined by computing $\overrightarrow{w_2}$:

$$\begin{gathered}\overrightarrow{w_2} = \overrightarrow{v_2} - \overrightarrow{u_1} \cdot \overrightarrow{v_2} * \overrightarrow{u_1} = \\ [1, -1] - \left[\frac{1}{\sqrt{2}}, \frac{1}{\sqrt{2}}\right] \cdot [1, -1] * \left[\frac{1}{\sqrt{2}}, \frac{1}{\sqrt{2}}\right] = \\ [1, -1] - 0 * \left[\frac{1}{\sqrt{2}}, \frac{1}{\sqrt{2}}\right] \\ [1, -1] = \\ \overrightarrow{w_2} = [1, -1]\end{gathered} \tag{31}$$

Normalizing gives:

$$\begin{gathered}\overrightarrow{u_2} = \frac{\overrightarrow{w_2}}{|\overrightarrow{w_2}|} = \frac{[1, -1]}{\sqrt{1^2 + 1^2}} = \frac{[1, -1]}{\sqrt{2}} = \\ \left[\frac{1}{\sqrt{2}}, \frac{-1}{\sqrt{2}}\right] \approx [0.707, -0.707]\end{gathered} \tag{32}$$

This yields the (unscaled but normalized) eigenfunction matrix:

$$[\boldsymbol{E}] = \begin{bmatrix} \frac{1}{\sqrt{2}} & \frac{1}{\sqrt{2}} \\ \frac{1}{\sqrt{2}} & \frac{-1}{\sqrt{2}} \end{bmatrix} \tag{33}$$

The weightings on the eigenfunctions are determined by calculating matrix $[\boldsymbol{V^T}]$**:**
This matrix can be calculated from the equation $[\boldsymbol{D}] = [\boldsymbol{E}] \cdot [\boldsymbol{S}] \cdot [\boldsymbol{V^T}]$
In which $[\boldsymbol{V^T}]$ is the only unknown. However, this does not allow for checking the outcome of the singular value decomposition.

The matrix $[\boldsymbol{S}]$ contains the square root of the eigenvalues, which is: $[\boldsymbol{S}] = \begin{bmatrix} \sqrt{25} & 0 \\ 0 & \sqrt{9} \end{bmatrix}$

$$[\boldsymbol{S}] = \begin{bmatrix} 5 & 0 \\ 0 & 3 \end{bmatrix}$$

The matrix $[\boldsymbol{V}]$ can be derived by solving:

$$[\boldsymbol{U}] = [\boldsymbol{D}]^T \cdot [\boldsymbol{D}]$$

$$[\boldsymbol{U}] = \begin{bmatrix} 3 & 2 \\ 2 & 3 \\ 2 & -2 \end{bmatrix} \cdot \begin{bmatrix} 3 & 2 & 2 \\ 2 & 3 & -2 \end{bmatrix} \tag{34}$$

$$[\boldsymbol{U}] = \begin{bmatrix} 13 & 12 & 2 \\ 12 & 13 & -2 \\ 2 & -2 & 8 \end{bmatrix}$$

Again solving equation (10):

$$[\boldsymbol{U}] \cdot [\boldsymbol{F}] = \lambda_k \cdot [\boldsymbol{F}]$$

$$\begin{bmatrix} 13 & 12 & 2 \\ 12 & 13 & -2 \\ 2 & -2 & 8 \end{bmatrix} \begin{bmatrix} \boldsymbol{F_1} \\ \boldsymbol{F_2} \\ \boldsymbol{F_3} \end{bmatrix} = \lambda_k \cdot \begin{bmatrix} \boldsymbol{F_1} \\ \boldsymbol{F_2} \\ \boldsymbol{F_3} \end{bmatrix} \tag{35}$$

Repeating equation (16) until (20) for this matrix results in:

$$\begin{bmatrix} 13-\lambda & 12 & 2 \\ 12 & 13-\lambda & -2 \\ 2 & -2 & 8-\lambda \end{bmatrix} = 0 \tag{36}$$

Using the characteristic that the determinant should have a zero solution:

$$(13-\lambda) * \det\begin{pmatrix} 13-\lambda & -2 \\ -2 & 4-\lambda \end{pmatrix} - 12 * \det\begin{pmatrix} -2 & 12 \\ 8-\lambda & 2 \end{pmatrix} + 2 * \det\begin{pmatrix} 12 & 13-\lambda \\ 2 & -2 \end{pmatrix} = 0 \tag{37}$$

After calculation the determinant and working out brackets the equation can be rewritten to

$$-\lambda^3 + 34\lambda^2 - 225\lambda = 0 \tag{38}$$

And:

$$-\lambda\,(\lambda - 25)(\lambda - 9) = 0 \tag{39}$$

This gives two non-zero solutions, $\lambda = 25$ and $\lambda = 9$
Eigenvectors can be determined by substituting the solutions in the outcome of matrix:
For $\lambda = 25$

$$\begin{bmatrix} -12 & 6 & 2 \\ 6 & -12 & -2 \\ 2 & -2 & -17 \end{bmatrix} \tag{40}$$

After applying row-reduction yields:

$$\begin{bmatrix} 1 & -1 & 0 \\ 0 & 0 & 1 \\ 0 & 0 & 0 \end{bmatrix} \tag{41}$$

This yields an unscaled eigenvector $e_1 = [1,1,0]$, corresponding to eigenvalue 25. The solution $\lambda = 9$ results in the following matrix:

$$\begin{bmatrix} 4 & 12 & 2 \\ 12 & 4 & -2 \\ 2 & -2 & -1 \end{bmatrix} \quad (42)$$

$$\begin{bmatrix} 1 & 1 & 0 \\ 0 & 1 & 0.25 \\ 0 & 0 & 0 \end{bmatrix} \quad (43)$$

This yields an unscaled eigenvector $e_2 = [1, -1, 4]$ corresponding to eigenvalue 9.
Normalizing the eigenfunctions corresponding to the equations results in the normalized eigenfunction matrix:

$$[\boldsymbol{V}] = \begin{bmatrix} 1/\sqrt{2} & 1/\sqrt{18} \\ 1/\sqrt{2} & -1/\sqrt{18} \\ 0 & 4/\sqrt{18} \end{bmatrix} \quad (44)$$

Now all required matrixes for the eigenfunction analysis are determined. The original dataset can be reconstructed using:

$$[\boldsymbol{D}] = [\boldsymbol{E}] \cdot [\boldsymbol{S}] \cdot [\boldsymbol{V^T}] \quad (45)$$

$$[\boldsymbol{D}] = \begin{bmatrix} \frac{1}{\sqrt{2}} & \frac{1}{\sqrt{2}} \\ \frac{1}{\sqrt{2}} & \frac{-1}{\sqrt{2}} \end{bmatrix} \cdot \begin{bmatrix} 5 & 0 \\ 0 & 3 \end{bmatrix} \cdot \begin{bmatrix} 1/\sqrt{2} & 1/\sqrt{2} & 0 \\ 1/\sqrt{18} & -1/\sqrt{18} & 4/\sqrt{18} \end{bmatrix} \quad (46)$$

$$= \begin{bmatrix} \frac{5}{\sqrt{2}} & \frac{3}{\sqrt{2}} \\ \frac{5}{\sqrt{2}} & \frac{-3}{\sqrt{2}} \end{bmatrix} \cdot \begin{bmatrix} 1/\sqrt{2} & 1/\sqrt{2} & 0 \\ 1/\sqrt{18} & -1/\sqrt{18} & 4/\sqrt{18} \end{bmatrix} \quad (47)$$

Equation (47) the right matrix gives the weightings on the scaled eigenfunctions in the left matrix. When calculating the dot product of both matrixes in equation (47) the original data in matrix $[\boldsymbol{D}]$ is reconstructed.

$$= \begin{bmatrix} 3 & 2 & 2 \\ 2 & 3 & -2 \end{bmatrix}$$

An interpretation from these eigenfunction could be that the first eigenfunction $\left[\frac{1}{\sqrt{2}}, \frac{1}{\sqrt{2}}\right]$ accounts for deviations from the mean (positive weight for first two columns), while the second eigenfunction $\left[\frac{1}{\sqrt{2}}, -\frac{1}{\sqrt{2}}\right]$ accounts for the differences in observations within one profile.

Appendix B: North Sea characteristics

Around the North Sea Region differences in the morphology can be observed. Along some parts of the coast, (migrating) sandbars are observed, while other parts of the coast no sandbars exist. Also, some coastal sections are structurally eroding while other stretches are stable or even have sediment accretion. This morphologic behaviour and differences in this behaviour can be caused by the larger dynamic systems of the North Sea, as various studies show likely correlations of characteristics like wave height or tidal current with bar existence/behaviour (Walstra, 2016; Wright & Short, 1984). Therefore, in this section, a general description of the North Sea and its main hydrodynamic processes is given.

Bathymetry

The North Sea is a semi-enclosed continental sea, connected to the Atlantic Ocean and the Norwegian Sea in the north and in the south to the Atlantic Ocean via the Straits of Dover and the English Channel. In the east, the North Sea is connected to the Baltic Sea via the Skaggerak and Kattegat. The North Sea is a shallow sea, with an average depth of 90 meters (Nauw et al., 2015). The northern part of the North Sea is relatively deep, with depths mostly between 50 and 200m. Close to the Norwegian Coast the sea is deeper, with depths up to 700m, see Figure 59. The southern part of the North Sea is relatively shallow, with depths ranging mostly between 20 and 50m (McGlade, 2002). The coasts of Belgium, The Netherlands, Germany and Denmark (the NSR) are all located in the Southern part of the North Sea. Close to the shore the water is shallower. The coastal areas along the NSR are comparable in bathymetry; the first kilometres offshore are in all cases relatively shallow.

An analysis of Naus (2018) showed that seabed of Flanders and the Dutch Frisian Islands Terschelling, Ameland and Schiermonnikoog coast is relatively flat, with slopes roughly around 1/200. The steepest slopes in the NSR are observed in the Dutch province Zeeland,

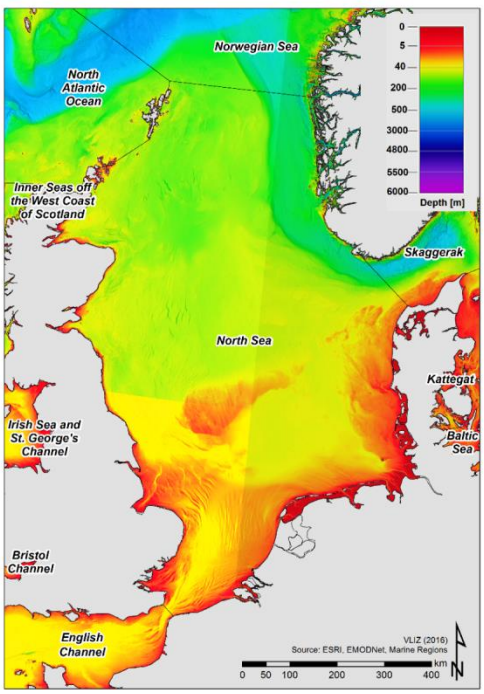

Figure 59:Bathymetry of the North Sea (De Hauwere, 2016)

with slopes generally steeper than 1/50. For the Dutch 'Holland' coast (provinces South- and North-Holland), Sylt (Germany) and parts of the Danish coast, slopes roughly around 1/100 are observed. However, different transects in the same region showed large variability in terms of slope. This variation is especially large for the Danish coast.

The North Sea bathymetry is influenced by glaciations. Until the last glaciation around 6000 years ago, invasions of mountain glaciers supplied sediments to the North Sea. In addition, the ice shaped elevations like the Dogger Bank and depressions like the Norwegian Trench (OSPAR, 2000). These ice layers, which could reach up to 2km in height, caused upon today an isostatic post-glacial rebound; an upward movement of areas that were first depressed by the weight of the ice (McGlade, 2002). In contrary to the upward movement of Scandinavian and Northern UK areas, areas that were not covered by the ice, such as the southern UK, Belgium and The Netherlands, sink. This declination causes increased relative sea level rise in southern parts of the NSR.

Sediments

Figure 60 shows the median grain size (D_{50}) of the North Sea bed. This figure is based on observations and kriging with external drift (Bockelmann et al., 2018). Around the NSR coast the grain size is around 1 to 2 ϕ, which corresponds with a grain size of respectively 500 to 250 μm (sand). The grain size along the Belgium and Dutch coast seems to be more constant compared to the German and Danish coast, where also areas with finer and coarser sediments are observed. In the region south of Norway, where the North Sea is relatively deep, the seabed is mainly built up of mud. At deeper locations, the shear stress is generally reduced and higher mud contents are found (Bockelmann et al., 2018).

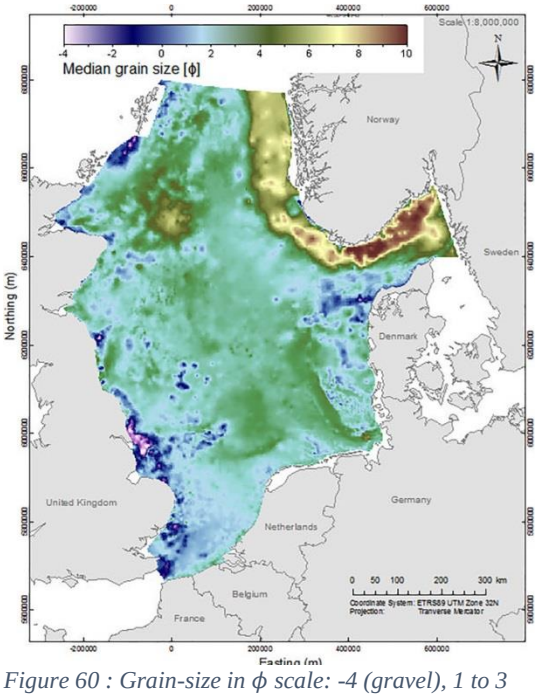

Figure 60 : Grain-size in ϕ scale: -4 (gravel), 1 to 3 sand, 4 to 10 mud (Bockelmann et al., 2018)

Currents

The hydrographic circulation in the North Sea influences the sediment transport in the North Sea. This hydrographic circulation is mainly formed by two processes; the tidal current and a wind induced current. Close to the coast currents also depend on wave direction and intensity. Therefore, also wave roses are provided for the various coasts in the NSR.

Tide

The dominant factor that creates a residual current in the North Sea is the tide. The semi-diurnal lunar tide (M2) and semi-diurnal sonar tide (S2) are the most significant tidal components in the North Sea. The North Sea is too small create a significant tide by itself, the tide observed in the North Sea is mostly a co-oscillation of the tide at the boundaries with the Atlantic Ocean (Sündermann & Pohlmann, 2011). Directly south of Norway an amphidromic point is located. At an amphidromic point there are no changes in elevation due to the tide; the tide rotates around this point. Observed from this amphidromic point, tide moves anti-clockwise trough the North Sea. The tide comes in at the Scottish coast, and travels along the eastern England coast southwards. Here it behaves like a near-perfect Kelvin wave. The tide travels along two other amphidromic points in the Dutch, German and Danish waters and leaves the North Sea via the South of Norway, see Figure 61a (Nauw et al., 2015).

Tidal amplitudes are the largest at the southernmost location in the North Sea, in the French and Belgian waters. Also, a relatively high tidal elevation is observed at the German and southern Danish coasts.

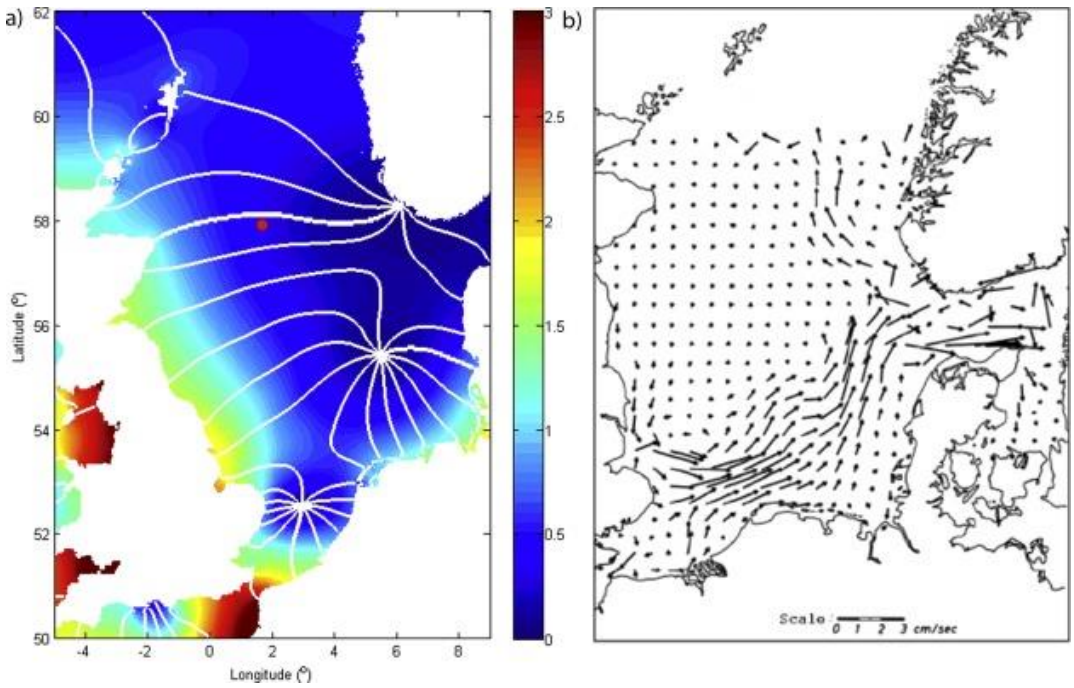

Figure 61: : Left: Tidal amplitude (colours, m) and tidal phases (white lines) derived from OSU tidal model (Egbert et al., 2010) reprinted from (Nauw et al., 2015). Right, residual current of M2 tide from (Brettschneider, 1967) reprinted from (Sündermann & Pohlmann, 2011) and (Nauw et al., 2015).

This tide generates a tidal current, which can reach speeds of a few decimetres per second (Sündermann & Pohlmann, 2011) to a roughly a meter per second during spring tide (Schloen et al., 2017; Van Dijk & Kleinhans, 2005; Walstra, 2016) . This tidal flow dominates other types of flow (Sündermann & Pohlmann, 2011). This tidal current amplitude does not coincide with the amplitude of the tidal elevation, i.e. peaks in tidal current are commonly not observed at locations where tidal amplitude is the highest. Residual currents of the tide in front of the NSR coast are directed towards the northeast, see Figure 61b. The length of the arrows indicates the velocity of the residual tidal current. In the southern part of Denmark and northern part of Germany, the residual tidal current tends to be southward. The strongest tidal residual currents in the NSR coast are observed in the northwest of the Netherlands. At the German and Danish coast, the tidal current is much weaker.

Wind and density

Another factor that influences the residual currents is the wind. West or south-westerly winds, which occur most frequently on the North Sea, cause a residual anti-clockwise current which is in direction comparable with the tidal current. In contrary, north-easterly winds cause a clockwise circulation against the direction of the tidal current. South-easterly and north-westerly causes stagnation of the wind-driven circulation in the north sea (Sündermann, 2003).

Density differences, caused by differences in temperature and salinity, in the North Sea also influence the residual circulation. The density driven current is only a small part of the total residual current (Langenberg, 1997) and is not studied in detail in this research.

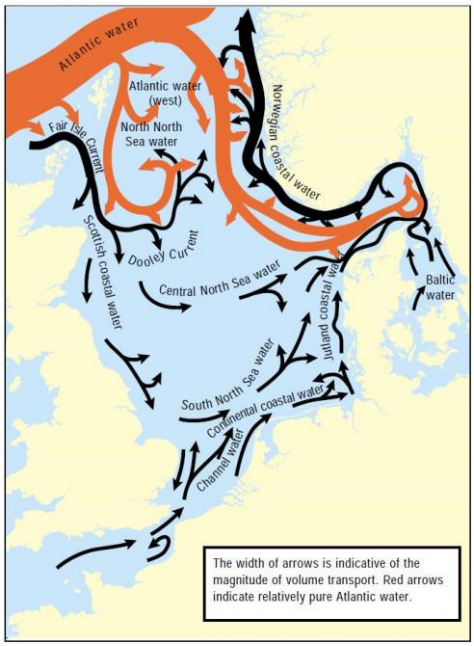

Figure 62: Schematic diagram of general (time-averaged) circulation pattern in the North Sea, (OSPAR, 2000) after (Turrell et al., 1992)

The mean residual circulation in the North Sea, resulting from these tide, wind and density driven currents is given in Figure 62. The width of the arrows indicates the magnitude of the total volume transport. This volume transport is not directly related to depth averaged flow velocity since the depth is variable in the area.

Wave climate

In this section the wave characterises for various location along the NSR coast are given. Waves influence morphologic behaviour at the coast a lot, since their energy is dissipated in this region. Wave roses are provided of various coast along the NSR since they give a complete overview of the wave intensity and direction. Wave intensity is often quantified through the significant wave height. The significant wave height is the mean wave height, so the vertical distance from trough to crest, of the highest one-third of the waves.

Denmark

Figure 64 gives an overview of the wave characteristics at the Husby measurement station (station number 2031) in the Danish North Sea. The wave data is obtained in a 4-year period, from January 2005 until January 2009 at a water depth of 17.5m. The dominant wave

direction is northwest. During high wave conditions, this direction is also dominant. The significant wave height barely exceeds 4 meters. Significant wave heights in the interval 3-4 meters are observed from the north-west to south-west direction. The significant wave height is exceeding 1m in approximately 56 percent of the time (Kaergaard et al., 2012).

The Netherlands

Figure 63 shows the wave rose obtained from measurement at the Noordwijk (NL) station in the period of January 1990 – December 1999 at a water depth of 18m (Walstra, 2016). The dominant wave directions are from the southwest and northwest. The waves entering from the southwest are very oblique to the shore, while the waves from the northwest are more perpendicular to the coast. The dominant wave direction during high waves events seems to be the northwest since this is the only direction from where significant wave height between 2.5-3.0m are observed. However, an unambiguous conclusion cannot be drawn from the wave rose. For less extreme (but still relatively high) wave conditions (1-2 m), the southwest direction is dominant.

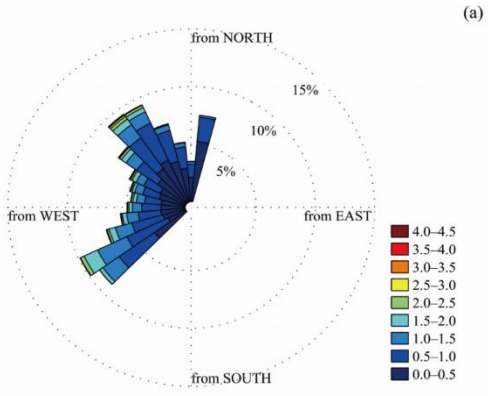

Figure 63: Wave roses at Noordwijk measurement station. Colours in wave rose indicate the significant wave height [m].(Walstra, 2016)

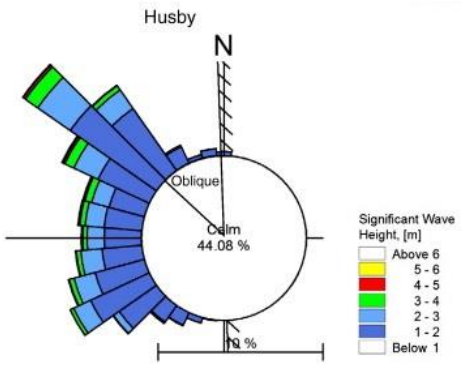

Figure 64: Wave rose at measurement station north of Husby (Kaergaard et al., 2012).

Differences

The dominant wave direction is northwest for the Danish measurement station, equally northwest/southwest for the Dutch measurement station. Significant wave height is higher in Denmark compared to The Netherlands.

Appendix C: Data-processing

In this appendix supporting data-processing steps and background information of the eigenfunction analysis data is listed. More essential data-processing steps are shown in the 3.3.4 *Data-processing* .

Stage 1: Collecting data and change format

In the first phase, the Jarkus-like profile measurements are transformed to a matrix representation. The Jarkus data is ordered with a header with information about the profile, after which the depth values are listed.

31000007		2011		70		0	2701	1602	257
-220	8541	-215	8771	-210	8711	-205	8631	-200	8671
-195	9251	-190	11071	-185	10681	-180	10951	-175	10831
-170	10871	-165	11011	-160	11181	-155	10601	-150	9811
-145	9551	-140	9261	-135	9321	-130	9331	-125	9441
-120	10391	-115	11881	-110	13431	-105	14621	-100	15031
-95	14311	-90	14111	-85	14011	-80	14121	-75	14251
-70	12291	-65	10321	-60	8461	-55	7471	-50	6621
-45	5761	-40	4931	-35	4041	-30	3242	-30	3243
-30	2984	-25	2302	-25	2293	-20	1702	-20	1663
-20	1374	-15	1392	-15	1333	-10	1312	-10	1173
-10	694	-5	1162	-5	1033	0	872	0	823
0	714	5	502	5	363	10	-22	10	-203
10	-434	15	-262	15	-443	20	-392	20	-623

Figure 65: Example of Jarkus data structure

The header contains seven numbers, it provides information about (between brackets the values in Figure 65):

1. The coastal area number (07, Noord-Holland coast)
2. The year of the measurement (2011)
3. The transect number, location in decametres from a reference point (70)
4. The type of measurement (e.g. yearly measurement or additional measurement) (0=Jarkus)
5. Date of the dry beach measurement (January 27th)
6. Data of the wet underwater measurement (February 16th)
7. The number of measurement point in the profile (257)

After this the bathymetry data within this profile is listed. The x-location (cross-shore distance from a reference point on the beach) and the y-location (e.g. elevation) are alternated. The x-location is in meters while the y-location is in centimetres. The last digit (from 1 to 6) of an altitude measurement provides information about how it was gathered. This digit should be deleted from the elevation data to get the actual elevation data. This number can have the following meanings (Deltares, 2017a)

1. Dry measurement
2. Dry measurement, in an area where also wet-measurement data is available
3. Interpolated data of the dry and wet measurement
4. Wet measurement, in an area where also dry-measurement data is available
5. Wet measurement
6. Adapted coordinate

To adjust the format of the data, there was made use of a MATLAB script constructed by Naus (2018) . This script is adjusted slightly. Firstly, the measurements ending with a 2 and 4 (dry and wet measurements, where also an interpolated value is available) are deleted, so that in an overlapping section only the interpolated data is taken into account. This is done because it is not possible to work with multiple depth values for one location later in the analysis.
Furthermore, the profiles are ordered by profile number and subsequently on year of measurement. Finally, two text files are written, containing the x and y location of the measurements. These text files are further processed in a Python based script.

0	0	0
1971	1972	1973
30	60	20
40	70	30
50	80	40
60	90	50
70	100	60
80	110	70
90	120	80
100	130	90
110	140	100
120	150	110
130	160	120
140	170	130
150	180	140
160	190	150
170	200	160
180	210	170
190	220	180

0	0	0
1971	1972	1973
-1.8	-3.8	-2.3
-2.1	-5.4	-2.6
-2.5	-9.7	-2.5
-3.2	-12	-3.2
-4.1	-15.2	-3.9
-6	-17.5	-4.7
-9.7	-20.4	-7.7
-12.8	-22.1	-10.7
-14.7	-23.2	-14
-18.2	-24.1	-17.2
-21.4	-24.1	-19.9
-23.1	-24.4	-22.2
-23.5	-24.5	-23.5
-24.3	-24.5	-24
-24.3	-24.9	-24
-24.7	-25	-24.2
-24.9	-24.7	-24.3

Figure 66:Structure of data after first processing. Left: location within transect, right: altitude at this location. The first two lines are the profile number (zero in this example) and measurement year respectively

Stage 2: Combining double profile measurements

For some years, multiple transect measurements are available. This is different than the multiple measurements at one location *within* a transect/profile, which is treated in stage 1. When two transect measurements are found within one year which are both marked as Jarkus

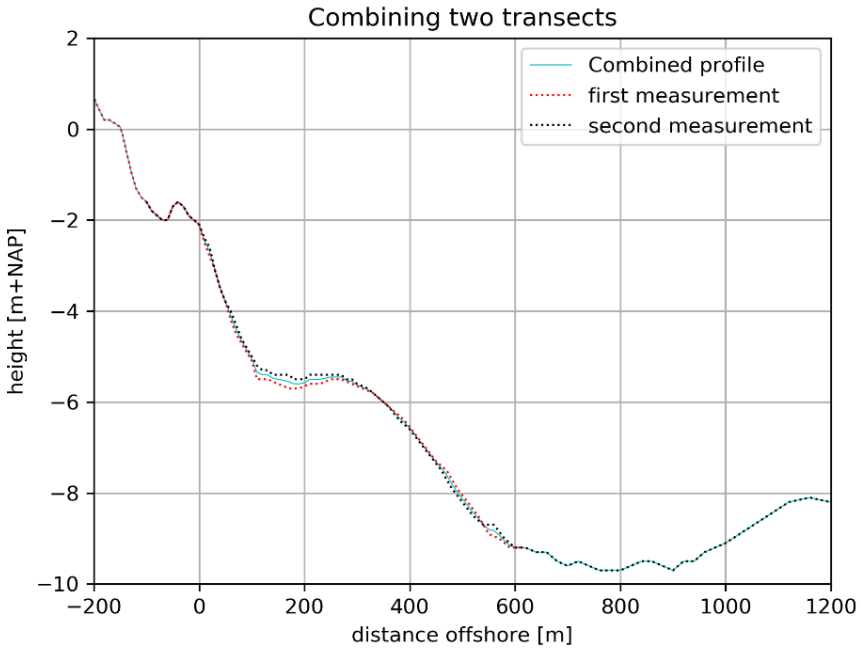

Figure 67: Combining transect measurements, profile 808 in 1980. For the clarity of the figure there is zoomed on the location where the axis overlaps, i.e. not the complete transect is shown

data (Column 4 equal to 0, see appendix B), these two are interpolated and combined, see Figure 67. This only happens for measurements the years 1965, 1970, 1975, 1980 and 1985. Mostly the additional measurement is a measurement that reaches further shoreward. At the overlapping cross-shore distance, the area for which both transect measurements have data (in Figure 67 roughly between -100m and 600m), both profiles are linearly interpolated to obtain continuous data of both transects. Next, the combined profile is obtained by the average of the interpolated data at the overlapping cross-shore distance. Since profiles are often very similar in the overlapping sections, no significant jumps are observed in the combined section at the borders of the overlapping section.

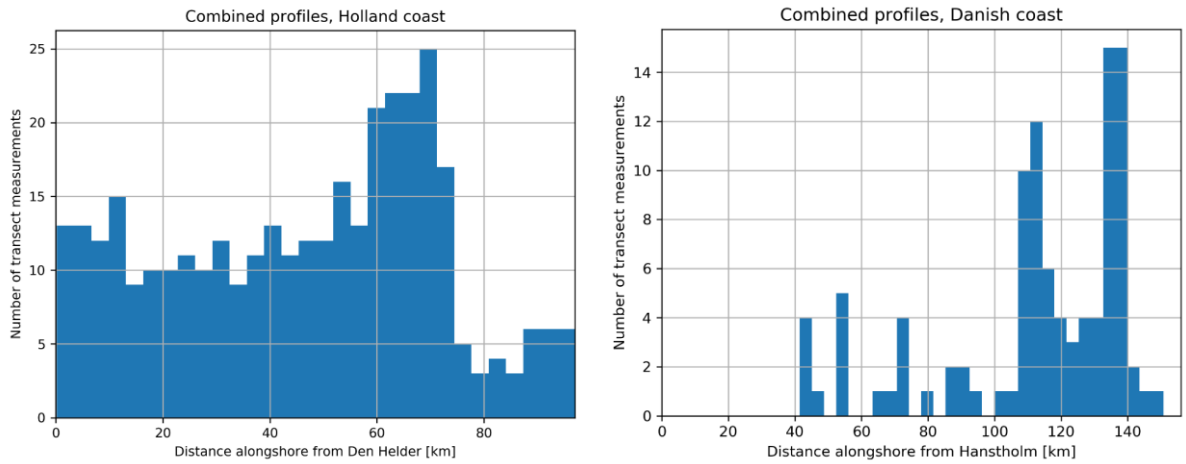

Figure 68: Number of combined profiles along the Holland and Danish coast

Interpolation errors

Although cubic spline interpolation works as desired for the majority of the profiles and gives a smoother and more natural looking result compared to linear interpolation, the interpolation can also result in unwished interpolation effects. By using cubic spline interpolation, a cubic polynomial is determined between each interval. At the endpoints, the interpolation satisfies boundary conditions of having a second derivative equal to zero. In this way, the chance of having large oscillations at the side of the interpolation interval (Runge's phenomenon) is minimized. This is a problem that typically shows up using polynomial interpolation.

Errors can however happen when the interval between measurement points are very irregular. An example is given in Figure 69. The measurement interval represented with the red dot and the first measurement offshore of this measurement is only 0.2m. The difference in depth between these measurements is 0.54m. Although this steepness on this small segment is questionable, it does not affect the overall shape of the cross-shore profile drastically.

The interval between this (red) datapoint and the next and the first more landwards measurement is 9.8m. Consequently, the polynomial fitted between these two measurements

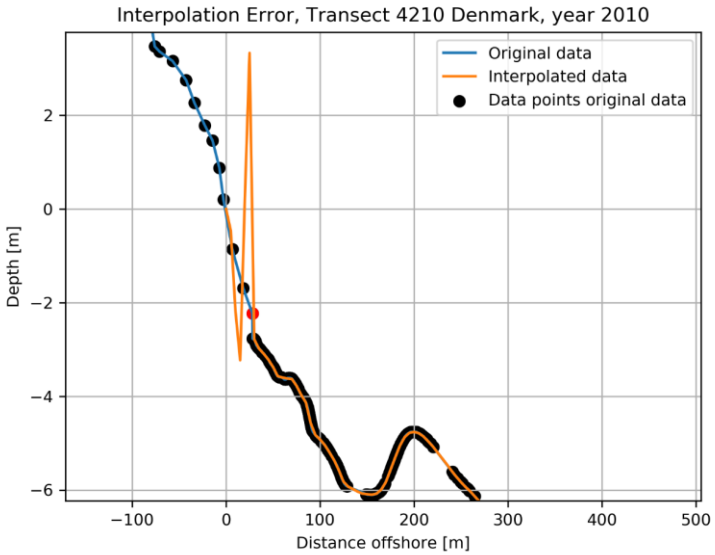

Figure 69: Example of interpolation error

is very much influenced by the extreme boundary conditions induced by the steep profile. This results in unrealistic interpolations. This interpolation error can also occur in a lesser extent and might not always be detected. Therefore, it is chosen to interpolate the data linearly.

Stage 3: Eigenfunction analysis

This stage is mainly treated in the main report. Only the scaling of the eigenfunctions is treated here.

Eigenfunction scaling

The eigenvectors as outcome of the SVD command are normalized, the sum of the squares of the eigenvector equals one. Hence, the eigenvectors do not represent the significance of the shape within the original dataset. This significance of the eigenvector is captured in its corresponding eigenvalue. These eigenvectors are scaled by multiplying with the square root of the corresponding eigenvalues. By using scaled eigenfunctions, eigenfunctions can be interpreted better. By multiplying with this scaling factor, a representation of the actual size within the original data is obtained. The first eigenfunction for example very much resembles the mean profile. Also, the amplitudes in the second and third eigenfunction give, by scaling with their eigenvalue, information about the height of the bars in the profiles.

The difference between an eigenvector and eigenfunction is not very sharp. In this report, eigenfunctions are the scaled eigenvectors.

Stage 4: Combining areas and plotting

In this last stage the data of different coastal areas is combined.

The Danish transect numbers do not, in contrary to the Dutch transect numbers, correspond with a distance measure. X and Y coordinate of the transects are available and used to determine the distance between two transects. With the help of Pythagorean theorem this distance between the transects is determined. The sum of the distances between the prior transect gives the distance from the reference location (Transect number 3100, south of Hanstholm).

The weightings of the transects are plotted using Delaunay triangulation. By using Delaunay triangulation, triangles are coloured based on the mean nearby measurements, which form the corners of the triangle. See for example Figure 70. between 2000-2001 and 2003-2004 for a schematisation of this triangulation. The black dots are the measurements and the lines form the triangles. This increases the readability of the weightings plot since individual outliers do have less influence on the result.

A negative consequence of triangulation is that also absence of data is filled with (larger) triangles. See Figure around the year 2002, where (hypothetically) no data is available. The blue lines here separate the triangles that are created by the Delaunay triangulation with absence of data in 2002. Triangles will now be coloured based on measurements in 2001 and 2003. This is however undesired.

To overcome this problem, in case of absence of data, data is created so triangles like the black lines are output of the triangulation. Next, triangles with more than one point attached to this newly created data are masked, in Figure 70 shown with the orange dashed lines.

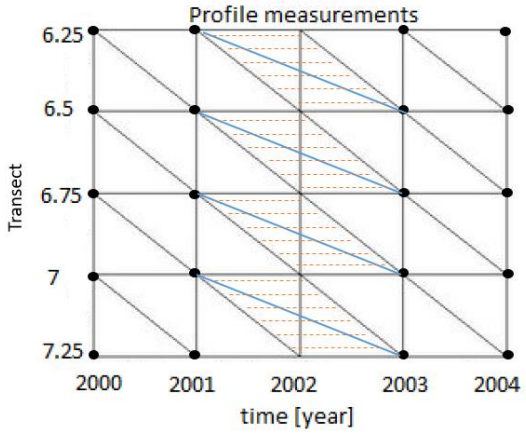

Figure 70: Schematization triangulation of rectangular grid

Appendix D: Year-to year variation in contour line

The MSL contour is used as a floating reference line which forms the start of the analysed profiles. If this MSL contour is prone to significant year-to-year fluctuations, the position of nearshore sandbars might change with respect to the floating reference line due to these fluctuations. However, if the reference line changed, there is a misinterpretation of the bar movement. To illustrate magnitude of the effect of the floating reference line, the year to year fluctuations are given in Figure 71 and Figure 72.

Figure 71 shows the year-to-year variations in the position of the Holland coast +1m NAP contour line. Mostly (85.1%), the difference in the contour position line is within 20m from the previous result. Incidentally (1.6%) the position of the contour line deviates more than 40m from the previous measurement.

This difference in contour position is quite large compared to the migration velocities of the bars, (approximately) 22 and 60-75m per year north and south of the IJmuiden harbour moles respectively. However, since the offshore migration is a relatively constant pattern, the variation of the coastline position is only expected to be 'noise' on this migration pattern.

Denmark

The majority (85%) of the year-to-year changes in the position of the MSL contour is within 25m. In 1.7 percent of the measurements the year-to-year variation is higher than 50m. The year-to-year variation in the MSL of the Danish coast is slightly higher than the year-to-year variation of the Holland +1m NAP contour. This could be due rougher wave conditions in Denmark. However, it could also be that this higher year-to-year variation is due to height of the contour line, i.e. it could be that a contour line above the MSL is more constant compared to a contour line at MSL.

Since the bar (reconstructions and eigenfunctions weights) do not show a constant migration as the Holland coast, this year-to-year variation is a larger problem. The coastline variation and therefore the supposed bar movement might be a consequence of the year-to-year variations.

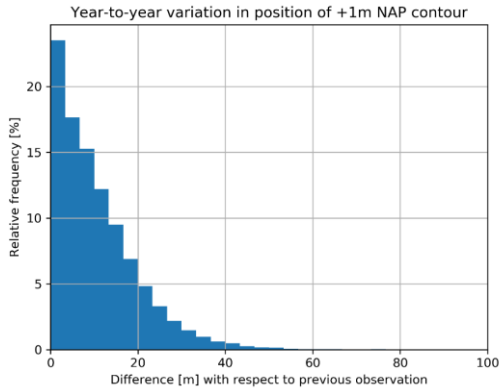

Figure 71: Year-to-year fluctuations in the position of the Dutch coastline contour

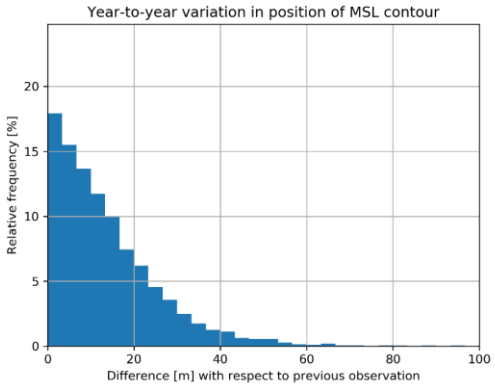

Figure 72: Year-to-year fluctuations in the position of the Danish coastline contour

Appendix E: Explained variance

The explained variance of the eigenfunctions gives an indication of how well the eigenfunctions can describe the actual dataset. If much of the variance in the dataset cannot be explained by the first three eigenfunctions, it means that the actual dataset and the reconstructed dataset have mismatches.

Netherlands

The first three eigenfunctions generally explain between 99 and 99.5 % of the total variance in the dataset, see Figure 73. The first eigenfunction mainly explains between 96 and 99% of the total variance. The second and third eigenfunction explain between 60 and 70% of the residual variance, i.e. variance that is not explained by the first eigenfunction, see Figure 74. The explained variance of the second and third eigenfunction correspond well with results of Wijnberg (1995). However, the explained (residual) of the second and third eigenfunction is lower (up to 5 percentage point) compared to Wijnberg (1995). She determined the explained variance in a similar way, but only with data until 1990. It is hypothesized that this difference has two main reasons:

1. The application of nourishments. From 1990 shoreface nourishments are increasingly applied. These nourishments affect the profile. Large bar-like shapes (nourishments) are observed in areas where they were first absent or barely present. Such changes in the profile are not incorporated in the second and third eigenfunction.
2. Very long-term changes in the profile, like flattening or steepening of the profile, are likely not spread equally over the profile (e.g., flatting mainly happened from -4m MSL, from MSL to -4m MSL no changes in steepness are present). These kinds of changes are not (fully) explained by the first eigenfunction, nor by the second or third eigenfunction, which generally represent migration of the sandbars. The variance due to unequal steepening or flattening might have contributed to the lowering of the percentage of explained residual variance by the second and third eigenfunctions.

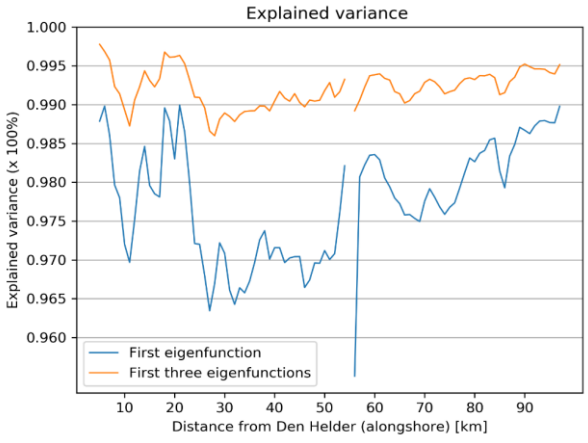

Figure 73: Explained variance of the first three eigenfunctions along the Holland coast

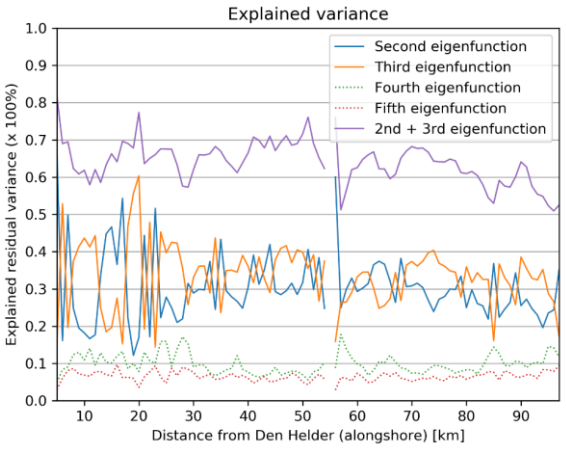

Figure 74: Explained variance of the second and third eigenfunction along the Holland coast

Although not analysed, also the explained variance of the fourth and fifth eigenfunction are given in Figure 74. Especially south of km. 30, there is a significant jump in the explained variance of the 4th eigenfunction and higher. This indicates that the second and third

eigenfunction are not random mixtures. Their explained variance is much higher compared to lower order eigenfunctions. Therefore, a (small) change in the dataset (e.g. adding data of new years) would not lead to a change of the shapes of the these eigenfunctions.

Denmark

In Denmark, an alongshore difference in the variance explained by the eigenfunctions can be observed. Between km. 0 and 79, the first eigenfunction explains between 98.5 and 99.5% of the variance. This is high with respect to the Holland coast. With the first three eigenfunctions, generally between 99.5 and 99.8% of the total variance is explained. This indicates that no major processes are missed in the eigenfunction analysis of the first three eigenfunctions.

Between km.80 and 165, generally between 97 and 98.5% of the variance is explained by the first eigenfunction. With the second and third eigenfunctions added, between 98.5 and 99.5% of the variance is explained. This is very similar to the Holland coast.
The second and third eigenfunction explain along the whole coast around 55 to 65% of the residual variance (i.e., variance not explained by the first eigenfunction).

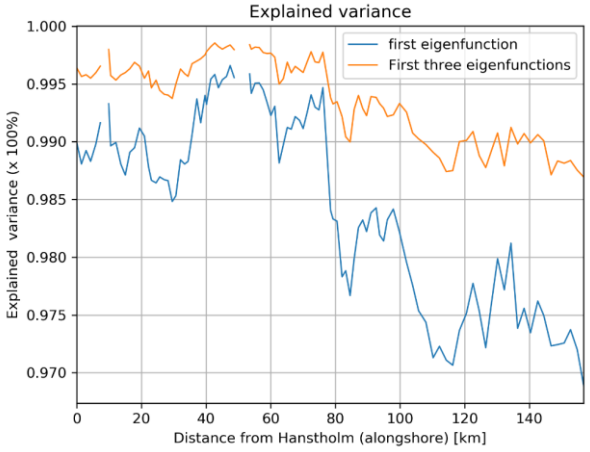

Figure 75: Explained variance of the first three eigenfunctions along the Danish coast

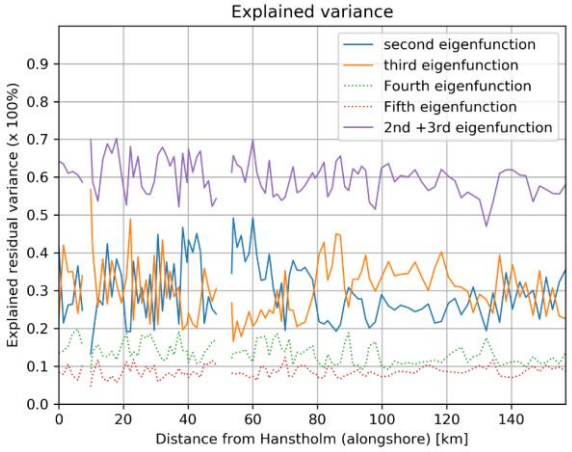

Figure 76:Explained variance of the second and third eigenfunction along the Danish coast

The difference between the second/third and fourth eigenfunction in terms of explained variance is less than the Holland coast. Especially between km. 0 and 40 this difference is sometimes very small. This indicates that the second and third eigenfunction do show signs of random mixtures. The shapes of the eigenfunctions can change when new data is added, since this new data might increase the explained variance part of the fourth eigenfunction. The shape of the fourth eigenfunction might in this case become the new third eigenfunction.

Appendix F: Danish coast analysis from 1900

From km. 22 until km. 79, data ranges back to 1874. However, the 1874 measurement is the only measurement in the before 1900. In this appendix, results from an eigenfunction analysis with data ranging back to 1900 are shown. Outcome of the analysis is briefly discussed.

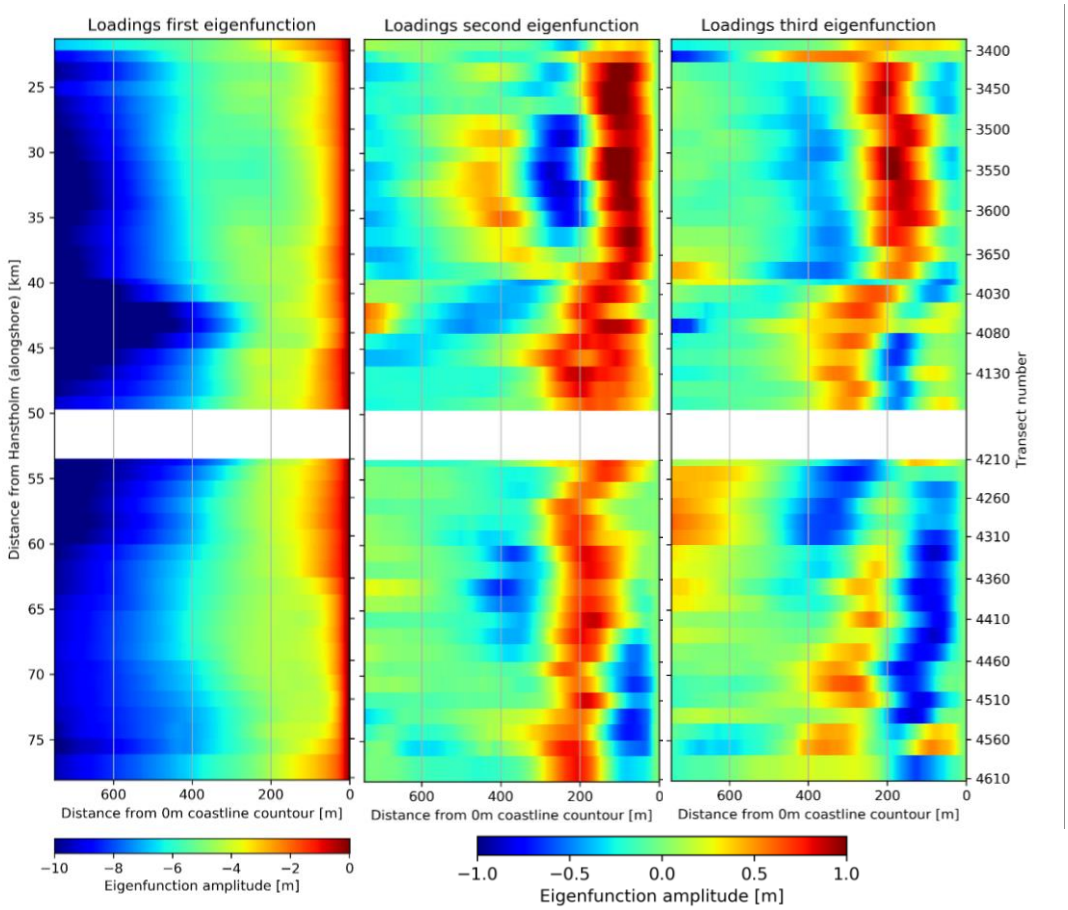

Figure 77: Eigenfunction loadings Daish coast from 1900

Nationalpark Thy, km 22-39

In this area, no clear short-term pattern or harmonic behaviour in the second and third eigenfunction weightings is observed. There is however a long-term development visible. Measurements before 1938 generally consist of a negative second eigenfunction weighting combined with a positive eigenfunction weighting for the third eigenfunction. From 1950 to 1980 the second eigenfunction is however positively weighted, while for the third eigenfunction as well positive as negative weightings can be observed. This positive second eigenfunction coincides with low first eigenfunction weightings in this area, Figure 78 and Figure 79. This high second eigenfunction weighting corresponds with two bars around 100 and 400m from the shoreline. This indicates that in case of a flatter shoreface generally coincides with a two-bar system.

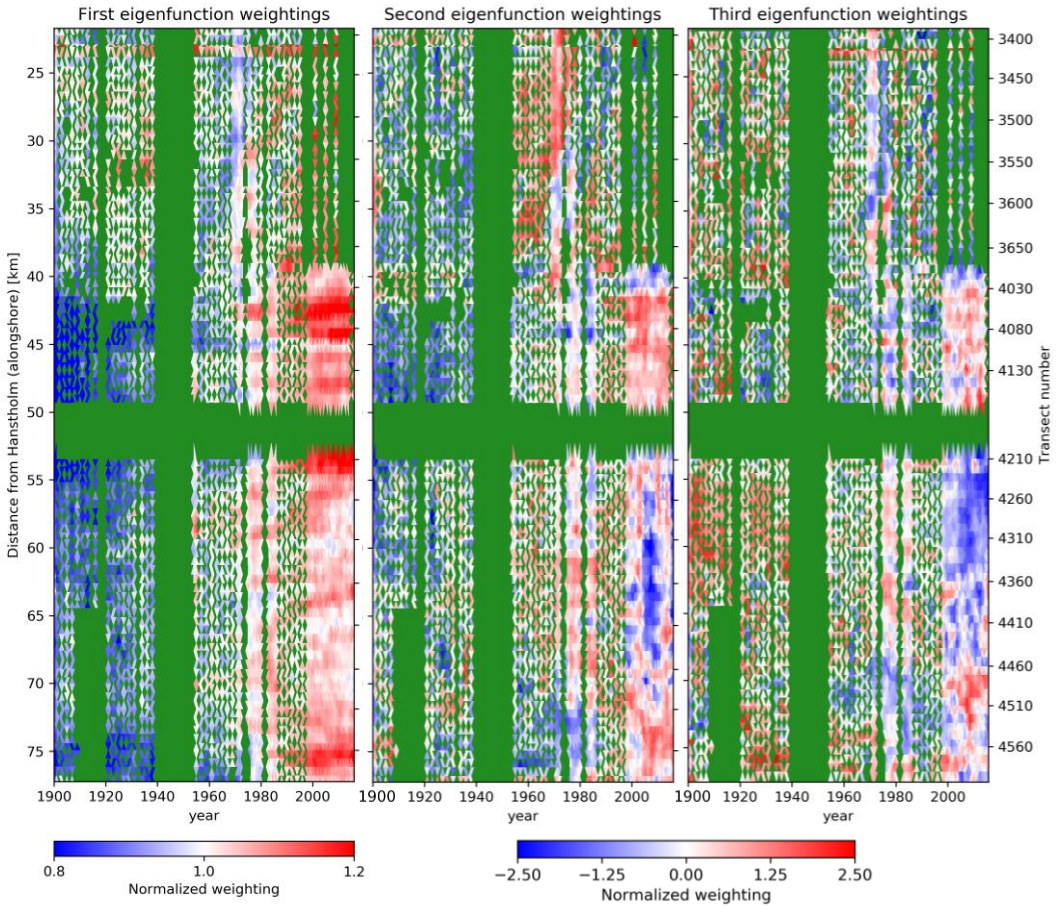

Figure 78: Eigenfunction weightings from 1900

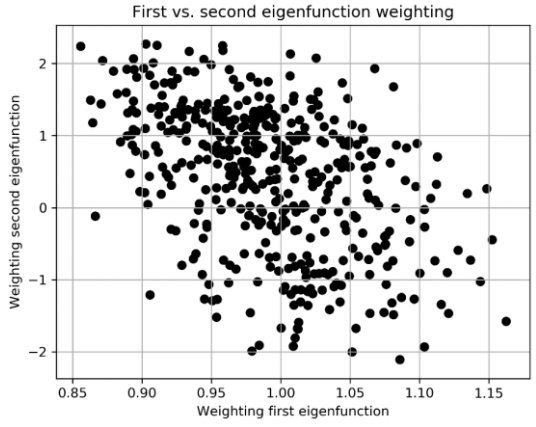

Figure 79: Correlation first and second eigenfunction weighting between km. 24 and 37.

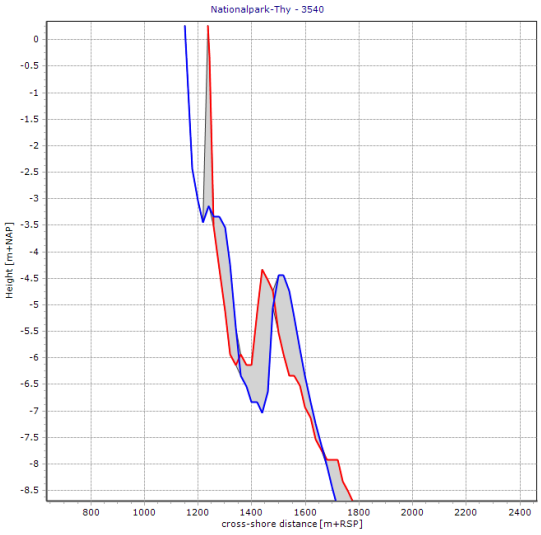

Figure 80: Transect km 30.7 in year 1938 (red) and 1955 (blue)

Agger and Midjylland north (km. 39-78)

The first eigenfunction increases gradually from 0.8 in the start of the 19th century up to 1.2 in the most recent years. This means that the steepness in the first 750m offshore has increased up to 50 percent from 1900. This 50 percent increase in eigenfunction is (amongst other locations) observed at km 42.

A very long-term trend (1900-2016) in the second and third eigenfunction can be observed in this area. The second and third eigenfunction rather describe abnormalities in the average profile shape than nearshore bars. The second eigenfunction gradually shifts from negatively weighted to positively weighted and the third eigenfunction decreases from positively weighted to weightings fluctuating around zero.

A negatively weighted second eigenfunction, yields a trough in the eigenfunctions within these positions close to the shoreline the shoreline, see Figure 77. The third eigenfunction, which is positively weighted in the early 1900s', also yields a high depth value close to the shore. Hence, both eigenfunctions in the early 1900's yields a negative amplitude with respect to the mean profile close to the shore. This is observable in the reconstruction in the year 1905, see Figure 81.

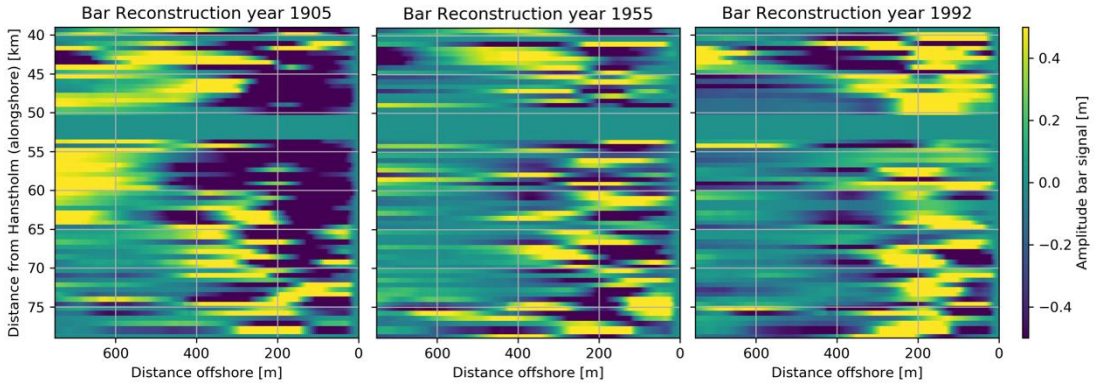

Figure 81: Bar reconstruction

Far from the shoreline, from 600m offshore, positive amplitudes can be observed. Hence, close to the shore the profile was relatively steep with respect to the mean profile, while the profile far from the shore was relatively shallow.

The eigenfunction weightings have reversed between 1905 and 1992. Hence, in 1992 the profile close to the shore was relatively flat with respect to the mean profile shape, while the profile far from the shore was relatively steep. This indicates that above average steepening occurred relatively far offshore (see Figure 82).

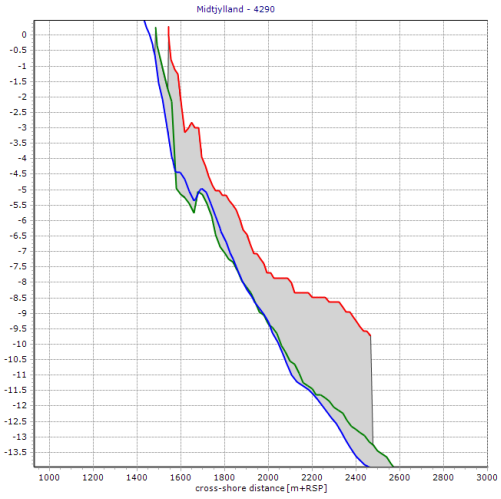

Figure 82: Measurements in the year 1905 (red), 1955 (green) and 1992 (blue) for transect 4290, km 58.3

Appendix G: Incomplete data

Not all transects can be used for the eigenfunction analysis. Many transects are too short or do not reach the coastline. When only little information is missing, profiles are filled with average data or data of measurement of adjacent years, according to Figure 83.

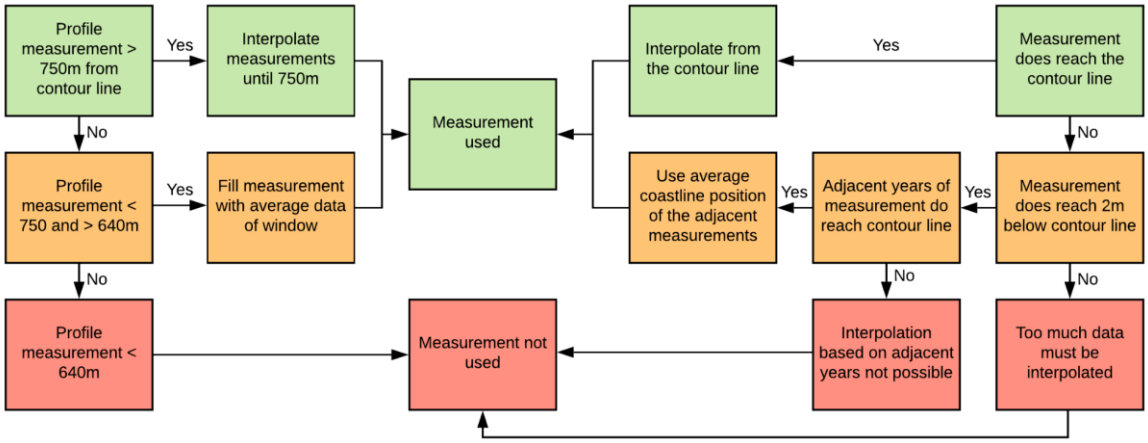

Figure 83: Handling of incomplete data

When measure grids are too short, i.e. not reaching 750m offshore from the intersection with the contour line, profiles are interpolated until where they contain data. When only a small section of the profile is missing (profile length above 630m), these profiles are extrapolated with data of the average profile. By doing so, no deviation from the average profile is created in the filled-up section. Therefore, this does barely affect the shape of the eigenfunctions.

When profiles are shorter than 630m, measurements are not extrapolated but deleted. This boundary is used because relatively a lot of measurements executed in The Netherlands reached until around 700m. When profiles are shorter than 640m, they are often way smaller (e.g. 300m).

When profiles do not reach the level of the contour line and only contain a wet measurement (i.e. only measurements below the reference line are available), the position of the reference line is interpolated based on measurements of adjacent years. In case of no data in an adjacent year, i.e. two years of incomplete data, the profile measurement is not extended with the reference line and the measurement remains unused.

Another requirement for interpolating the reference line based on adjacent years is that the most landward measurement of the incomplete 'wet' profile is at most 2m below this measurement line. If the most landward observation is even more than 2m below this reference line, a too large part of the profile is interpolated.

Location of incomplete profiles

To assess the impact of the filling of incomplete data, the total number of filled and deleted profiles are investigated. In Figure 84 and Figure 85 the profiles that do not reach 750m offshore or that do not reach the contour line are shown. Length of bars indicate the total number of insufficient transects. For example, at km. 20 almost 400 profile measurements were insufficient, of which around 280 were below the -1 MSL contour and are not used. The other 100 profiles did reach between -1 and +1m MSL and are interpolated if the measurements of adjacent years did reach the contour line.

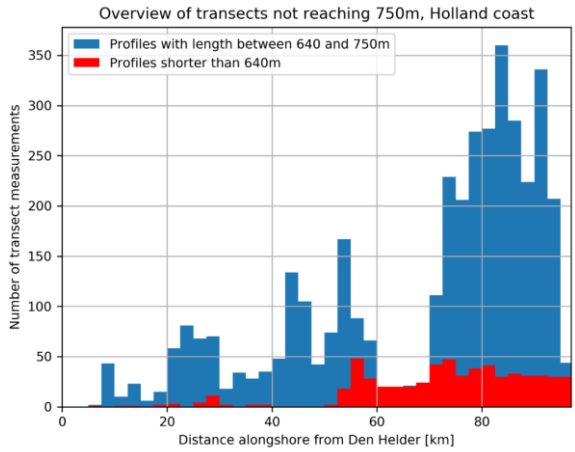

Figure 84: Overview of too short profiles for the Holland coast.

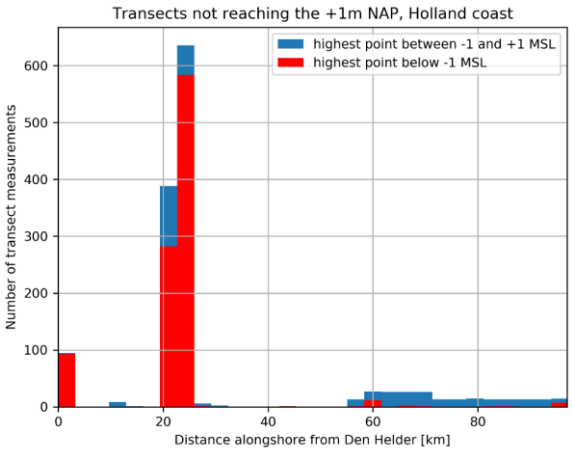

Figure 85: Overview of profile measurement not reaching the +1m NAP contour line.

Especially at the Hondsbossche zeewering (km.20-26) measurements did not reach the +1m contour line. Likely no dry measurements have been performed here since the coastal defence is a hard structure, so no significant morphologic changes can be expected. At all other locations measurements generally reach the +1m contour line.

South of the IJmuiden harbour moles (km. 50) many profiles that not reach 640m offshore are observed. Per bar of 2.5km length, generally between 20 and 50 measurements are too short to be used. Based on a transect interval of 250m (ten transects per bar) and 52 years of measurement (1965-2016), at maximum 520 measurements are performed. This means that between four and almost ten percent of the measurements remain unused.

South of km. 70 many transects do reach between 640-750m offshore. This is generally between 180 and 250 measurements per bar (2.5 km). However, also spikes of over 300 measurements are observed. Roughly between 35 and 58% of theoretical maximum of measurements are extended. This number of extended profiles is large and should be taken into account when interpreting the results. It negatively influences the significance of the eigenfunction analysis along this coastal stretch.

Since these transects are filled with average data, no sandbars are present in the filled section (see shape of first eigenfunction). Since this filling occurred over a significant part of the total data, it might have affected the shape of the second and third eigenfunction loadings. Resulting in flattening of the eigenfunction shape from 640m offshore.

In Figure 86 and Figure 87 the insufficient profiles along the Danish coast are shown. Compared to the Holland coast, much less profiles are manually extended sea- or landwards. If the +1m MSL contour line was used as reference line, many more transects measurements would be insufficient.

The number of insufficient profiles along the Danish coast is small. The filled measurements do likely not influence the eigenfunction analysis much.

The used data in this analysis is data between 1957 and 2016, not the data ranging back until 1874 (Appendix F).

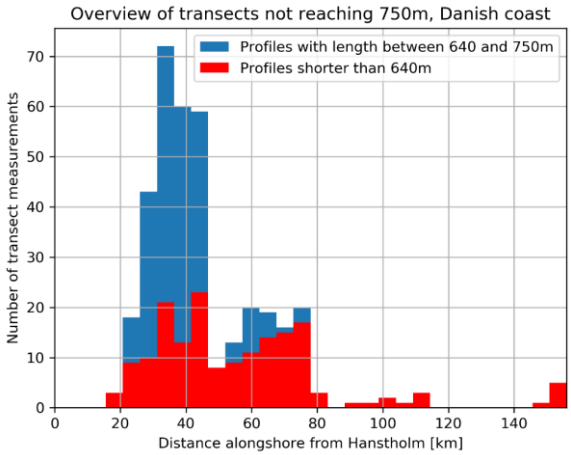

Figure 86:Overview of too short profiles along the Danish coast

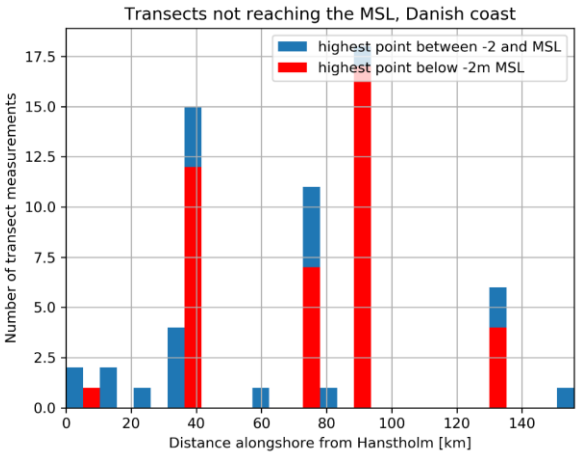

Figure 87: Overview of profile measurements not reaching the MSL contour

Appendix H: Post-nourishment development of coastline contour

The development of the average coastline position at the alongshore section of nourishments is shown in Figure 88 and Figure 89. These figures are made to assess the effect of the horizontal replacement of the contour line on the observed bar migration from bar reconstructions in Chapter 5.

The mean position of the coastline is shown with respect to the mean of the last observation prior to the nourishment. The values between brackets represent the area (km.) over which the shoreline position is determined. This is generally the same alongshore section as where the nourishment is applied.

The average post-nourishment migration of the coastline is seaward directed. When the contour line moves seaward, there is an underestimation in the seaward transport since the position to the bars is determined with respect to this coastline.

The standard deviation of the position of the coastline is after all nourishments quite high. The standard deviation is determined by subtracting the position of the last pre-nourishment observation from the post-nourishment data. Inspection of the data suggest that this is mostly due to alongshore variability on km. scale.

The nourishments at the Hondsbossche Zeewering, Camperduin and Noordwijk all show the effect of large beach nourishments on the position of the contour line. Severe seawards migration of the contour line is observed.

For the Danish coast, both the development the coastline of the nourished section and the reference areas in Chapter 5 are shown. Often the graphs are discontinuous, since (suitable) measurements are missing.

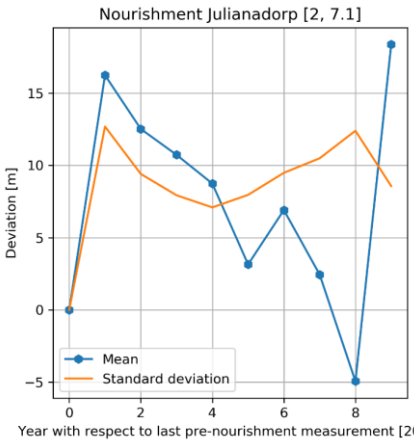
Nourishment Julianadorp [2, 7.1]
Deviation [m]
Mean
Standard deviation
Year with respect to last pre-nourishment measurement [2007]

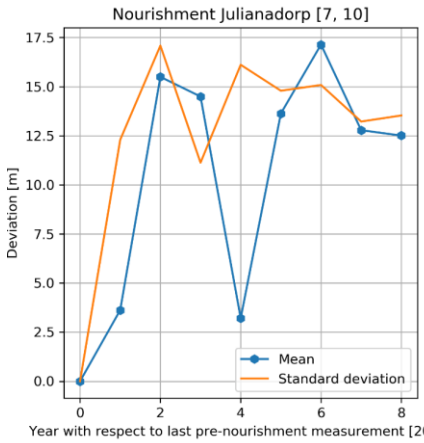
Nourishment Julianadorp [7, 10]
Deviation [m]
Mean
Standard deviation
Year with respect to last pre-nourishment measurement [2008]

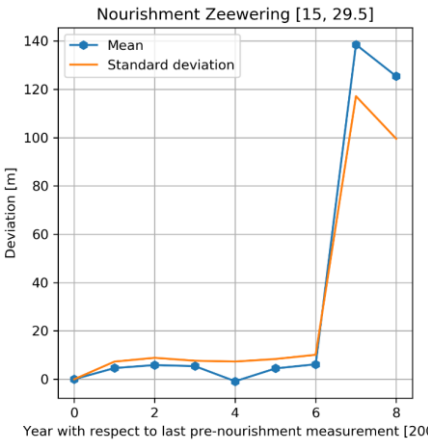
Nourishment Zeewering [15, 29.5]
Deviation [m]
Mean
Standard deviation
Year with respect to last pre-nourishment measurement [2008]

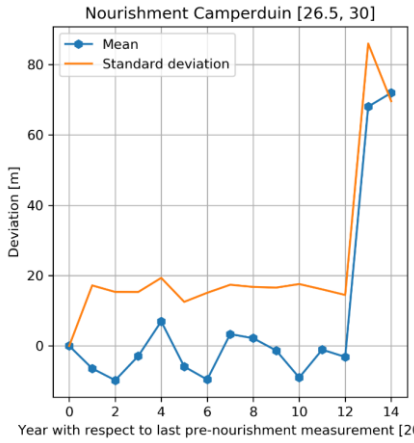
Nourishment Camperduin [26.5, 30]
Deviation [m]
Mean
Standard deviation
Year with respect to last pre-nourishment measurement [2002]

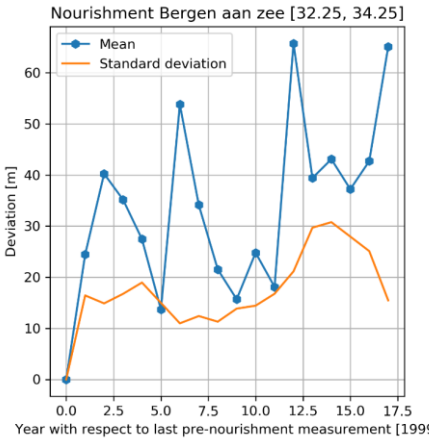
Nourishment Bergen aan zee [32.25, 34.25]
Deviation [m]
Mean
Standard deviation
Year with respect to last pre-nourishment measurement [1999]

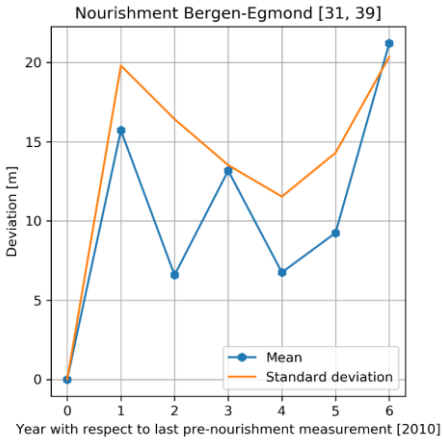
Nourishment Bergen-Egmond [31, 39]
Deviation [m]
Mean
Standard deviation
Year with respect to last pre-nourishment measurement [2010]

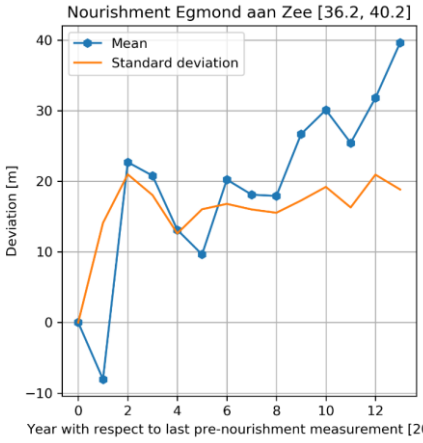
Nourishment Egmond aan Zee [36.2, 40.2]
Deviation [m]
Mean
Standard deviation
Year with respect to last pre-nourishment measurement [2003]

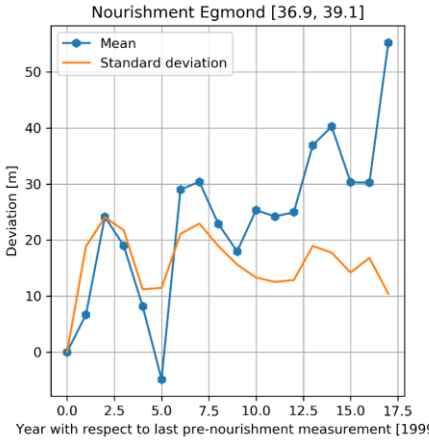
Nourishment Egmond [36.9, 39.1]
Deviation [m]
Mean
Standard deviation
Year with respect to last pre-nourishment measurement [1999]

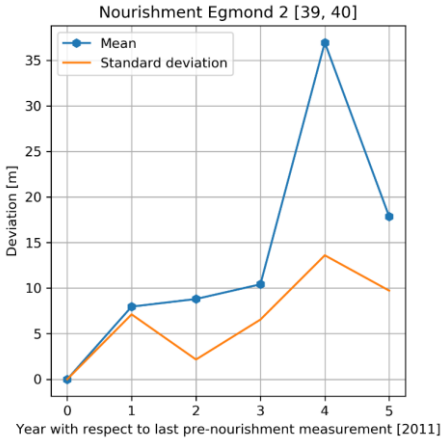
Nourishment Egmond 2 [39, 40]
Deviation [m]
Mean
Standard deviation
Year with respect to last pre-nourishment measurement [2011]

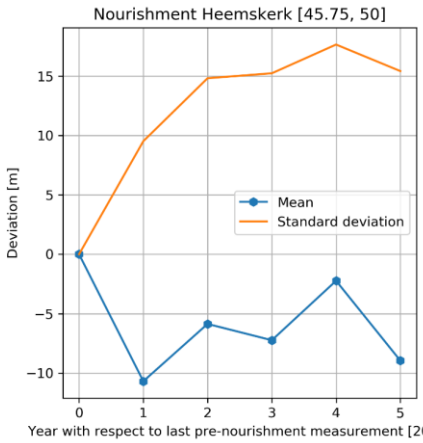
Nourishment Heemskerk [45.75, 50]
Deviation [m]
Mean
Standard deviation
Year with respect to last pre-nourishment measurement [2011]

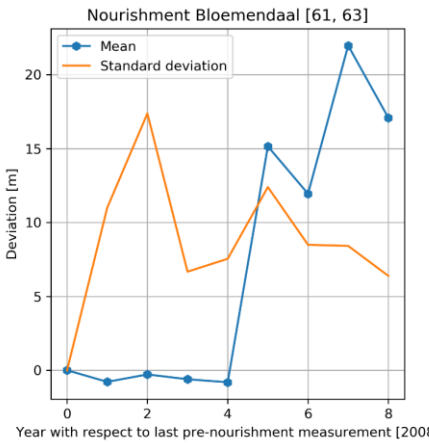
Nourishment Bloemendaal [61, 63]
Deviation [m]
Mean
Standard deviation
Year with respect to last pre-nourishment measurement [2008]

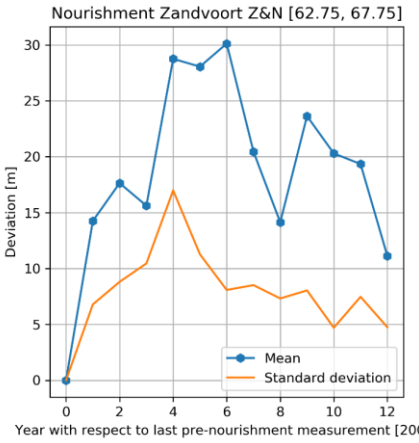
Nourishment Zandvoort Z&N [62.75, 67.75]
Deviation [m]
Mean
Standard deviation
Year with respect to last pre-nourishment measurement [2004]

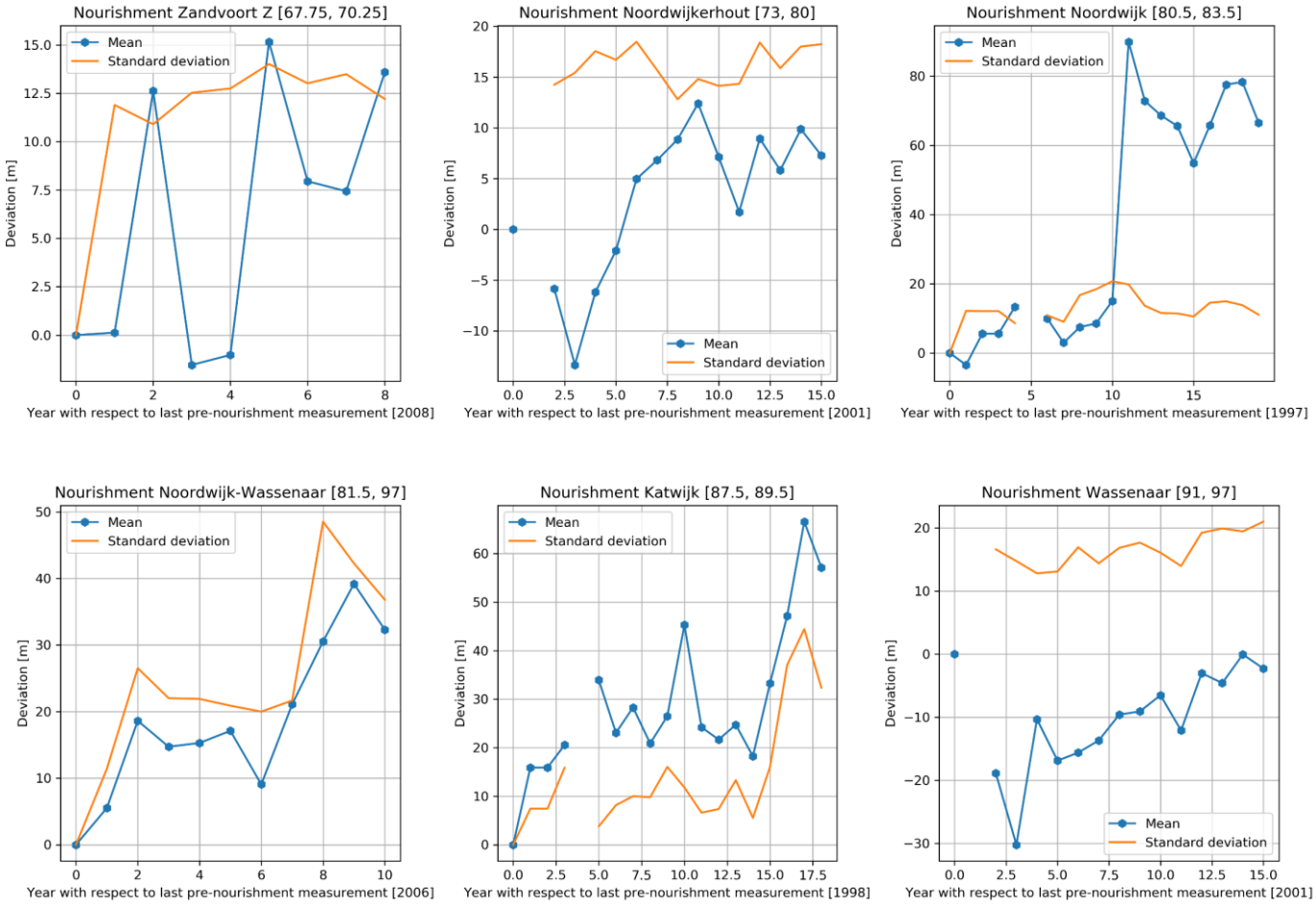

Figure 88: Development of +1m NAP contour after application of nourishments (Netherlands)

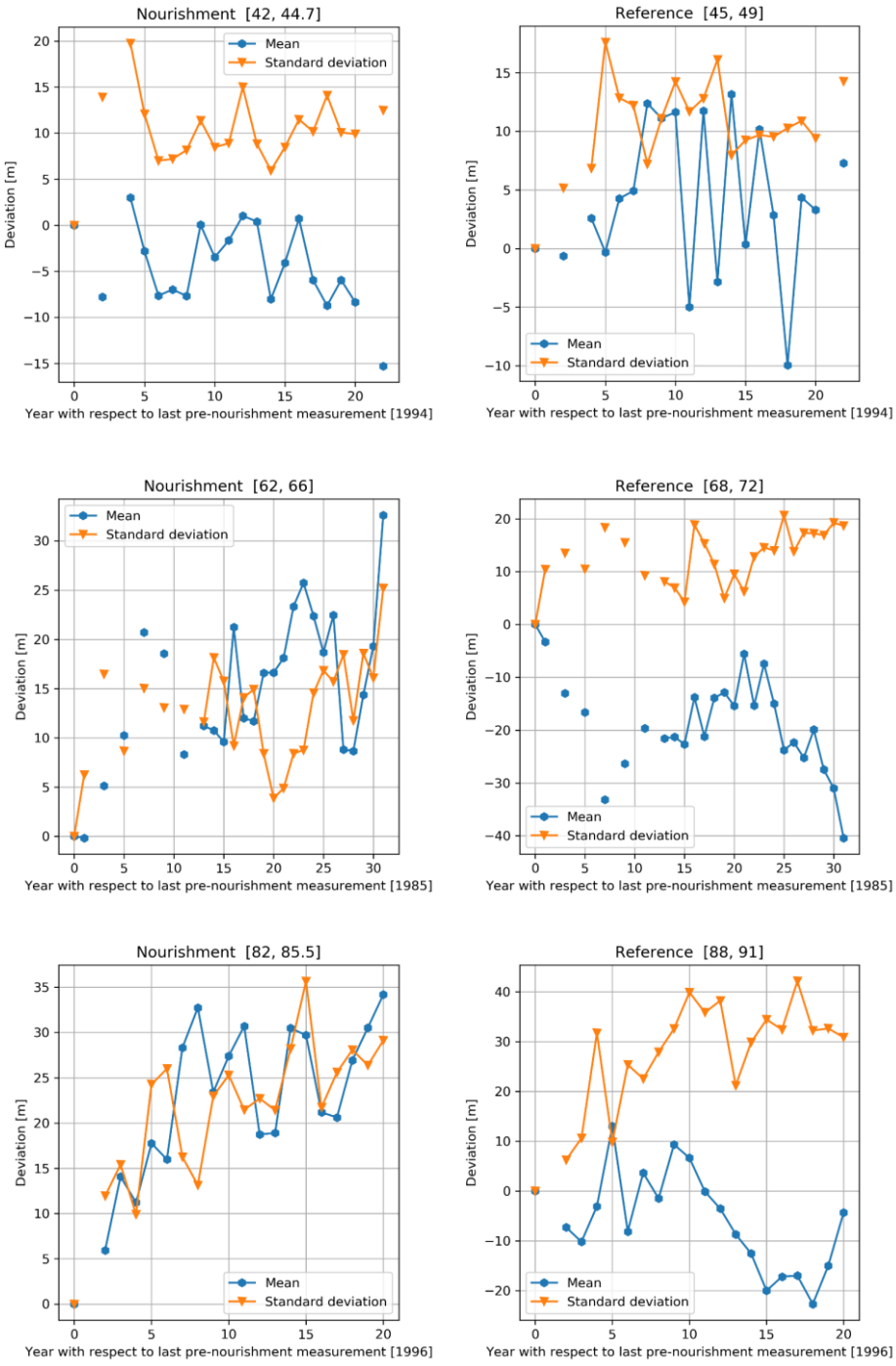

Figure 89:Development of coastline after application of nourishments (Denmark). Part 1

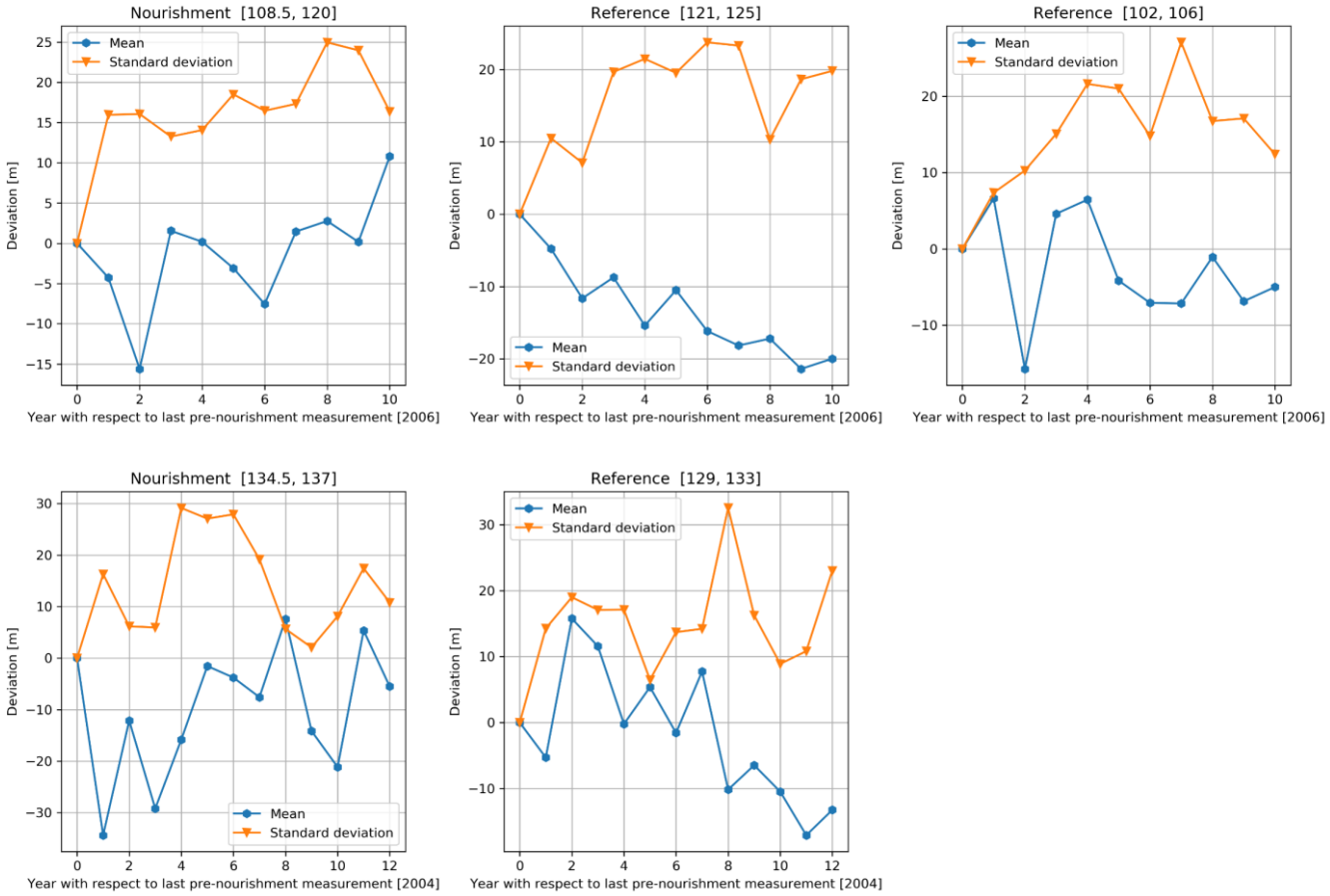

Figure 90: Development of coastline after application of nourishments (Denmark). Part 2

Appendix I: Cross- and autocorrelation

Holland coast, km. 30-50

Cross correlation

The normalized cross-correlation is shown in Figure 91. The cross-correlation of the eigenfunction reaches a maximum average with a time lag of three years. This means that the weightings of second eigenfunction correspond quite well with the third eigenfunction weightings three years later.

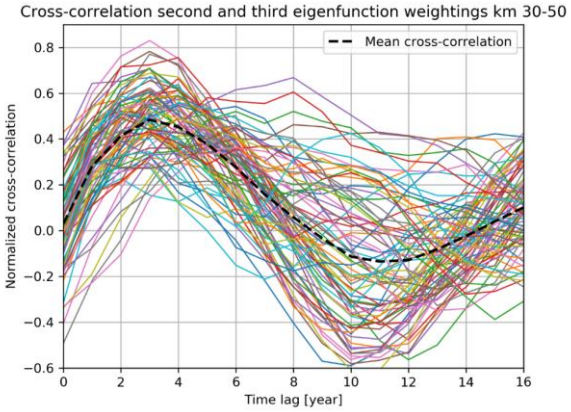

Figure 91: Normalized cross-correlation for section km. 30-50 of the Holland coast, pre-nourishment data

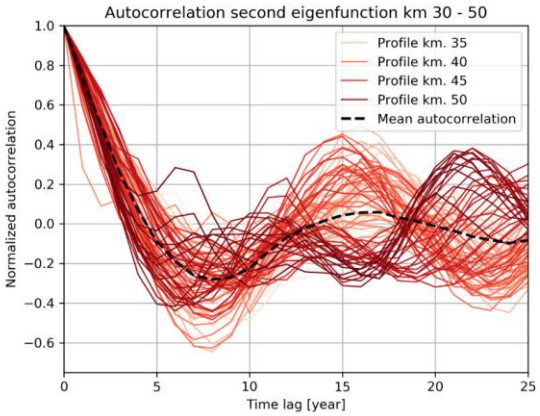

Figure 92: Autocorrelation of the second eigenfunction for km. 30-50 of the Holland coast

Bar cycle return period

In Figure 92 the autocorrelation of the second eigenfunction weightings in the section north of IJmuiden are given. Figure 92 shows that the highest autocorrelation for many transects is found with a time lag of 15 years, which is in correspondence with the bar cycle return period of around 15 years observed by Wijnberg (1995). Between km. 45 and 50 the autocorrelation is different. This is likely the effect of a bar switch at this location, see also Figure 31. Because the measurement period prior to nourishments is short compared to the bar cycle return period, one bar switch can influence the outcome of the autocorrelation significantly. Based on Figure 31, there is no reason to conclude that the bar cycle return period is significantly different along this coastal stretch.

Holland coast, km. 56-90

Cross correlation

The cross-correlation of the second and third eigenfunction is shown in Figure 93. The cross-correlation of the eigenfunction reaches a maximum with a time lag of one year. The second eigenfunction corresponds well with the third eigenfunction weightings one year later. Since as well the loadings as the weightings of the third eigenfunction lag behind the second eigenfunction, this sequence indicates offshore moving bars.

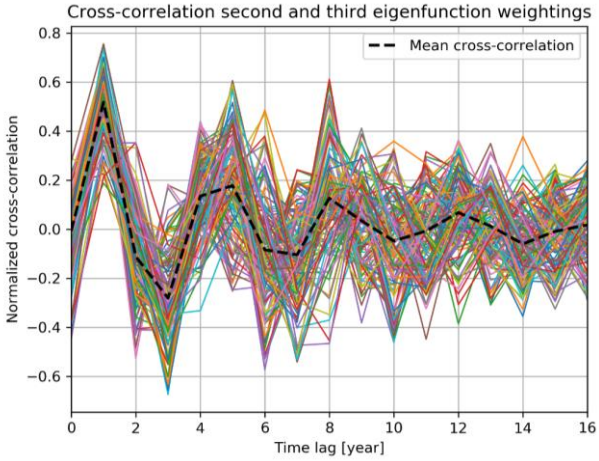

Figure 93: Cross-correlation of the second and third eigenfunction of the Holland coast, pre-nourishment data. Profiles between km. 56 and 90.

Bar cycle return period

Figure 94 shows the autocorrelation of the second eigenfunction for the area south of IJmuiden. Just as in section km 30-52, the autocorrelation varies slightly alongshore. The left figure shows the autocorrelation between transects km 56 and 70, while the figure on the right is based on the transects between km 70 and 90. The latter figure shows a clear and consistent autocorrelation for a time lag of 4 years.

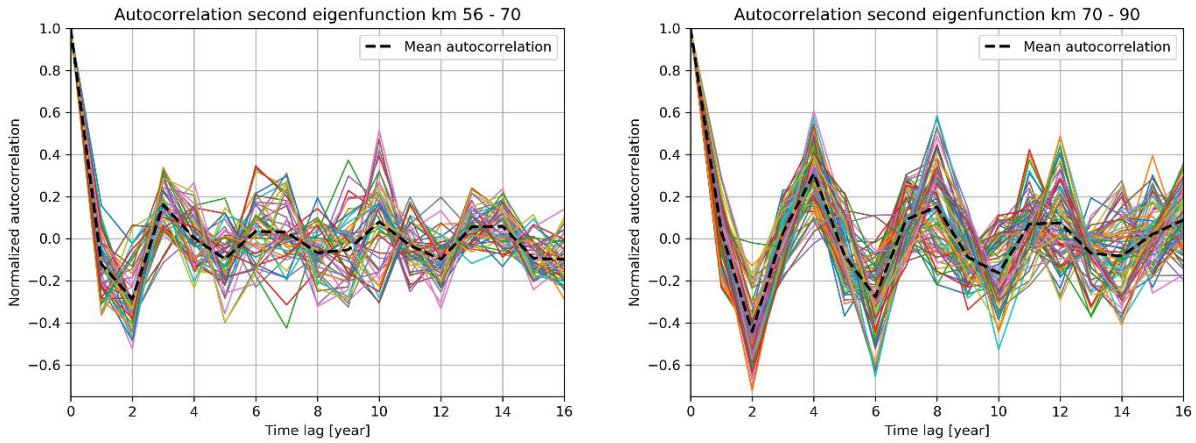

Figure 94: Autocorrelation for different sections of the Rijnland coast. Left: km 56-70, right: km 70-90.

The autocorrelation between transects km 56 and 70 is less consistent and shows a peak with a time lag 3 years. Peaks for higher time lags occur at 6-7 years and 10 years, which indicates that the bar cycle return period is just over 3 years.

Danish coast, km. 122-129

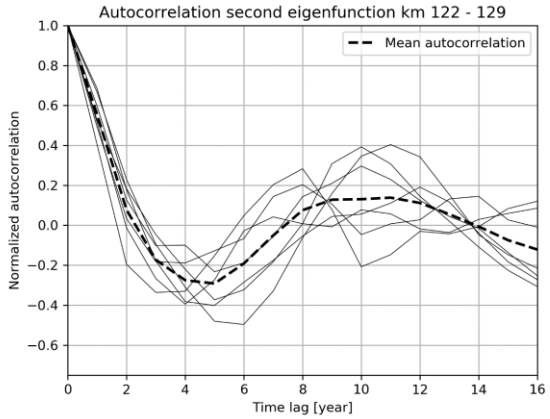

Figure 95: Autocorrelation second eigenfunction km. 122 - 129

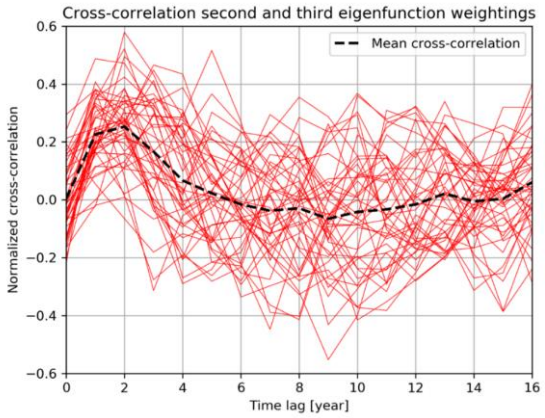

Figure 96: Cross correlation second and third eigenfunction km. 90 to 133

Appendix J: Reconstruction of bar signal and bathymetry measurements

With the eigenfunction loadings and their corresponding weightings, the bar signal, captured in the second and third eigenfunction, can be reconstructed. This is done to interpret and visualise the findings based on the figure of the eigenfunction weightings and loadings. Also, bathymetry figures have been constructed to compare with the eigenfunction results.

Section 5-26

Along this section, no bar signal was reconstructed. For this section, only the position of the bar in the first eigenfunction is compared with a bathymetry measurement.

In Figure 97, the bathymetry in the year 1980 of the North Holland coast is shown, based on the position with respect to the Rijksstrandpalenlijn (RSP). The bar in Figure 97 does show similarities with the bar in the first eigenfunction (Figure 25). Around km. 10 (blue arrow) the bar is located relatively far offshore, at km. 16 (orange arrow) the bar is connected to the shore and the distance to the shoreline varies south of km. 16.

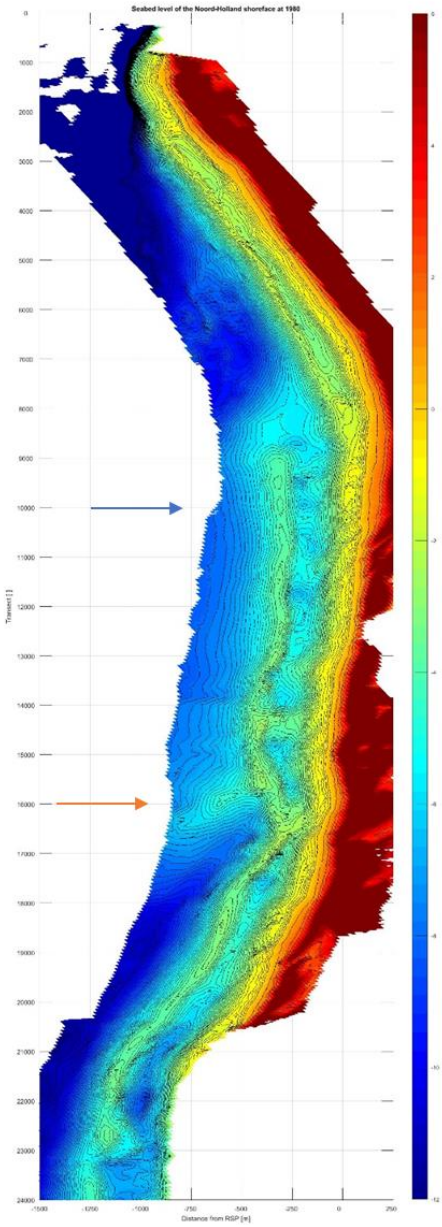

Figure 97: Bathymetry of the North Holland Coast in 1980 (km. 0-24), based on the RSP (Rijksstrandpalen)

In contrary to the result of the first eigenfunction the bar looks less shore-oblique. This is partly because the cross-shore and alongshore axes are more in equally divided. However, it could also be that the cross-shore bar position seems variable due to the variable position of the shoreline but is actually straight. This can however not be assessed based on Figure 97, since this figure also contains a disputable reference (RSP). This line is neither a straight reference line. This figure for example suggests that the that the coast is located more in the west in the north compared to 10km further south. This is not the case for the Holland coast.

Scaling and reference line choices have to be made when mapping a coast with a (small) bend over large alongshore lengths (e.g. 50km), while only analysing 750m or 1000m cross-shore. These choices can influence the interpretation of the bar position. For this report, it is important to realize that the axes in the eigenfunction figures of both areas (Dutch and Danish coast) are highly unequal in scale. 100m cross-shore corresponds with 4700m alongshore In the Netherlands, in Denmark with 5700m alongshore. Therefore, the obliqueness of the of the bars is strongly accentuated. Moreover, due to the use of a floating reference, the position of a bar can seem variable alongshore. However, based on the figures in this report, it is not possible to determine whether this is due to obliquity of the shoreline or obliquity of the sandbar.

Section 26-55

In Figure 98, section 30-55 of the North-Holland coast is reconstructed in the period 1982-1995. Although the reconstructed bars show alongshore coherence, the bar position varies alongshore. In Figure 98, 3 bars are highlighted with red lines. These bars are:

1. The bar indicated with '1'. This bar is the outer bar in the year 1982. This bar slowly migrates offshore over the years. The development of this bar is not analysed in detail since this bar migrates out of the 750m border relatively quick.
2. Bar 2 is a middle bar in the year 1982. Its position from the shoreline varies alongshore. Generally, the bar migrates offshore over time. However, between km. 45 and 47 the bar does barely migrate offshore. Because of this lack of offshore migration in this area, the bar between km 47 and 53 disconnects in the year 1987 from the main middle bar. Between 1989 and 1991, the bar reconnects to the former inner bar, marked with a '3'. In 1991, the connected bars form a shore parallel bar between km 40 and 53. However, this alongshore uniformity is lost between 1993 and 1995.
3. The bar indicated with a '3' migrates offshore remarkably fast. It connects to bar '2' between 1989 and 1991. By 1995, the original bar '3' forms the most offshore part of the original bar '2'.

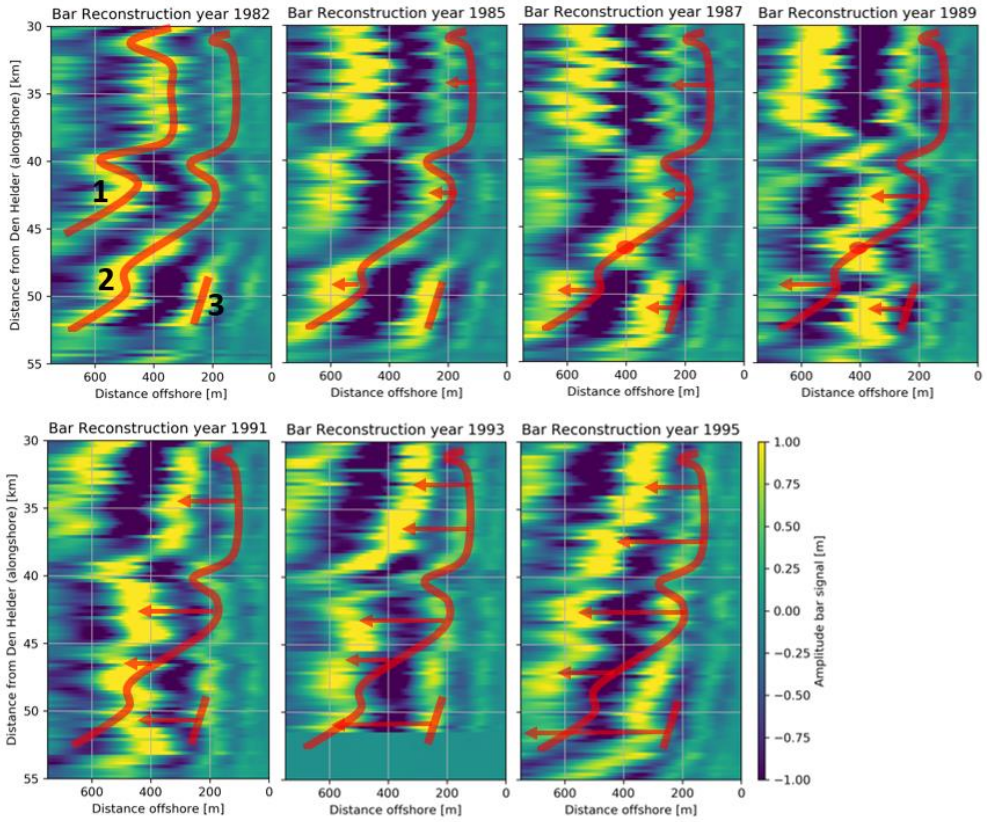

Figure 98: Bar reconstruction km. 30-55 between 1982 and 1995

The rapid offshore migration in the southernmost part of the analysed section is in correspondence with Figure 33. This figure also shows that between 1965 and 1982 no signs of faster migrating bars can be observed in the southern area. In contrary, in this period even slower than average bar migration is observed in the southernmost section. However, the figure also shows that from 1995 until 2005 faster bar migration is still present along this stretch.

Section 56-97

In Figure 18, reconstruction of section km. 55-97 between 1978 and 1982 is given. An alongshore relatively uniform bar similar to the eigenfunction loadings can be observed, which is a logical result given the alongshore consistent weightings in this area.

In between 1978 and 1982 one bar cycle is gone through. While the bars migrate seawards they largely remain their shape. In four years, the prior outer bar fades away and the former middle bar becomes the outer bar. The shapes of the bars in the year 1982 correspond well with the shape of the bars four years earlier.

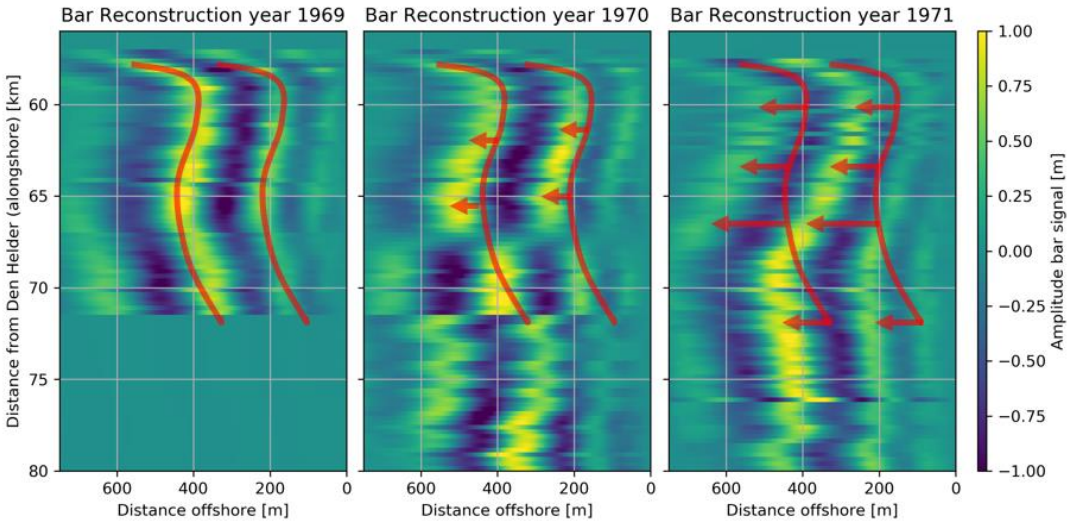

Figure 99: Bar reconstruction km. 56-97 between 1969-1971

However, bars are not always as uniform as between 1978 and 1982. A reconstruction between 1969 and 1971 does s

how differences in migration speed alongshore, resulting in a bar switch, see Figure 99.

Denmark

Various reconstructions of the bar signal in the second and third eigenfunctions are made. These are made to visualize the bar behaviour, which can be helpful to interpret the obtained eigenfunction results. Firstly, a reconstruction of the bar signal between km 0 and 39 is made for the years 1957-1975. Secondly, a representative figure for the section km. 39 and 79 is shown. Thirdly, reconstructions of the Midtjylland section are made to gain insight in the patterns that are observed in the eigenfunction weightings.

Nationalpark Thy, km. 0-39

Reconstruction of the second and third eigenfunction often results in bars without any visible trend or alongshore coherence in it, e.g., km section 0-15 in Figure 100. However, along some locations trends can be discovered. The red transparent oval shape indicates where a bar close to the shore existed. As visible from Figure 100 this bar close to the shore tends to migrate northwards. Moreover, also a negative amplitude, which position in 1967 is indicated with a red line, shows northward movement. However, in the period from 1975 the reconstruction from eigenfunctions does show less consistent bars. No trend or migration direction can be identified. The absence of bar behaviour can partially be explained by the low percentage of

variance that is captured in the second and third eigenfunction along this coastal stretch, see appendix E.

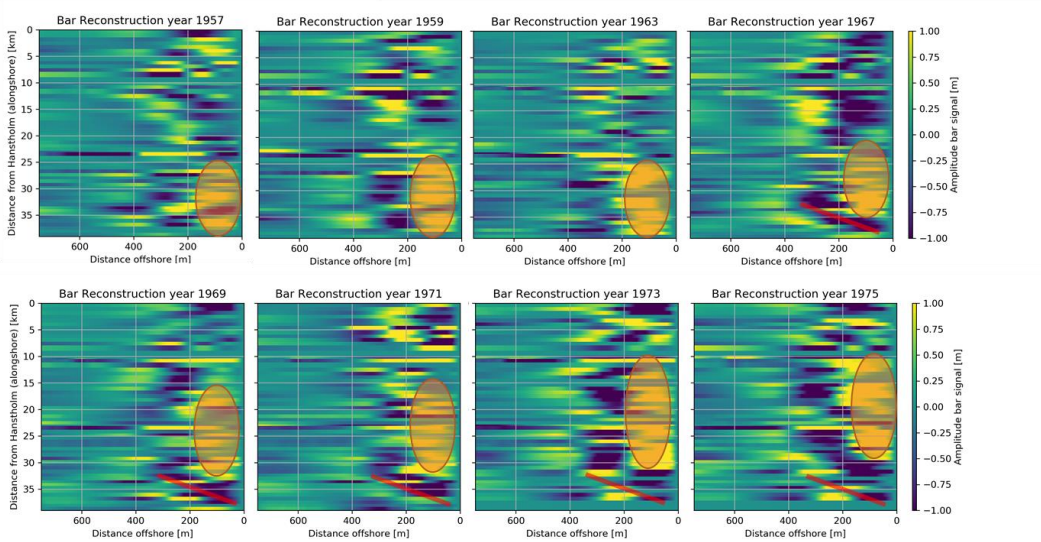

Figure 100: Bar reconstruction Nationalpark Thy 1957-1975

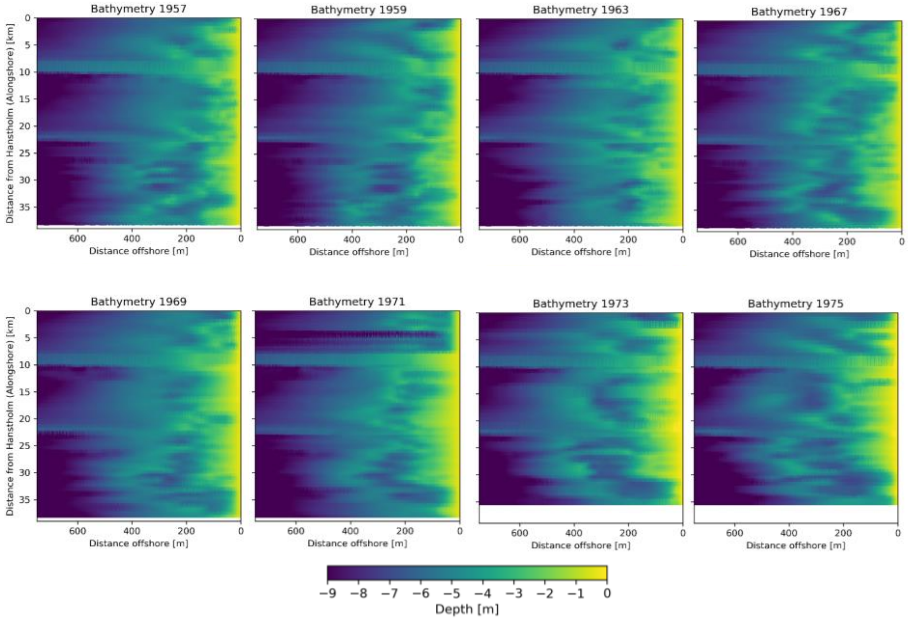

Figure 101: Bathymetry measurements corresponding to Figure 100.

Bathymetry measurements indicate that the reconstructions observed in the second and third eigenfunction do not show bars, but rather the steepness of the nearshore profile, see Figure 101.

Agger and Midjylland North, km. 40-80

Based on eigenfunction loadings and weightings, it was concluded that bars are regularly located further offshore from 2004. Bathymetry measurements support this finding, see Figure 102.

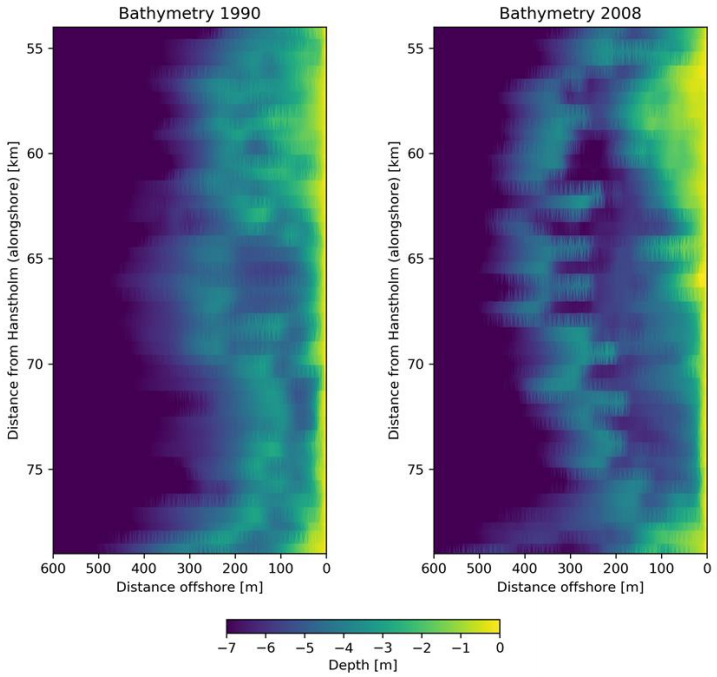

Figure 102: Bathymetry km. 54-70. Bars are located further offshore in the 2008 measurement

Midtjylland north, km. 80-90

Offshore migrating shore parallel bars is observed in the north of the Midtjylland area (km 80-90), see Figure 103.

Since the reconstructed bars in 1967 are quite weak, the bathymetry measurements are used to compare with the eigenfunction signal, see Figure 104. This corresponds with the findings of the reconstruction. However, the offshore migration is far from a clear and uniform movement.

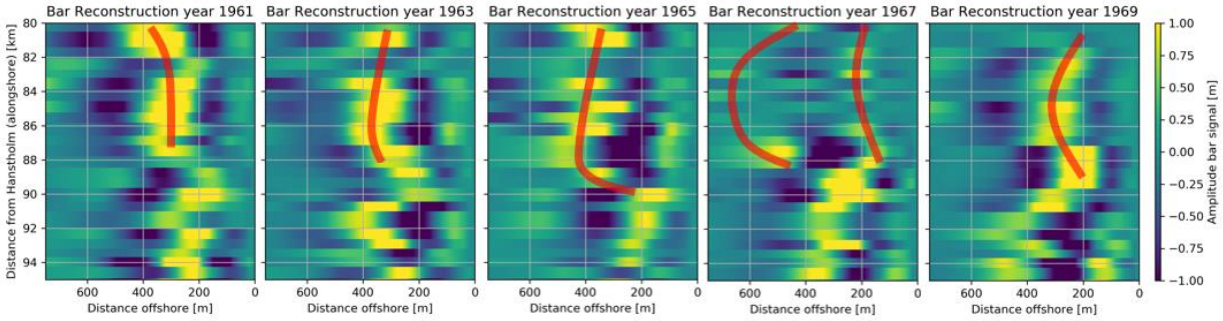

Figure 103: Bar reconstruction Midtjylland north coast.

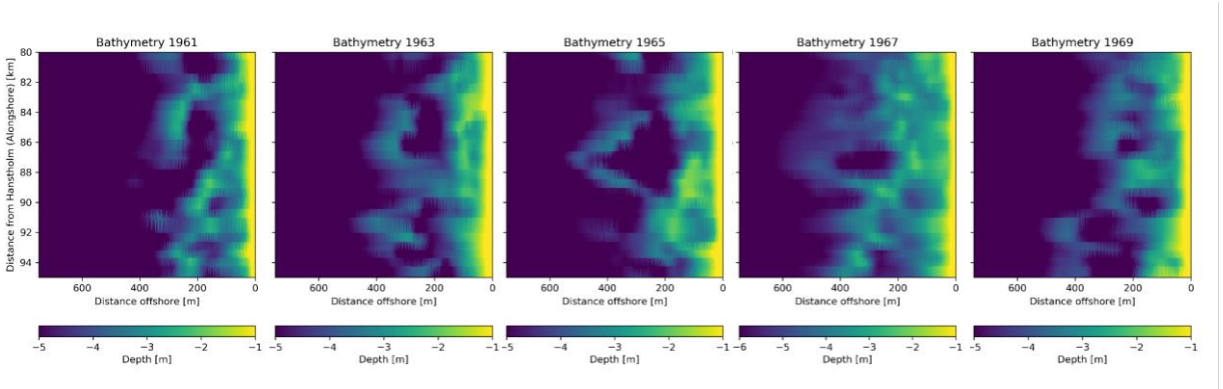

Figure 104: Bathymetry measurements corresponding to Figure 103. Please note that the colormap used for the year 1967 is slightly different to highlight the position of the bar.

Midtjylland South

The bar signal of in the second and third eigenfunction is reconstructed in Figure 105 from 1990 until 2001. The red (transparent) lines indicate the position of bars where they were first observed as a bar. Changes in the bar position are indicated with the red arrows.

One first observation regarding the shape of the bars, is that they stretch out seawards in the south. This is in correspondence with findings of Kaergaard et al. (2012).

In the year 1990 in Figure 105, two bars are marked between km 90 and 115. Two years later, in 1992 the position of bar '1' barely changed. The bar signal in the south got less strong and it seems like in the north, around km. 90, the bar moved a bit seaward. No clear trend can be identified in this bar.

The bar marked with '2' migrates from 1990 to 1994 northwards while it largely remains in the same shape. This migration is in the order of 3 km. From 1994, the bar falls apart in two bars. One part (relatively offshore and south) which migrates further northwards and vanishes in the year 2000. The other part (more landwards and north) primally migrates seaward and does not vanish.

The bar marked with a 3 shows similar behaviour as bar '2'. The bar seems to move northward between 1994 and 2001. Again, this might be caused by the offshore migration of the oblique oriented bar. In this period the shape of the bar did not change as drastically as bar 2. The bar extends more seaward over time and the amplitude close to the shore decreases. Also, the bars indicated with '4'and '5' show this northward migration. Both bars do show variations in shape over time.

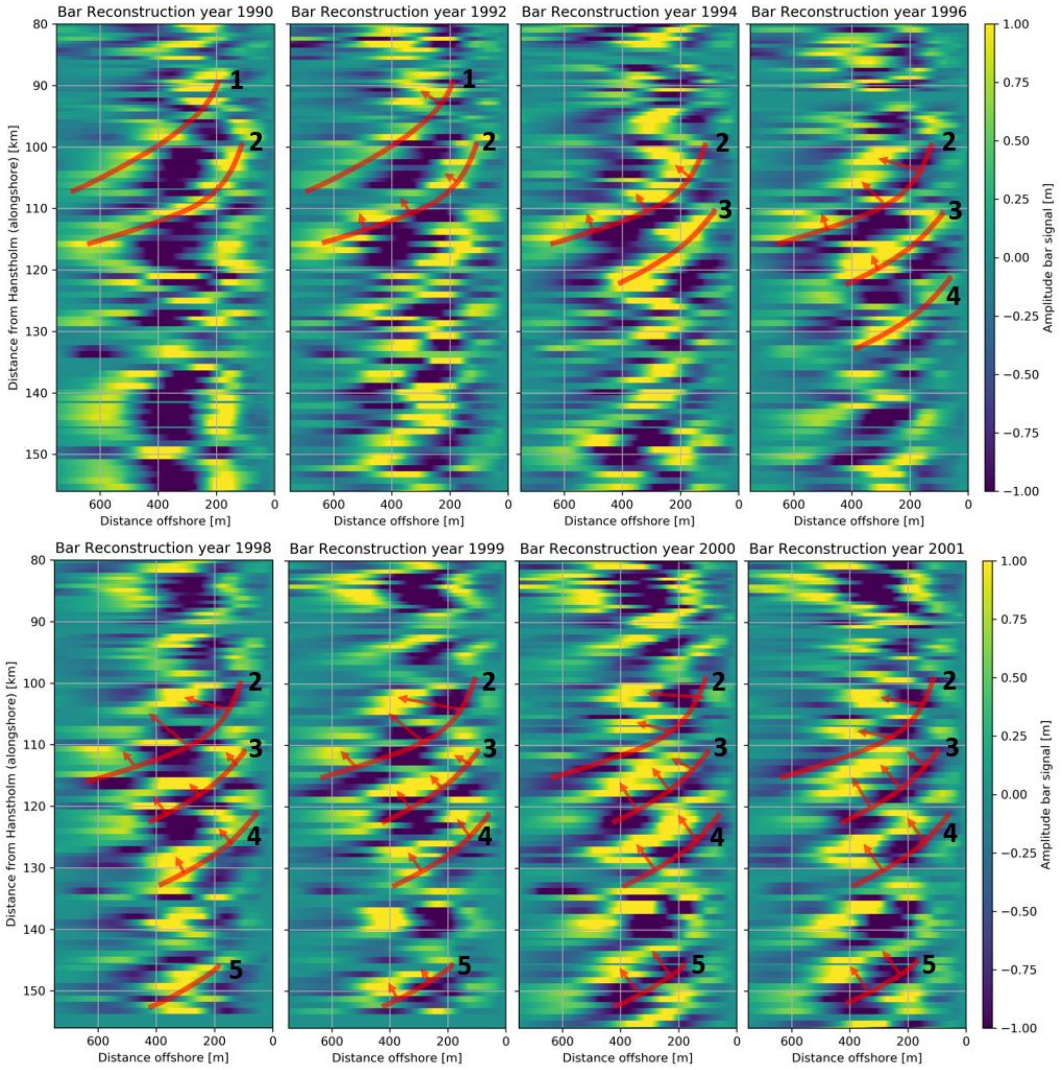

Figure 105: Bar reconstruction of the Midtjylland coast